UNIVERSITY
OF TASMANIA

Role of Neurofilaments in Ageing and Neurodegenerative Disease

by

Yao Liu MSc

School of Medicine

Submitted in fulfillment of the requirements

for the Degree of

Doctor of Philosophy

University of Tasmania

September 2013

COPYRIGHT STATEMENT

This thesis contains no material which has been accepted for a degree or diploma by the University, or any other institution, except by way of background information duly acknowledged in the thesis, and to the best of my knowledge and belief no material previously published or written by another person except where due acknowledgement is made in the text of the thesis, nor does the thesis contain any material that infringes copyright.

(Signed)_____ (Date) _____

Yao Liu

STATEMENT OF AUTHORITY OF ACCESS

This thesis may be made available for loan and limited copying in accordance with the *Copyright Act 1968*.

(Signed)_____ (Date) _____

Yao Liu

Part of the work presented in this thesis has been published as follows;

Liu Y, Staal JA, Alison JC, Kirkcaldie MT, King AE, Bibari O, Mitew S, Dickson TC, Vickers JC (2013). Cytoskeletal changes during development and ageing in the cortex of neurofilament light protein knockout mice. Journal of Comparative Neurology 521:1817-1827.

SUMMARY

Cytoskeletal protein abnormalities are common features of a number of neurodegenerative conditions. However, the potential roles of neurofilaments (NFs) in neurodegenerative disease and in ageing-related cellular changes are poorly understood. Many models of NF abnormalities in mice have been reported, but how ageing affects the NF pathology and the role of ageing in neurodegenerative diseases are still unknown. This thesis, therefore, sought to examine the effects of the absence of a major class of NF proteins, in NF light (NF-L) knockout (KO) mice, on the ageing-related adaptive capacity of other cytoskeletal elements in neurons, and also on neurodegeneration-linked alteration of cytoskeletal proteins, cytoskeletal RNA-binding proteins (TDP-43) and myelin proteins.

The NF-L subunit is considered as an obligate subunit polymer for the assembly of NF triplet proteins into neuronal intermediate filaments (IFs). Previous studies have shown that NF-L KO mice have substantially reduced axonal intermediate filaments. NF abnormalities such as NF accumulation, reduced NF-L mRNA, and NF mutations have been described in human neurodegenerative disease.

This thesis has used immunohistochemical and quantitative Western blot techniques to examine cytoskeletal changes in the brains of NF-L KO and wild-type (WT) mice at different ages. It was demonstrated that depletion of NF-L protein resulted in alteration of the expression of a range of cytoskeletal proteins, and disrupts other neuronal IF proteins, through ageing. However, there were no gross structural

changes in neurons or cytoarchitecture in regions such as the cerebral cortex. In this regard, alterations in the expression of other cytoskeletal proteins may compensate for decreased NFs.

TDP-43, an NF-L mRNA binding protein, has recently been pathologically associated with a number of neurodegenerative diseases of ageing. However, mechanisms of TDP-43 pathogenesis are unknown. As TDP-43 is known to bind to NF-L mRNA, this thesis used immunohistochemical and quantitative Western blot approaches to characterize and quantify the changes of TDP-43 expression and distribution in brain and spinal cord of ageing NF-L KO mice as compared to WT animals. It was found that a significant increase of TDP-43 protein levels occurred in the cortex and lumbar spinal cord in NF-L KO mice at 12 months of age, compared to WT mice. Moreover, an increase of phosphorylated TDP-43 was found in the cervical spinal cord of NF-L KO mice at 12 months, compared to WT controls.

NFs have a critical role in myelination by regulating axonal diameter. To investigate whether deficiency of NF-L protein results in myelin alteration during ageing, this thesis measured the relative protein level of myelin basic protein (MBP) by using quantitative Western blot. It was demonstrated that the level of MBP was significantly reduced in the cortex of NF-L KO mice at 12 months, compared to WT mice.

In summary, these findings indicate that pathological and compensatory neuronal effects of NF-L KO and reduced NFs are affected by ageing. The absence of NF-L protein results in the alteration of NFs and other cytosekeletal, mRNA-binding and

myelin proteins during ageing. These results indicate that the absence of NF proteins can lead to abnormalities in neurodegenerative disease-related proteins, but also that the central nervous system (CNS) is capable of adaptive alterations in the absence of NFs.

ACKNOWLEDGEMENTS

First and foremost, I would like to express my greatest appreciation to my supervisors, Prof. James Vickers, A/Prof. Tracey Dickson and Dr. Anna King. I am grateful for their patient guidance and supervision towards the completion of this project and sacrificing their precious time to meet me on a regular basis despite their busy schedule. It is Prof. James Vickers who encouraged and helped me, not only in my academic development but also in getting a PhD scholarship, which provided a financial support for me. I feel extremely fortunate to have been a PhD student working under his supervision. Secondly, I would like to extend a special thank to my previous co-supervisor Dr. Jerome Staal. Although Dr. Jerome Staal went to America in 2011, the skills I learnt under his guidance became a firm basis to overcome the challenges ahead.

I would also like to thank Dr. Carmen Fernandez-Martos, Justin Dittmann and Kimberley Stuart for their help with the behavioural tests of NF-L KO and WT mice, to extend many thanks to Graeme McCormack for the perfusion of NF-L KO and WT mice, and to thank Steve Weston, Clara Lee and John McManus for help with tissue sectioning and immunohistochemistry. I would like to thank Dr. Shijie Liu, Dr. Hao Cui and Yanling Hu for help with Western blot, and to thank Dr. Olivier Bibari and Dr. Stan Mitew for the help with the confocal microscope. Additionally, I would like to thank the staff at the UTAS animal facility.

I would also like to acknowledge Dr. Matthew Kirkcaldie and Dr. Carmen

Fernandez-Martos. Their statistical knowledge has benefited me greatly in understanding some complex statistical terms and concepts, and this has led to a significant improvement in my statistical skills.

Thank you to all the staff and students of the Wicking Centre and Menzies Institute, for their kindness and making my time enjoyable and memorable. A special thank to A/Prof. Changhai Ding, A/Prof. Meng Inn Chuah, Dr. Alison Canty, Dr. Adele Woodhouse, Jessica Collins, Kimberley Stuart, Rachel Atkinson, Jeng Tang and David Ward for their friendships, constant support and encouragement.

I would also like to acknowledge the University of Tasmania, School of Medicine, Wicking Centre, for providing me a scholarship over my PhD period. My PhD study was supported by JO and JR Wicking Trust (ANZ Trustees) and the National Health and Medical Research Council of Australia.

Finally, I would like to sincerely express my great thanks to my family and friends, for their understanding and support, especially my husband and my mum.

TABLE OF CONTENTS

ABBREVIATIONS

ABC	Avidin-biotin complex
AD	Alzheimer's disease
ALS	Amyotrophic lateral sclerosis
ANOVA	Analysis of variance
BSA	Bovine serum albumin
°C	Degrees Celsius
CC	Corpus callosum
CCD	Charge-coupled device
CNPase	2', 3'-cyclic nucleotide 3'-phosphodiesterase
CNS	Central nervous system
CR	Calretinin
CTX	Cortex
DAPI	4', 6-diamidino-2-phenylindole
DNA	Deoxyribonucleic acid
DPX	Di-N-Butyle Phthalate in Xylene
FTLD	Frontotemporal lobar degeneration
FUS/TLS	Fused in sarcoma/translocated in liposarcoma
g	Gram
GAP-43	Growth-associated protein 43
GAPDH	Glyceraldehyde 3-phosphate dehydrogenase
GFAP	Glial fibrillary acidic protein
HIP	Hippocampus

hnRNP	Heterogeneous nuclear ribonucleoprotein
IF	Intermediate filament
IgG	Immunoglobulin
INT	Alpha-internexin
kDa	Kilo Dalton
KO	Knockout
KSP	Lys-Ser-Pro
L	Litre
µl	Micro litre (10^{-6}l)
µm	Micrometre (10^{-6}m)
µM	Micro molar (10^{-6}M)
M	Molar
ml	millilitre
mm	millimetre
MAP	Microtubule associated protein
MBP	Myelin basic protein
miRNA	MicroRNA
mRNA	Messenger ribonucleic acid
MS	Multiple sclerosis
MT	Microtubule
NES	Nuclear export signal
NFTs	Neurofibrillary tangles
NF	Neurofilament
NF-DP	Dephosphorylated neurofilament

NF-P	Phosphorylated neurofilament
NF-H	neurofilament heavy subunit
NF-M	neurofilament medium subunit
NF-L	neurofilament light subunit
NFTP	Neurofilament triplet proteins
NIH	National Institutes of Health
NLS	Nuclear localization signal
nm	Nanometer
PBS	Phosphate buffered saline
PFA	Paraformaldehyde
PD	Parkinson's disease
PLP	Proteolipid protein
PNS	Peripheral nervous system
PVDF	Polyvinylidene fluoride
RNA	Ribonucleic acid
RRM	RNA recognition motif
SC-C	Cervical spinal cord
SC-T	Thoracic spinal cord
SC-L	Lumbar spinal cord
SDS-PAGE	Sulfate-polyacrylamide gel electrophoresis
SEM	Standard error of the mean
TBS	Tris-buffered saline
TDP-43	TAR-DNA-binding protein 43
TTL	Tubulin-tyrosine ligase
UPS	Ubiquitin proteasome system

WT	Wild-type

Chapter 1: Literature review and introduction

1.1 Overview

Abnormal accumulations and mutations of neurofilament (NF) proteins are associated with human neurodegenerative diseases, including amyotrophic lateral sclerosis (ALS), Charcot-Marie-Tooth disease, Alzheimer's disease (AD) and Parkinson's disease (PD) (reviewed in Ching and Liem, 2006; Abe et al., 2009; reviewed in Perrot and Eyer, 2009; Szaro and Strong, 2010).

Mutations in the NF genes have a close relationship with neurodegenerative diseases. For example, mutations in the NEFH gene in humans, have been identified in a small number of sporadic ALS patients (reviewed in Al-Chalabi and Miller, 2003). Mutations in NEFL gene are associated with Charcot-Marie-Tooth disease (reviewed in Liu et al., 2011). Moreover, mutations of the NF-M rod domain have occasionally been identified in early-onset PD (Lavedan et al., 2002).

Pathologically, NF abnormalites are frequent findings in many neurodegenerative conditions. For example, abnormal phosphorylation of NFs leads to their accumulation in cell bodies and has been observed in the brains of AD patients and those suffering from other neurodegenerative disorders (Rudrabhatla et al., 2011). Moreover, abnormally phoshorylated NFs which are rich in cytoskeletal NF triplet proteins (NFTPs) are accumulated in dystrophic neurites adjacent to amyloid plaques (Adalbert et al., 2009) and spheroids in proximal axons of lower motor

neurons of ALS patients (reviewed in Pasinelli et al., 2006). The accumulation of NFs is believed to arise in part from impaired axonal transport. However, it is not known if NF disruption precedes transport disruption or whether transport disruption is the cause of NF accumulation. These pathological changes may precede overt clinical symptoms (Price et al., 1998). However, it is currently unclear if axon swellings are associated with overt cell death (Adalbert et al., 2009)

The use of various mouse models provides a better knowledge of the role played by the disorganization of intermediate filaments (IFs) in the pathogenesis of neurodegenerative disorders (reviewed in Perrot and Eyer, 2009). However, the mechanisms leading to the formation of these aggregates remain elusive. In addition, previous studies have not looked at how ageing affects NF pathology, an important consideration since ageing is central to many neurodegenerative diseases. In this thesis, NF light subunit (NF-L) knockout (KO) mice, especially 12-month-old mice, were used to explore the roles of NFs in the adult and ageing in the central nervous system (CNS), the possibile capacity of the neuronal cytoskeleton to adapt to the absence of NFs and the possible role of NF dysregulation in neuropathological pathways responsible for neurodegenerative disorders.

1.2 Neuronal cytoskeleton

The neuronal cytoskeleton comprises three different components: NFs (neuronal IFs), microtubules (MTs), and microfilaments (MFs) (Figure 1.1). Because neuronal cytoskeletal structure plays a particularly prominent role in the nervous system, cytoskeletal proteins represent a large fraction of total brain protein, comprising perhaps a third or more of the total (Kirkpatrick et al., 1999).

1.2.1 NFs

NFs are a type of IFs exclusively expressed within neuronal cells, most prominently in large axons (Fliegner and Liem, 1991). IFs are components of the cytoskeleton of eukaryotic cells involved in the maintenance of cell shape, locomotion, intracellular organization, and transport (Bershadsky and Vasiliev, 1988; reviewed in Ku et al., 1999). IFs have an average diameter of 10 nm, which is between that of MFs and MTs, and consist of six distinct classes of proteins that share common structural and sequence features. These types are acidic and basic keratins (type I and II); desmin, vimentins, glial fibrillary acidic protein and peripherin (type III); NFs, alpha-Internexin (INT), syncoilin and synemins (type IV); lamins, phakinin and filensin (typeV) and nestin (type VI) (Omary et al., 2004; reviewed in Goldman et al., 2008).

1.2.1.1 The components of neuronal IF

The primary components of NFs are the NFTPs, INT and peripherin (Fliegner and Liem, 1991; reviewed in Ching and Liem, 2006). NFs are heteropolymers that are composed of NFTPs and INT in the CNS; whereas, in the peripheral nervous system

Figure 1.1 The neuronal cytoskeleton comprises three different components: microtubules, neurofilaments and microfilaments (modified from Fletcher and Mullins, 2010, review). A**,** microtubules consist of 13 protofilaments of tubulin dimers arranged in a hollow tube. B, neurofilaments have flexible polymer arms that repel neighbouring neurofilaments and determine the radius of the axon. C, actin filaments are arranged into networks with a variety or structural features, including the branched structures depicted here, which are formed by the Arp2/3 complex (blue).

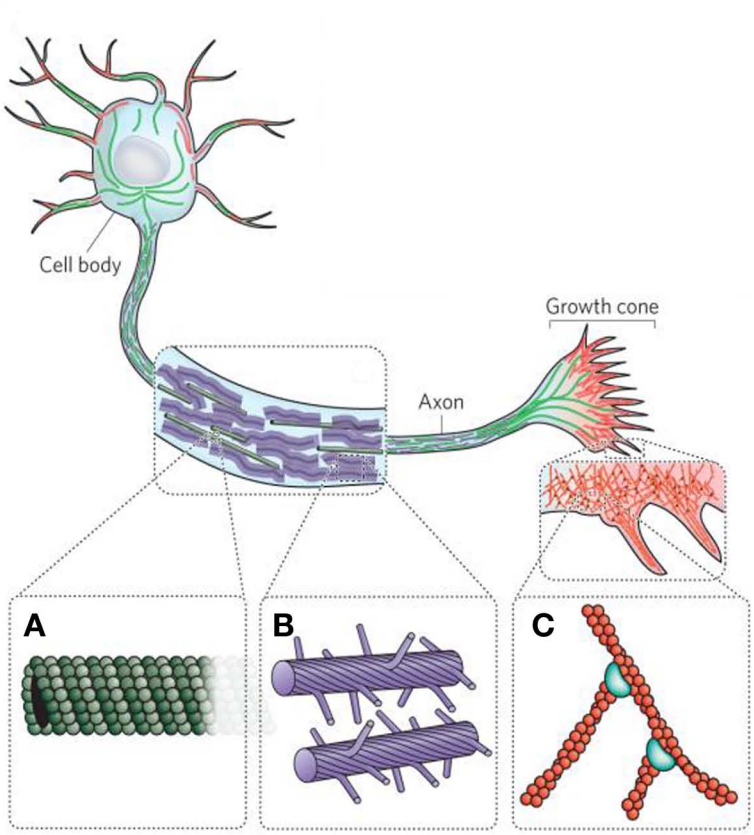
Cell body
Growth cone
Axon
A
B
C

(PNS), NFs are comprised of NFTPs and peripherin (Parysek et al., 1991; Ching and Liem, 1998; Beaulieu et al., 1999a).

NFTPs are formed from three subunit proteins: NF high-molecular-weight subunit (NF-H, 180 to 200 kDa), NF middle-molecular-weight subunit (NF-M, 130 to 170 kDa) and NF low-molecular-weight subunit (NF-L, 60 to 70 kDa) (Fliegner and Liem, 1991; reviewed in Lee et al., 1996). Mouse NF-H, NF-M and NF-L subunits are unable to self-assemble into homopolymer filaments, although human NF-L can do so *in vitro* (Carter et al., 1998). In this regard, the NFTP subunits are co-expressed throughout the neocortex (Vickers and Costa, 1992). NFTPs are expressed abundantly in both the CNS and PNS (Fliegner and Liem, 1991; reviewed inLee et al., 1996). However, it may not be that all nerve cells comprise these proteins. For example, in the cerebral cortex (CTX), NFTPs are predominantly expressed in a subpopulation of pyramidal cells of cortical layers II-VI that give rise to corticocortical connections (Vickers and Costa 1992; Hof et al. 1995; van der Gucht et al. 2007; Paulussen et al. 2011). In the rat neocortex, NFTP-immunopositive pyramidal neurons account for approximately 10-13% of all neurons (Kirkcaldie et al. 2002).

INT is found primarily in the CNS and minimally in the PNS (Kaplan et al., 1990; Fliegner et al., 1994). In the developing mammalian nervous system, INT proteins are expressed earlier and more abundantly than the NFTPs (Kaplan et al., 1990; Fliegner et al., 1994). In addition, INT upregulation in injured motoneurons suggests that INT may play a role in neuronal regeneration (McGraw et al., 2002). While peripherin is predominantly expressed in the PNS and in some neuronal populations

of the CNS, this protein also plays a role in neurite elongation during development of the nervous system (reviewed in Lariviere and Julien, 2004). Moreover, its synthesis appears necessary for axonal regeneration in the adult, but its exact function is unknown (Portier et al., 1993). It has been reported that peripherin and INT can self-assemble or co-assemble with NFTP subunits to form filamentous structures before their translocation into the axon (Cui et al., 1995; Beaulieu et al., 1999a, b).

Neurons also express other IF proteins, including nestin (200 kDa), synemin (Low, 41 kDa, Middle/beta 150 kDa or High/alpha synemin180 kDa), syncoilin (Sync1 64 kDa, Sync2 64 kDa) and vimentin (57 kDa) (Perrin et al., 2005). Some of these are developmentally regulated in neurons and may not be in adult neurons (reviewed in Guérette et al., 2007). IFs in astrocytes are primarily composed of glial fibrillary acidic protein (GFAP) (reviewed in Liem et al., 2009). Astrocyte precursors of the CNS usually express vimentin as the major IF. Astrocyte maturation is followed by a switch between vimentin and GFAP expression, with the latter being recognized as an astrocyte maturation marker (Gomes et al., 1999).

1.2.1.2 The stucture of NF

Like other IFs, NF subunits consist of a globular amino-terminal head, a highly conserved α-helical rod domain, and variable carboxy-terminal tail domains (Figure 1.2). All NF subunits (NF-H, NF-M, NF-L, INT and peripherin) share a highly conserved central rod domain of 310 amino acid residues, which is responsible for the formation of coiled-coil structures (Parry et al., 1985; Hisanaga et al., 1988; reviewed in Herrmann et al., 2009). Flanking this central rod domain are the amino-

Figure 1.2 Structure of NF proteins (adapted from Lariviere and Julien, 2004a, review). All IF subunits share a highly conserved central domain of 310 amino acid residues involved in the formation of coiled-coil structures. Flanking this central rod domain are the amino- and the carboxy-terminal domains. These two end domains present a higher degree of variability among NFs and they may confer functional specificity to the different types of NF proteins.

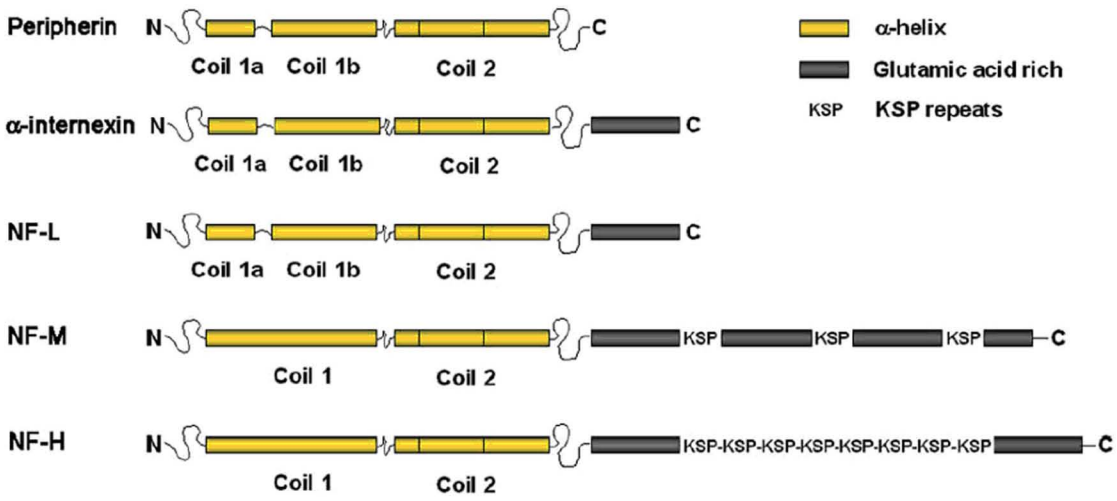
Peripherin
N
C
Coil 1a
Coil 1b
Coil 2
α-helix
Glutamic acid rich
KSP
KSP repeats
α-internexin
N
C
Coil 1a
Coil 1b
Coil 2
NF-L
N
C
Coil 1a
Coil 1b
Coil 2
NF-M
N
KSP
KSP
KSP
C
Coil 1
Coil 2
NF-H
N
KSP-KSP-KSP-KSP-KSP-KSP-KSP-KSP
C
Coil 1
Coil 2

and the carboxy-terminal domains. These two end domains present a higher degree of variability among NFs and they may confer functional specificity to the different types of NF proteins (Carpenter et al., 1996). Interestingly, the NF-M and NF-H carboxy-terminal regions contain multiple repeats of the motif Lys-Ser-Pro (KSP), which is a site for phosphorylation and accounts for the unusually high content of phosphoserine residues in these proteins (reviewed in Lariviere and Julien, 2004).

1.2.1.3 NF assembly

The current model of a 10-nm IF structure (Steinertet al., 1988; reviewed in Liu et al., 2004a) is that of two coiled-coil dimers of protein subunits that line up in a staggered fashion to form an antiparallel tetramer. Eight tetramers packed together in helical array are required to make a ropelike 10-nm filament (Figure 1.3).

However, there are features of NF assembly that differ from other types of IFs (reviewed in Liu et al., 2004a). First, NFs consists of four subunit proteins: NF-L, NF-M, NF-H and INT or peripherin (Parysek et al., 1991), whereas other IFs are either homopolymers, or heteropolymers consisting of two polypeptides. Secondly, only NFs demonstrate 4-6 nm wide sidearm structures, which correspond to the carboxy-terminal domain of the proteins. In axons, these sidearms span the intracellular space between filaments, appearing to cross-link them together (Hisanaga and Hirokawa, 1989). Because of this morphological specialization, NFs often appear parallel to one another and to the long axis of the axon. In this regard, NF spacing is widely believed to be an important determinant of axonal caliber in large myelinated axons (Hoffman et al., 1987). Thirdly, the NFTPs possess carboxy-

Figure 1.3 Schematic model of NF assembly (adapted from Liu et al., 2004a, review). In the NF assembly process, two NF subunits (NF-L, and either NF-H or NF-M) form head-to-tail coiled-coil dimers, anti-parallel half-staggered tetramers, protofilaments, and 10-nm NFs. There are ~32 molecules in the crosssection, and hyperphosphorylated side arms formed by the C-termini of NF-H and NF-M project out of the stem of the filament.

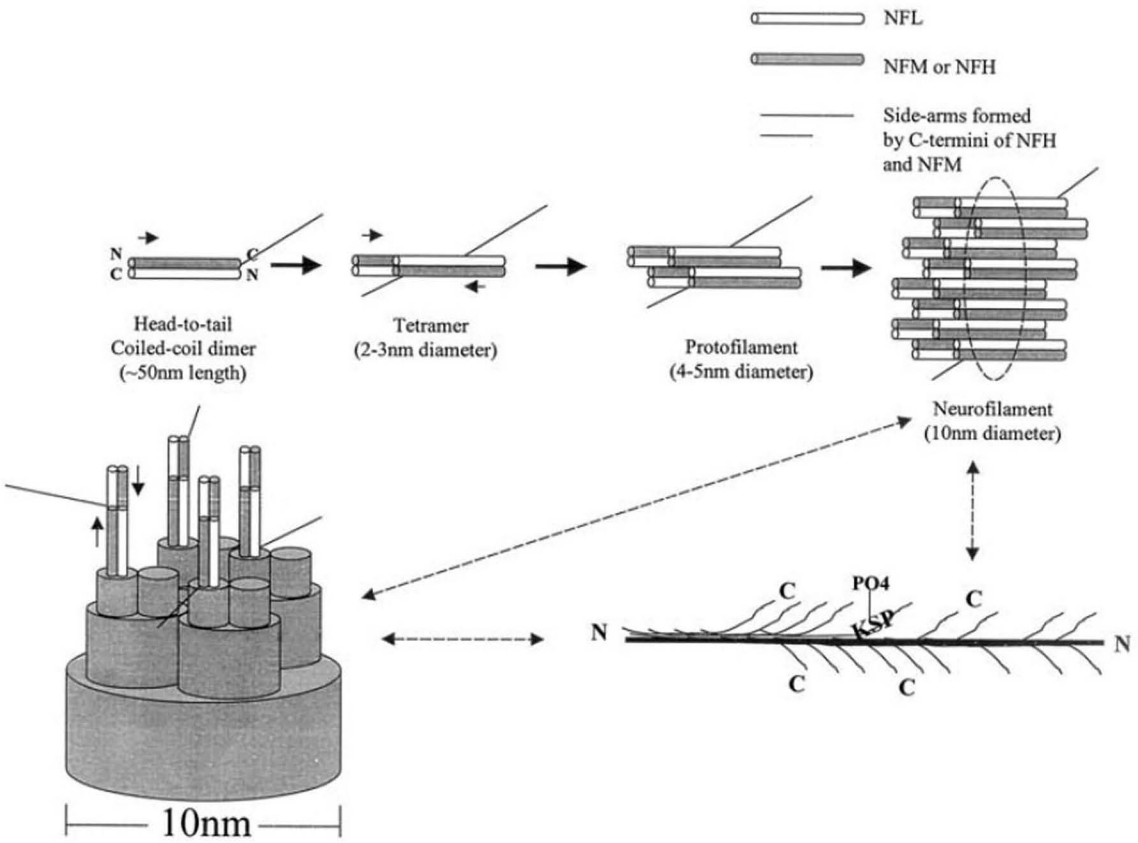
NFL
NFM or NFH
Side-arms formed
by C-termini of NFH
and NFM
N
C
C
N
Head-to-tail
Coiled-coil dimer
(~50nm length)
Tetramer
(2-3nm diameter)
Protofilament
(4-5nm diameter)
Neurofilament
(10nm diameter)
C
PO4
C
N
KSP
N
C
C
10nm

terminal tail domains that differ greatly in size and type of sequence motifs. All three NF proteins contain one or more glutamic acid-rich regions. As described earlier, NF-M and NF-H have atypically long tail domains containing multiple KSP repeats, which are phosphorylation sites (Carpenter et al., 1996). The tail domains of these two polypeptides are therefore expected to be highly charged, and are believed to provide repulsive forces that maintain NFs in an axon at finite separations (reviewed in Liu et al., 2004a).

NFTPs play important roles in NF assembly (Jones and Safinya, 2008). NF-L is essential for the precise assembly of NFs, for NF formation is believed to start with the dimerization of NF-L with either NF-M or NF-H subunits (Ching and Liem, 1993; Lee et al., 1993; Zhu et al., 1997). NF-M participates in the formation of cross-bridges, stabilization of the filament network and longitudinal extension (Elder et al., 1998a; Elder et al., 1999a, b; Jacomy et al., 1999). NF-H also contributes to the formation of cross-bridges and may interact with MTs/MFs and other cytoskeletal elements (Elder et al., 1998b; Elder et al., 1999b; Jacomy et al., 1999).

1.2.1.4 Modifications of NFs

NFs demonstrate a variety of post-translational modifications, such as phosphorylation, glycosylation and ubiquitination (reviewed in Perrot et al., 2008). The phosphorylation of the conserved KSP motifs located on the tail domain of NF-H and NF-M are the most frequent post-translational modification (Julien et al., 1981, 1982, 1983). However, phosphorylation of "non-KSP" serine residues within head domain of NF-M and NF-L has been described (Zheng et al., 2003).

Phosphorylation of the tail domain of NFs is specific for particular domains within the nerve cell, with non-phosphorylated tails predominately found in the cell bodies, with this region of the NF protein becoming highly phosphorylated in mature axons (Hashimoto et al., 2000). Phosphorylation of the tail domain can regulate both the interactions between the NF domains themselves and with MTs (Hisanaga and Hirokawa, 1989; Hisanaga et al., 1991). Tail phosphorylation is also the crucial modification that confers the resistance of NFs to proteolysis (Pant, 1988).

Phosphorylation of the head domain of NFs may play a role in maintaining the disassembled state of NFs, as head domain phosphorylation of NF-L inhibits NF assembly (Hisanaga et al., 1990a; Sihag and Nixon, 1991; Sihag et al., 1999). Phosphorylation of the NF head domain is mediated by the second messenger dependent kinases, protein kinase A and C (Sihag et al., 1988; Sihag and Nixon, 1989; Sihag and Nixon, 1990) and possibly also by Cam kinase II (Hashimoto et al., 2000). The kinases and phosphatases that are known to control phosphorylation of NFTPs are deregulated in the disease state (reviewed in Yuan et al., 2012). The accumulated NFs in neuronal perikarya and proximal axons are aberrantly phosphorylated (reviewed in Julien et al., 1999).

1.2.1.5 NF protein expression during development

Nervous system development is accompanied by a differential expression of the various NF proteins. The NFTP subunits appear early and simultaneously in central and peripheral neurons and are also expressed in mature neurons of both the CNS

and PNS (Cochard and Paulin, 1984; Ching and Liem, 1993). Initial NF-L expression is detected at the beginning of neuronal differentiation, often overlapping with INT and peripherin expression (Willard and Simon, 1983; Carden et al., 1987). The NF-M subunit is expressed shortly after with the emergence of neurite formation whereas the NF-H subunit is expressed later in neuronal differentiation during the postnatal period in mouse development (Carden et al., 1987). INT is expressed abundantly in young neurons of the developing the CNS and PNS, but in the adult it is found primarily in the central neurons (Pachter and Liem, 1985; Chien and Liem, 1994). However, in most adult peripheral nerves, INT is markedly downregulated during embryonic development to hardly detectable levels, and its disappearance from the PNS coincides with the appearance of peripherin (Escurat et al., 1990).

1.2.1.6 NF transport

NFs in most neurons are continually synthesized in the perikarya and transported along axons (Hoffman and Lasek, 1975; Black and Lasek, 1980; Willard and Simon, 1983; reviewed in Nixon, 1998a, b, c). The mechanism is known as the "Stop and Go" model of slow axonal transport, and has been extensively validated for the transport of the NFs (Brown, 2003). However, the movement of NFs is actually rapid, but unlike fast axonal transport, they pause frequently, making the overall transit rate much slower (Sunil et al., 2012).

The current understanding of NF transport is that they are transported bi-directionally in the axon along MTs through motors. The molecular motors that regulate axonal transport of NF subunits have been proposed to be the MT-based

motors, kinesin and dynein (Prahlad et al., 2000; Wagner et al., 2004), and MF-based motor myosin Va interactions with actin (Alami et al., 2009). Kinesin regulates anterograde axonal transport of NFs (Prahlad et al., 2000; Xia et al., 2003) while dynein regulates retrograde NF transport (Yabe et al., 1999; Roy et al., 2000; Wang et al., 2000). In addition, phosphorylation of NFs (mainly on NF-H) results in their dissociation from the kinesin motor, thereby decreasing their transport speed (Yabe et al., 1999).

Transport of NF subunits does not require the formation of complete NFs. Minimal requirement for axonal transport is the formation of heterodimers that involve specific NF subunits (reviewed in Yuan et al., 2012). NF-M and INT have been identified as the subunits that are crucial for the transport of dimers of NFs, as deleting both prevents transport of NF-L and/or NF-H, whereas deleting either NF-H, NF-L or both, only minimally alters NF-M or INT transport in optic axons (Yuan et al., 2003; Yuan et al., 2006a; Yuan et al., 2006b).

Studies on mouse optic nerve have led to the proposal that only a small proportion of NFs are being transported in axons and that the majority are localised to a persistently stationary and extensively cross-linked cytoskeletal network that remains fixed in place for months without movement (Li et al., 2012). Gene-targeting of KIF5A, which encodes a neuronally expressed isoform of conventional kinesin, has been found to lead to the accumulation of NF-H, NF-M, and NF-L within the cell bodies of peripheral sensory neurons (Xia et al., 2003). Moreover, inhibition of dynein activity leads to the accumulation of NFs in the axons of dynamitin-transgenic mice (LaMonte et al., 2002). The regulated action of molecular motors on

NFs can have dramatic effects on NF organization, which may have important implications for the mechanisms by which NFs accumulate normally in axons during development, and the mechanisms by which they accumulate abnormally and excessively in many neurodegenerative diseases (Li et al., 2012).

1.2.1.7 The roles of NF

In neurons, NFs exhibit an unusual degree of metabolic stability, which makes them potentially well suited for a role in stabilizing and maintaining neuronal morphology (Lasek et al., 1988). NFs have been proposed to be essential for the maintenance of axon caliber, the radial growth of axons during development and dendritic arborization (Friede and Samorajski, 1970; Ohara et al., 1993; Eyer and Peterson, 1994; reviewed in Yuan et al., 2012). However, the precise functions of NF proteins in neurons have remained elusive, also as to why neuronal subpopulations are comprised of differing sets of neuronal IF proteins.

The basic function of NF may be to support the axonal structure. NFs interact with MTs and MFs to enhance structural integrity, cell shape, and cell and organelle motility (reviewed in Liu et al., 2004a). The head domains of all NFs have a MT polymerization inhibitory domain that regulates the number of MTs in the axon (Bocquet et al., 2009). The rod domains have important roles in the polymerization of NF subunits into IFs, and serve as a binding site for the myosin Va motor protein, which modulates levels and local topography of specific vesicular organelles (endoplasmic reticulum, endosomes, synaptic vesicles) within the axoplasm (Rao et al., 2011). Loss of NF-L or myosin Va partially depletes these organelles from axons

(Rao et al., 2011).

NFs, particularly in phosphorylated forms, can regulate cellular and axonal volumes, and are primary determinants of axonal caliber in large fibers (Zhu et al., 1997). In addition, NFs play an important role in the radial growth of axons during development. Replacement of NF-M (Garcia et al., 2003; Rao et al., 2003) or both NF-M and NF-H (Garcia et al., 2003) with versions missing the C-terminal tails that extend from the filament surface and contain the KSP repeat motifs resulted in axons with diminished radial axonal growth (Garcia et al., 2003; Rao et al., 2003). However, phosphorylation of NF-M KSP repeats is not an essential component for the acquisition of normal axonal caliber mediated by myelin-dependent outside-in signaling (Garcia et al., 2009). Relatively decreased axon caliber accompanied by reduced conduction velocity has been observed in mutant Japanese quail that lack the NF-L gene (Sakaguchi et al., 1993). Normal axonal caliber but decreased conduction velocity has been observed in NF-H KO mice, indicating that NFs potentially have roles beyond being determinants of the physical dimensions of axons (reviewed in Nixon and Shea, 1992; Kriz et al., 2000). A recent report by Schulz and his colleagues suggests that Merlin-iso2 expressed in axons, mediates NF phosphorylation and axonal radial growth (Schulz et al., 2013). However, the precise mechanism by which NF protrusions regulate axonal diameter remains to be fully understood.

NFs are thought to be potential candidates for contributing to axonal outgrowth. The evidence suggesting that NF proteins might facilitate axonal elongation by stabilizing the cytoskeleton and inhibiting the retraction of long axons, comes from the injection

of anti-NF-M antibodies into *Xenopus* laevis embryos at the two-cell stage followed by the analysis of dissociated spinal cord cultures (Lin and Szaro, 1995). By the second day of axon outgrowth, the injected anti-NF-M antibodies produced shorter axons, both in intact embryos and in culture (Lin and Szaro, 1995). On average, the neurites from anti-NF-M containing neurons grow slower than the normal ones (Lin and Szaro, 1995; Walker et al., 2001).

NFs may also be required for regulating dendritic arborization. For example, a deficiency of NF-L levels in mice can cause reduction of dendritic arborization (Zhang et al., 2002). In addition, overexpression of NF-H or NF-M in mice leads to alteration in dendritic arborization (Kong et al., 1998).

1.2.2 MTs

Electron crystallography studies have demonstrated that MTs are composed of α- and β-tubulin dimers (Nogales et al., 1998). Heterodimers of α- and β-tubulin align end to end to form protofilaments, 13 of which join laterally to form a hollow tube with an outer diameter of 25 nm (Hyams et al., 1994). MTs have been regarded as essential structures for stable neuronal morphology, motility in development and neuroplasticity following injury (Bouquet et al., 2004), but new studies are highlighting their role in dynamic neuronal processes, such as the identity of axons and the dynamics of dendritic spines (Hoogenraad et al., 2009).

MT-associated proteins (MAPs) interact with MTs to regulate their stability rather than with free tubulin and maintain constant stoichiometry with the tubulin in MTs

through cycles of assembly and disassembly (reviewed in Schoenfeld and Obar, 1994). The identified MAPs have been classfied into two categories based on their molecular weights: Type I (the high-molecular-weight MAPs, >270 kDa) including MAP1A, MAP1B, MAP2A and MAP2B, and type II (the low molecular weight MAPs, 30-60 KDa) including tau proteins, MAP3, MAP4 and the molecular motors such as kinesin and dynein (Maccioni and Cambiazo, 1995; reviewed in Lace et al., 2007). Some MAPs are differentially distributed in neurons. For example, MAP1 is localised to axons and dendrites, MAP2 is present primarily in cell bodies and dendrites, and tau is enriched in axons (reviewed in Schoenfeld and Obar, 1994; Matsunaga et al., 1999). In contrast to the MAPs described above, MAP4 is not only confined to nerve cells, but also be found in all non-neuronal vertebrate cells (reviewed in Schoenfeld and Obar, 1994).

Both MAP2 and tau are able to stabilize MTs by binding to the outer surface of the tubulins to promote tubulin assembly into MTs (reviewed in Drewes et al., 1998). Misfolded tau proteins can form extremely insoluble aggregates that contribute to a number of neurodegenerative diseases (Santarella et al., 2004). Like MAP2 and tau, MAP4 can contribute to the stabilization of MTs (Santarella et al., 2004). In addition, MAP4 has been involved in the process of cell division (Permana et al., 2005). These categories of MAPs possess similar carboxyterminal amino acid sequences despite the difference in molecular weights. MAPs are primarily cytoskeleton structural components, involved in MT-dependant organization of the cytoplasm through interactions with other subcellular components (Avila et al., 2008). While MAPs regulate nucleation and stability of MTs, these may not be their primary functions. Other MAP functions include roles in MT spacing and organization,

compartmentation and interaction with other cellular structures (reviewed in Van der Vaart et al., 2009). Because they contribute to most cellular functions, MAPs are likely regulated in response to extracellular and intracellular signals (reviewed in Etienne-Manneville et al., 2010). One of the major mechanisms is the modification of the phosphorylation state of MAP proteins via changes in the relative activities of protein kinases and phosphatases within neurons. For example, the MAP2 proteins serve as substrates for most of protein kinases present in neurons and MAP2 phosphorylation is developmentally regulated (Sánchez et al., 2000). The regulation of MAP2/tau protein function in signaling networks can control the morphogenesis of neurons (Reviewed in Cassimeris and Spittle, 2001). However, the connection between signaling pathways and regulation of MT dynamics by MAPs remain obscure.

The interactions of MTs with MAPs and motor proteins are also essential for the formation and maintenance of the polarized morphology of neurons and are regulated in part by post-translational modifications of tubulin (Peris et al., 2009). Both α- and β-tubulin subunits of neuronal MTs are subject to a variety of modification (Westermann et al., 2003), such as acetylation of α-tubulin, phosporylation of β-tubulin and the tyrosination/detyronisation of α-tubulin (Mullins et al., 1994; Utreras et al., 2008).

The two best-studied post-translational modifications of tubulin are α-tubulin detyrosination and acetylation (reviewed in Luduena, 1993). Most α-tubulins are expressed with a carboxy-terminal tyrosine residue, which can be removed by tubulin carboxypeptidase and then replaced by tubulin tyrosine ligase, in a rapid

cycle that occurs on the majority of available tubulin. Since the carboxypeptidase acts only on assembled tubulin and the ligase acts on unassembled tubulin, this tyrosination/detyrosination cycle is linked to MT dynamics (Myers et al., 2006). The longer that MTs remain polymerized, the higher the content of de-Tyr-tubulin or Glu-tubulin (detyrosinated tubulin, in which the C-terminal tyrosine of α-tubulin is removed by tubulin carboxypeptidase) (Myers et al., 2006). It has been inferred that stable neuronal MTs are detyrosinated, because inhibiting the tubulin-tyrosine ligase did not alter the global dynamics of MTs (Webster et al., 1990). α-Tubulin is also acetylated at position lysine 40 (reviewed in Palazzo et al., 2003). This modification is predominantly associated with stable MTs in structures such as the axoneme (reviewed in Palazzo et al., 2003). Acetylation might affect MT stability, directly or indirectly, through the binding of plus-end proteins such as Bim1 and Bik1 (the homologs of mammalian EB1 and CLIP-170, respectively) at Glu-tubulin ends (reviewed in Schuyler and Pellman, 2001; reviewed in Palazzo et al., 2003; Blake-Hodek et al., 2010).

However, the precise mechanisms of the properties of post-translationally modified MTs have been poorly understood until recently. The identification of tubulin deacetylase, such as histone deacetylase 6, and discovery of its specific inhibitors (Matsuyama et al., 2002) has paved the way to understand the roles of acetylated MTs in kinesin-mediated axonal transport and neurodegenerative diseases. Recent work has demonstrated that detyrosination impairs MT disassembly in neurons and inhibits the activity of the neuronal depolymerizing motor KIF2A *in vitro*, which indicates that MT depolymerizing motors are directly inhibited by the detyrosination of tubulin, resulting in the stabilization of cellular MTs (Peris et al., 2006). Tubulin-

tyrosine ligase (TTL), the enzyme that catalyzes the addition of a C-terminal tyrosine residue to α-tubulin in the tubulin tyrosination cycle, is involved in tumor progression and has a vital role in neuronal organization(Peris et al., 2006). In TTL-null fibroblasts, tubulin detyrosination and cytoskeleton-associated protein glycine (CAP-Gly) protein mislocalization correlate with defects in both spindle positioning during mitosis and cell morphology during interphase (Peris et al., 2006). Studies with TTL- KO mice have shown that tyrosinated MTs are essential in normal brain development (Erck et al., 2005). The discovery of TTL-like genes encoding polyglutamylase has led to the finding that polyglutamylated MTs which accumulate during brain development are involved in synaptic vesicle transport or neurite outgrowth through interactions with motor proteins or MT-associated proteins, respectively (reviewed in Fukushima et al., 2009). However, a mechanistic explanation for the long-recognized correlation between MT stability and tubulin tyrosination remains elusive.

MTs are highly dynamic and play an important role in the elongation of axons and the guidance of growth cones (Dent et al., 2003). In neuronal growth cones, interactions between MTs and actin filaments in filopodia are necessary for growth cones turning (reviewed in Geraldo and Gordon-Weeks, 2009). Growth-cone turning is a fundamental behaviour during axon guidance, as correct navigation of the growth cone through the embryo is required for it to locate an appropriate synaptic partner (reviewed in Geraldo and Gordon-Weeks, 2009). Some studies have demonstrated that attractive growth cone turning can be initiated by localized MT stabilization in conjunction with actin dynamics (Buki and Zheng, 2002). Recent experiments suggest that microtubule-actin filament interactions might also be

important for the formation of dendritic spines from filopodia in mature neurons (reviewed in Geraldo and Gordon-Weeks, 2009).

MTs not only play a vital role during neuronal development but also modulate the post-injury sprouting response of damaged axons (Chuckowree and Vickers, 2003). However, MTs are not restricted to growth cones and can dynamically reorganize to form axon collateral branches (Dent and Kalil, 2001; Schaefer et al., 2002; Wang and Brown, 2002; Kalil and Dent, 2005). In this regard, calcium transients are proposed to play an important function in modulating MT dynamics (Dent et al., 2004; Hutchins and Kalil, 2008).

In addition, MTs play an important role in axonal transport required to maintain proper neuronal function in nerve cells. MT networks are responsible for the bi-directional (anterograde and retrograde directions) movement of membrane bound organelles along axons and dendrites (Baas et al., 2006) that is facilitated by the motor proteins—kinesin for anterograde transport (Myers et al., 2006) and dynein for retrograde transport (reviewed in Hirokawa, 1998). Kinesins move towards the MTs' plus end, while dyneins "walk" to the minus end of the MTs (Karp, 2005). Kinesins and dyneins both use the energy of ATP hydrolysis to move along the surface of MTs (Karp, 2005; Uchida et al., 2009; reviewed in Verhey and Hammond, 2009).

The C-terminal domains of NF-M and NF-H bind MTs, either directly (Hisanaga et al., 1990b; Hisanaga et al., 1991; Miyasaka et al., 1993) or using MAPs as linkers between NFs and MTs (Hirokawa et al., 1988). In addition, NF-L contain sites in its N-terminal domains able to bind un-polymerized tubulin (Berges et al., 2012). The

bi-directional motility of NFs along MTs has been reconstituted in vitro (Shah et al., 2000).

1.2.3 MFs

MFs are formed by polymerization of the monomeric globular protein—actin that are arranged like two strings of pearls intertwined into fibrils 7nm in diameter (Theriot et al., 1994). MFs play an important part in cell migration, cell adhesion, cell division, and many other essential cellular functions.

MFs are found throughout neurons and glia, but they are enriched in cortical regions of the cell near the plasmalemma and are particularly concentrated in presynaptic terminals, dendritic spines and growth cones (Kuczmarski and Rosenbaum, 1979). MFs primary role in mature neurons is as the main components of the membrane cytoskeleton (Hitt and Luna, 1994). MFs also play critical roles in growth cone motility and axon outgrowth (Dent and Gertler, 2003). The rapid remodeling of filopodia-actin-rich plasma-membrane protrusions, is required for cell migration and neurite outgrowth (reviewed in Mattila and Lappalainen, 2008). In addition, MFs are involved in the transportation of vesicles along the axon, and in their clustering at the plasma membrane sites where exocytosis takes place (Noda and Sasaki, 2008). The dense filamentous network of MFs beneath the plasma membrane is reorganized upon cell stimulation to allow the access of vesicles to fusion sites (Noda and Sasaki, 2008).

The submembrane actin cortex and/or its associated motor myosin may facilitate

axonal transport of NFs (Jung et al., 2004). Within the super family of myosin motors, myosin V is highly enriched in brain, and exists as three different isoforms in vertebrates: Myo Va, Vb and Vc (Rodriguez et al., 2002). It has been found that Myo Va binding to NF-L modulates the distribution of vesicular organelles in axons (Rao et al., 2011).

1.3 Pathology of NF

NF abnormalities including NF mutation, disregulation of protein synthesis, defective axonal transport, and abnormal phosphorylation, have been demonstrated in many human neurodegenerative diseases such as Alzheimer's disease, Amyotrophic lateral sclerosis, Pakinson's disease, Frontotemporal Lobar Degeneration and Charcot-Marie-Tooth disease (reviewed in Liu et al., 2011). Abnormal accumulation of NFs is a common hallmark of these disorders (reviewed in Yuan et al., 2012).

1.3.1 Alzheimer's disease (AD)

AD is the most common neurodegenerative disease in the elderly and is the major subtype of dementia (Sosa-Oritz et al. 2012). Patients with AD suffer from neurological dysfunctions resulting in memory loss, as well as cognitive and functional decline. AD is characterized pathologically by the formation of intracellular neurofibrillary tangles (NFTs) (Terry, 1963), extracellular deposition of amyloid plaques (reviewed in Kidd, 1964; Terry et al., 1964; Busche et al., 2008) and the loss of neurons and synapses in certain brain areas (Whitehouse et al., 1982).

NFTs consist predominantly of abnormally modified tau protein, but also contain NF proteins, ubiquitin and other cytoskeleton proteins (Perry et al., 1985; Vickers et al., 1992, 1994). Tau protein and NF proteins found in NFTs are extensively phosphorylated (Perry et al., 1987). The vulnerability of NFTs containing subpopulations of pyramidal neurons in AD has been attributed to co-expression of abnormally phosphorylated NF and tau protein revealing an interference between tau

and NF phosphorylation (Ahlijanian et al., 2000; Yang et al., 2009). It has been reported that amyloid plaques in AD can result in structural and functional disruption of neuronal networks (Kuchibhotla et al., 2008), and that the earliest stages of plaque formation are associated with dystrophic neurites principally comprised of NF proteins (Vickers et al., 1996). The evidence that NFs play a role in the pathogenesis of AD is strengthened by the finding that NF protein expression levels are altered (McLachlan et al., 1988) and phosphorylation of NF-M is increased (Deng et al., 2008) in the AD brain.

1.3.2 Amyotrophic lateral sclerosis (ALS)

ALS is a progressive, fatal neurodegenerative disease caused by the degeneration of motor neurons (Carpenter et al., 1968; Hirano et al., 1984). Intraneuronal accumulation of phosphorylated NF proteins in the perikarya and axons of degenerating motor neurons is a primary neuropathologic hallmark of ALS (Manetto et al., 1988; reviewed in Leigh et al., 1989; Murayama et al., 1992). A five-fold increase of NF-H level in cerebrospinal fluid samples of ALS patients compared to controls has been reported, suggesting NF-H level can be a marker of axonal damage (Brettschneider et al., 2006).

Pathogenic NEFH mutations have been found in a small number of sporadic and familial ALS (reviewed in Liu et al., 2004a). Four novel codon deletions and one novel insertion in the KSP region have also been detected in the tail domain of NF-H in a small number of sporadic cases of ALS (Al-Chalabi et al., 1999; Tomkins et al., 1998). These mutations would likely affect NF assembly in the neurons (Sasaki

et al., 2006) and NF transport (Yates et al., 2009).

NF-L protein is very susceptible to peroxynitrite-mediated nitration, which has been suggested as one possible mechanism of ALS pathogenesis (Crow et al., 1997). The reduced NF-L mRNA levels by up to 70% seen in degenerating neurons of ALS patients has been linked to perikaryal accumulation of NF proteins and axonal hypertrophy in motoneurons (Strong et al., 1998; Wong et al., 2000). The decline in NF-L mRNA levels associated with degenerating neurons in ALS (Bergeron et al., 1994) may contribute to increased oxidative damage of other cellular components and, therefore, may exacerbate disease progression (reviewed in Julien et al., 1999).

1.3.3 Pakinson's disease (PD)

PD is a neurodegenerative disorder, characterized by progressive degeneration of dopaminergic neurons in the substantia nigra (Trimmer et al., 2004). The major pathological hallmark of PD is the Lewy body in the degenerating neurons. Lewy bodies are an inclusion composed of numerous proteins including alpha-synuclein, NFTP subunits, ubiquitin and proteasome subunits, torsinA and parkin (Galloway et al., 1992; Trimmer et al., 2004).

Reduced protein level of NF-M and NF-L has been detected in brain of PD patients (Basso et al., 2004). NF-L mRNA is also decreased, correlating with the severity of the disease of PD (Hill et al., 1993). A 16-year-old PD patient showed a point mutation in the region of the NEFM gene coding for the rod domain 2B of NF-M protein, which results in substitution of serine for glycine at residue 336, and was

argued to disrupt NF assembly (Lavedan et al., 2002). However, this NEFM gene mutation was screened in another 322 PD patients and no further similar mutations were found (Kruger et al., 2003).

1.3.4 Frontotemporal Lobar Degeneration (FTLD)

FTLD is the second most common form of early-onset neurodegenerative dementia after AD, sharing a propensity to produce selective brain atrophy predominantly involving the temporal or frontal lobes due to deposition of pathogenic proteins (reviewed in Graff-Radford and Woodruff, 2007).

Neuronal cytoplasmic inclusions, which are ubiquitin-positive, in the neocortex, striatum and the dentate fascia of the hippocampus (HIP) are the pathological hallmarks of FTLD (Mackenzie et al., 2005). A number of different proteins such as tau, TDP-43 and FUS pathology are associated with pathological includions in FTLD (van der Zee et al., 2007). Approximately 50% of FTLD cases will present with tau pathology at post-mortem (Bugiani, 2007). TDP-43 pathology, which is described as dementia with ubiquitin positive, tau- and alpha-synuclein negative inclusions with and without motor neuron degeneration, accounts for approximately 40% of FTLD (reviewed in Lee et al., 2011). FTLD-FUS represents only 5–10% of clinically diagnosed FTLD (reviewed in Lee et al., 2011).

Several genetic mutations have been found that are the cause of FTLD and result in these pathological inclusions. A mutation in the gene encoding the progranulin protein was found to be a common cause of FTLD in families with a strong family

history (Baker et al., 2006; Mackenzie et al., 2006b). When patients have a progranulin mutation, they always have TDP-43 inclusions at autopsy (Josephs et al., 2007). Similarly, families with mutations in the gene coding for TDP-43 gene have been found to develop ALS, but so far such patients have not been found to show signs of FTLD (Lagier-Tourenne et al., 2010). In addition, mutations in the valosin containing protein gene and the gene encoding the charged multivesicular body protein have been reported in a small number of FTLD with TAR-DNA-binding protein 43 (TDP-43) positive ubiquitinated inclusions (FTLD-TDP) families (Watts et al., 2004; Skibinski et al., 2005).

1.3.5 Charcot-Marie-Tooth disease

Charcot-Marie-Tooth disease is one of the most commonly inherited disorders of the motor and sensory PNS, characterized by muscular atrophy and weakness (reviewed in Skre, 1974). CMT is classically subdivided into "primary demyelinating" forms (Charcot-Marie-Tooth disease type 1), which are defined by a characteristic reduction of nerve conduction velocity and segmental demyelination and remyelination, and "primary axonal" forms (Charcot-Marie-Tooth disease type 2) that show preservation or mild reduction of nerve conduction velocities and loss of axons (reviewed in Patzkó and Shy, 2011).

Mutations in the NEFL gene have been recently reported in many cases of Charcot-Marie-Tooth disease type 2 (Mersiyanova et al., 2000; De Jonghe et al., 2001; Georgiou et al., 2002; Jordanova et al., 2003). Aggregation of NF-L is a common pathological hallmark of motor neuron degeneration in Charcot-Marie-Tooth disease

type 2 (reviewed in Liu et al., 2011). Three hundred and thrity three Charcot-Marie-Tooth patients showed six pathogenic mis-sense mutations and one 3-base-pair in-frame deletion in the NFEL gene (Jordanova et al., 2003). To date, up to 18 NEFL mutations have been associated with axonal Charcot-Marie-Tooth disease type 2 (reviewed in Lupski et al., 2000; Gentil et al., 2012). In cell culture studies, three mutations- P22S, P8R, Q333P- in the NFEL gene (Perez-Olle et al., 2005) affected the axonal transport of both mutant and non- mutant NFs.

Ageing is the biggest risk factor for most neurodegenerative disorders. For example, AD, PD, and ALS all are ageing-related disorders. Neuritic dystrophy and synapse loss is recapitulated in mouse models of familial AD (reviewed in Duyckaerts et al., 2008) and in animal models that naturally develop amyloid pathology with ageing (Martin et al., 1991; Cummings et al., 1996). Moreover, an ageing-related decline in axonal transport may make axons particularly vulnerable in older individuals (Adalbert and Coleman, 2012). Both anterograde and retrograde axonal transport proteins decline with age (Adalbert and Coleman, 2012). It is likely then that ageing could affect many aspects of cytoskeletal structure, though less is known about how ageing affects cytoskeletal function.

1.4 TDP-43

TDP-43 protein is a 414 amino-acid heterogeneous nuclear ribonucleoprotein (hnRNP) encoded by the TARDBP gene (Ou et al., 1995), which was originally identified as a transcriptional repressor. TDP-43 is an NF-L mRNA binding protein, which can stabilize mRNA transcription and is involved in NF mRNA metabolism and transport (Strong et al. 2007). An increase in the expression of TDP-43 protein has been found in injured young NF-L KO mice (Mossie et al., 2009).

In 2006, TDP-43 was identified as the major ubiquitinated species present in the cells of the majority of patients with ALS and a number of cases of FTLD (Neumann et al., 2006). While initially thought to be relatively specific to ALS and FTLD with TDP-43 positive ubiquitinated inclusions refered as FTLD-TDP (Neumann et al., 2006), TDP-43 pathology has now been detected in a number of other neurodegenerative diseases, including AD (Uryu et al. 2008) and PD (Mosca et al. 2012). TDP-43 mislocalization from the nucleus to the cytoplasm is associated with a reduction in NF-L mRNA levels (Caccamo et al., 2009).

Evidence suggsts that neurofilament pathology results from disruption to TDP-43. Double immunofluorescence labelling revealed the detection of NF-H protein and NF-M protein in inclusion bodies with peripherin in the spinal cord of TDP-43G348C mutant mice (Swarup et al., 2011a). Moreover, it was found that NF-L protein was downregulated in the spinal cord lysates of TDP-43G348C mutant mice, a phenomenon that has also been observed in motor neurons of ALS cases (Wong et al., 2000). A decrease in NF-L protein levels may explain in part the age-related

axonal atrophy detected in TDP-43 mutant mice, and may result in a reduction of axon conduction velocity similar to that found in NF-L KO mice (Kriz et al., 2000). In large animals with long peripheral nerves, this may cause neurological disease. A loss of NFs due to a homozygous recessive mutation in the NEFL gene was recently identified to cause a severe early-onset axonal neuropathy (Yum et al., 2009).

Human TARDBP is located on chromosome 1p36 and contains 5 coding and 2 noncoding exons (Rutherford et al., 2008). The TARDBP gene is highly conserved in human, mouse, drosophila and *C elegans* (Wang et al., 2004). TDP-43 binds to both DNA and RNA and has multiple functions in transcriptional repression, pre-mRNA splicing and translational regulation (reviewed in Buratti and Baralle, 2008; Wang et al., 2008). Although it is ubiquitously expressed in all tissues, it is highly expressed in the brain and kidney (Buratti et al., 2001). It has been found that TDP-43 protein is ubiquitously expressed in the postnatal mice and rats, but is markedly decreased in the adult rodents (Huang et al., 2010). In adulthood, TDP-43 protein was even undetectable in peripheral organs including skeletal muscles, liver, and kidney, but was constantly expressed at substantial levels in the CNS (Huang et al., 2010).

1.4.1 Structure

TDP-43 has two RNA recognition motif (RRM) domains (reviewed in Buratti and Baralle, 2008) including RRM1 and RRM2 (both involved in DNA and RNA binding and protein–protein interactions), and a carboxy -terminal glycine-rich region, a bipartite nuclear localization signal (NLS) and a nuclear export signal

(NES) (Figure 1.4).

1.4.1.1 RRM domains

The RRMs contain two conserved segments: a ribonucleoprotein 2 hexapeptide sequence located at the N-terminus of the domain and a ribonucleoprotein 1 octapeptide consensus sequence (Maris et al., 2005). TDP-43 binding to other TDP-43 molecules is enhanced by the presence of an intact N-terminus and thus this domain may be important in determining TDP-43 aggregation in neurodegenerative disease (Zhang et al., 2013). RRM1 domain is the predominant functional RNA binding domain for binding to single-stranded RNA (Ou et al., 1995; Buratti et al., 2001; Wang et al., 2004). RRM2 domain has an atypical RRM-fold with an additional β-strand involved in making protein–protein interactions (Kuo et al., 2009).

1.4.1.2 C-terminal glycine-rich domain

TDP-43 interacts with other hnRNP by its C-terminal glycine-rich domain (Buratti et al., 2001). Within the nervous system, TDP-43 binds to >6,000 pre-mRNAs through this domain and affects the levels of about 600 mRNAs (Arnold et al., 2013a). Almost all ALS-associated TDP-43 mutations are dominantly inherited and located in the glycine-rich region (Lagier-Tourenne et al., 2010), suggesting that this domain drives neurotoxic effects of TDP-43.

Figure 1.4 The structure of TDP-43 protein (adapted from Lee et al, 2011, review). Numerous mutations (shown by short vertical lines) have been linked to sporadic and familial forms of ALS and FTLD (these sites are indicated by asterisks).

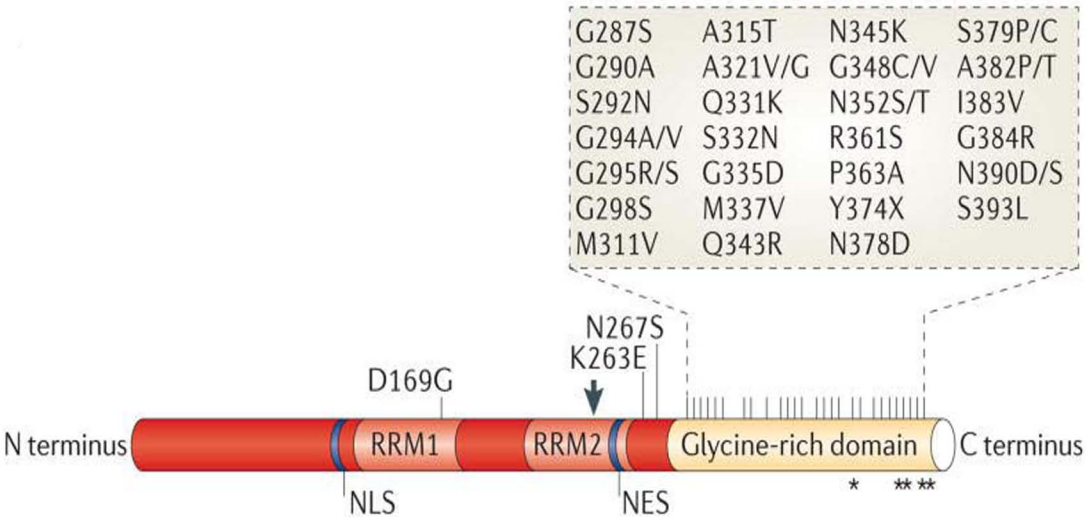
G287S
G290A
S292N
G294A/V
G295R/S
G298S
M311V
A315T
A321V/G
Q331K
S332N
G335D
M337V
Q343R
N345K
G348C/V
N352S/T
R361S
P363A
Y374X
N378D
S379P/C
A382P/T
I383V
G384R
N390D/S
S393L
N267S
K263E
D169G
N terminus
RRM1
RRM2
Glycine-rich domain
C terminus
NLS
NES
*
** **

1.4.2 Function

TDP-43, which is both a DNA and RNA-binding protein, has multiple functions (Figure 1.5) in RNA processing, including transcription, pre-mRNA splicing, and RNA metabolism (reviewed in Buratti and Baralle, 2008). TDP-43 binds to a large proportion of the transcriptome, preferentially localizing to introns (including deep intronic sites), 3′ untranslated regions and non-coding RNAs (reviewed in Buratti and Baralle, 2008).

1.4.2.1 Transcriptional repression

TDP-43 can affect mRNA stability and turnover by binding to DNA — in particular, single-stranded DNA sequences, resulting in inhibition of transcription through unknown mechanisms. For example, TDP-43 was originally identified as a transcriptional factor, repressing mRNA levels of HIV-1 gene (Ou et al., 1995), cyclin-dependent kinase 6 gene (Ayala et al., 2008), HDAC6 gene (Fiesel et al., 2010), Futsch gene (the Drosophila melanogaster homologue of MAP1B; Godena et al., 2011) and acrosomal protein SP-10 gene (Abhyankar et al., 2007).

1.4.2.2 Pre-mRNA splicing

TDP-43 is a component of hnRNP complexes that consists of mRNAs, noncoding RNAs and RNA-binding proteins (Elvira et al., 2006). HnRNP complexes are known to regulate splicing of pre-mRNA species. For example, TDP-43 acts as a splicing factor binding to the intron 8/exon 9 junction of the human CFTR gene (Buratti et al., 2001), and the intron 2/exon 3 junction of apolipoprotein A2 (APOA2) gene

Figure 1.5 The functions of TDP-43 (modified from Lagier-Tourenne et al., 2010 and Lee et al., 2011, review). TDP-43 is involved in transcriptional repression (A), pre-mRNA splicing (B), RNA metabolism (C), RNA transport and local translation (D), miRNA biogenesis (E), and acts as a component of stress granules (F).

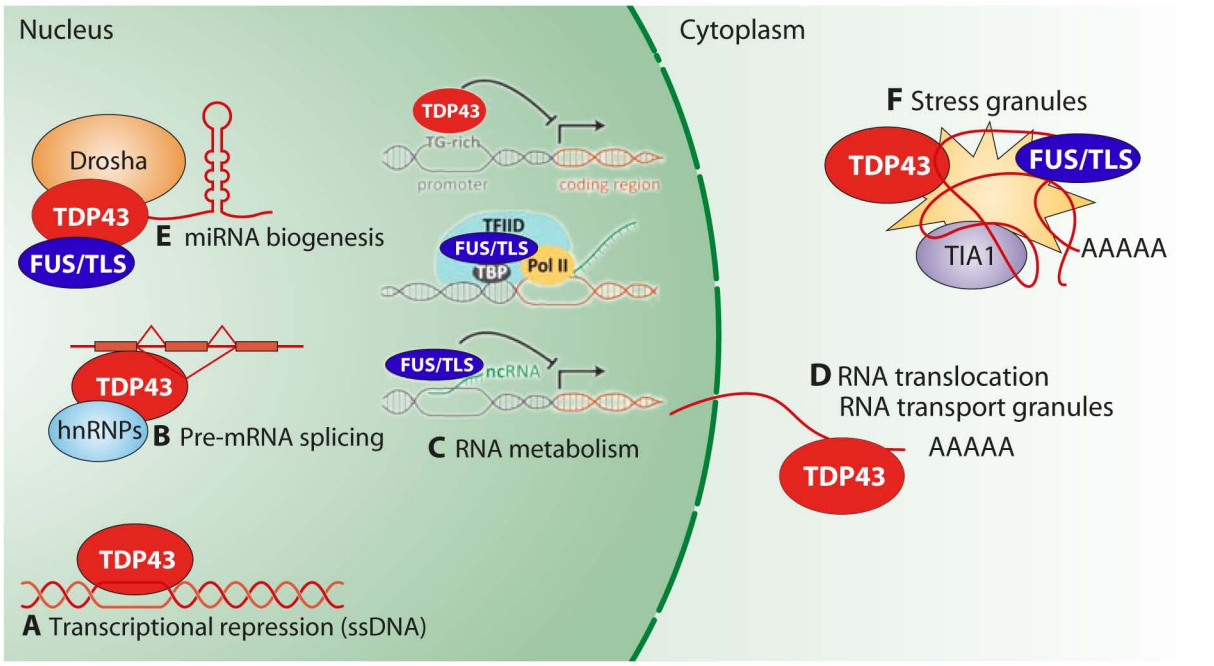
Nucleus
Cytoplasm
TDP43
TG-rich
promoter
coding region
Drosha
TDP43
FUS/TLS
E miRNA biogenesis
TFIID
FUS/TLS
TBP
Pol II
F Stress granules
TDP43
FUS/TLS
TIA1
AAAAA
TDP43
hnRNPs
B Pre-mRNA splicing
FUS/TLS
ncRNA
C RNA metabolism
D RNA translocation
RNA transport granules
AAAAA
TDP43
TDP43
A Transcriptional repression (ssDNA)

(Mercado et al., 2005) to inhibit exon splicing.

1.4.2.3 RNA metabolism

TDP-43 interacts with the RNA-binding protein FUS/TLS (fused in sarcoma/translocated in liposarcoma) and mutations in FUS have been identified as a primary cause of familial ALS (Lagier-Tourenne et al., 2010; Ling et al., 2010). FUS/TLS is involved in RNA metabolism to regulate transportation, translation and degradation of RNA (Colombrita et al., 2009; Vance et al., 2009).

The localization of TDP-43 in RNA granules within neuronal processes suggests that TDP-43 is involved in RNA trafficking (Elvira et al., 2006; Wang et al., 2008). Thus the mRNA binding properties of TDP-43 may facilitate mRNA trafficking from the nucleus to the cytoplasm as part of the biological machinery that regulates mRNA metabolism (Liu-Yesucevitz et al., 2010).

TDP-43 and FUS/TLS may additionally play roles in microRNA (miRNA) biogenesis, as they associate with drosophila and mouse miRNA processor complexes to degrade or translationally silence mRNA (Feiguin et al., 2009; Ling et al., 2010). Knockdown of TDP-43 alters the level of several miRNAs (Buratti et al., 2010). Mutations in TDP-43 and FUS/TLS lead to abnormal protein expressions (reviewed in Verma et al., 2011).

TDP-43 and FUS/TLS are also integral components of RNA stress granules under stress conditions (Wang et al., 2008; Colombrita et al., 2009; Lagier-Tourenne et al.,

2010). The role of these TDP-43-positive stress granules remains unknown, but they were proposed to mediate the stabilization and transport of the NF-L mRNA to the injury site for local translation of NF-L protein required for axonal repair (Strong et al., 2007; Moisse et al., 2009).

1.4.3 Pathology of TDP-43

1.4.3.1 Genetic mutation

The list of genes that are associated with either ALS or FTLD include TDP-43 (Gitcho et al., 2008; Sreedharan et al., 2008; Yokoseki et al., 2008), FUS (Kwiatkowski et al., 2009), copper/zinc superoxide dismutase (Deng et al. 1993), UBLN2 (Deng et al., 2011), optineurin (Maruyama et al. 2010), granulin (Baker et al., 2006; Cruts et al., 2006), valosin containing protein (Watts et al. 2004), ataxin 2 (Elden et al., 2010), sigma non-opioid intracellular receptor 1 (Al-Saif et al., 2011; Luty et al., 2010) and C9ORF72 (Dejesus-Hernandez et al., 2011; Renton, 2011). Despite the variety of genes that are implicated in ALS and FTLD, there is remarkable homogeneity in terms of downstream pathology: nearly every patient with ALS or FTLD that is linked to a genetic mutation exhibits TDP-43 pathology (reviewed in Cook et al., 2008 and Lee et al., 2011)

Pathogenic mutations in the TDP-43 gene (Figure 1.4) have been found in sporadic and familial ALS (Gitcho et al., 2008; Sreedharan et al., 2008; Yokoseki et al., 2008; reviewed in Al-Chalabi et al., 2012), FTLD (Winton et al., 2008), and recently in PD (Mosca et al., 2012), providing evidence of a direct link between TDP-43 abnormalities and neurodegeneration. Approximately 2–3% of patients affected by

sporadic and familial forms of ALS carry specific mis-sense mutations in the C-terminus of TDP-43 (Gitcho et al., 2008; Kabashi et al., 2008; Kuhnlein et al., 2008; Rutherford et al., 2008; Sreedharan et al., 2008; Van Deerlin et al., 2008; Yokoseki et al., 2008; Lemmens et al., 2009).

1.4.3.2 TDP-43 cytoplasmic inclusions in FTLD-TDP and ALS

Normally, TDP-43 protein is localized to the nucleus. However, ubiquitin-positive TDP-43 immunoreactive cytoplasmic inclusions in neurodegenerative disorders are present in the cytoplasm as well as TDP-43 inclusion in the nucleus (Neumann et al., 2006; Winton et al., 2008). Pathologic TDP-43 in the cytoplasm is present with abnormal posttranslational modifications, including phosphorylation, ubiquitination and proteolytic cleavage (reviewed in Lee et al., 2011). The reason that this occurs is not known. One possible mechanism is that the transport of TDP-43 back into the nucleus is faulty. Researchers have explored the factors that regulate the transport of TDP-43 and found that a TDP-43 nuclear transport factor (called celluar apoptosis susceptibility) is deficient in FTLD and ALS patients (Nishimura et al., 2010). In addition, it has been found that sequestration into polyglutamine aggregates causes TDP-43 to be cleared from the nucleus and become detergent-insoluble (Fuentealba et al., 2010).

The cytoplasmic ubiquitin-positive inclusions are present in the lower motor neurons and, less frequently, upper motor neurons of ALS patients (Leigh et al., 1991; Ince et al., 1998). In cases of ALS with dementia, and in some ALS patients with minor cognitive changes, ubiquitin-positive inclusions are also present in other brain

regions including the extramotor neocortex and hippocampus (Okamoto et al., 1991; Wightman et al., 1992; Mackenzie and Feldman, 2005; Geser et al., 2008). In ALS, TDP-43 inclusions were predominantly localized to the neuronal cytoplasm (Van Deerlin et al. 2008; Giordana et al. 2010), dystrophic neurites (Neumann et al., 2006), and are also found in the glial cytoplasm (Van Deerlin et al., 2008; Giordana et al., 2010).

The relative amount of inclusions in different cellular structures differs among the FTLD-TDP types (Josephs et al., 2009; Mackenzie et al., 2006a). For example, Type 1 is associated with widespread cortical and subcortical neuronal cytoplasmic inclusions, dystrophic neurites and neuronal intraneuronal inclusions, while Type 2 has predominantly dystrophic neurites in the CTX and Pick-body like neuronal cytoplasmic inclusions in the dentate fascia, amygdala and basal ganglia, and Type 3 has mainly neuronal cytoplasmic inclusion in medial temporal lobe structures and in cases with motor neuron disease, neuronal cytoplasmic inclusions in motor neurons (reviewed in Cook et al., 2008).

TDP-43 cytoplasmic inclusions observed in cell culture models of ALS appear to correspond to stress granules, which are cytoplasmic compartments composed of RNA and proteins, formed under stressful conditions to consolidate mRNA and prevent further translation of protein (Chernov et al., 2009; Colombrita et al., 2009). However, the mechanisms by which TDP-43 might associate with stress granules are unknown. In addition, it remains unclear whether aggregation of TDP-43 into inclusions is detrimental (Hanson et al., 2010), or whether cellular distress is caused by cytoplasmic expression of TDP-43 or by loss of TDP-43 from the nucleus

(reviewed in Lee et al., 2011).

1.4.3.2.1 Phosphorylation

Aberrant phosphorylation of full-length TDP-43, resulting in a product of 45 kDa, was first observed in FTLD-U and ALS brains (Neumann et al., 2006). Using rabbit polyclonal antibodies against 36 of the 64 potential phosphorylation sites within TDP-43, Hasegawa et al. (2008) determined that five Serine residues localized at the C-terminal extremity of TDP-43 were specifically phosphorylated (S379, S403, S404, S409, S410). One of the kinases responsible for the abnormal phosphorylation of TDP-43 may be casein kinase 1 (Hasegawa et al., 2008). Phosphorylation-dependent antibodies to pS409/S410 label all types of abnormal inclusions, such as dystrophic neurites, neuronal cytoplasmic and nuclear inclusions, as well as glial cytoplasmic inclusions, in various TDP-43 proteinopathies (Hasegawa et al., 2008). Importantly, antibodies against pS409/S410 fail to detect non-pathologic nuclear TDP-43 by immunohistochemistry (Hasegawa et al., 2008), providing further support that phosphorylation is a disease-specific phenomenon. By comparing the levels of labelling of "preinclusions" by these antibodies described above with anti-ubiquitin antibodies, it has also been possible to determine that phosphorylation precedes ubiquitination (reviewed in Segref and Hoppe, 2009). Phosphorylated TDP-43 proteins exhibit a longer half-life than non-phosphorylated proteins, suggesting that phosphorylation may inhibit ubiquitin proteasome system (UPS)-mediated degradation and thus contribute to aggregate formation (Zhang et al., 2010). Alternatively, as TDP-43 phosphorylation is associated with TDP-43 insolublility, it remains possible that aggregation may render TDP-43 C-terminal fragments less

vulnerable to proteasome-mediated degradation and that phosphorylation is merely a marker of aggregation (reviewed in Lee et al., 2011).

1.4.3.2.2 Ubiquitination

The UPS is the major eukaryotic protein degradation pathway, and plays a very important role in normal neuronal development, as reviewed recently by Segref and Hoppe (2009). At present, the residues involved in TDP-43 ubiquitination are still unknown although they presumably occur in the lysine residues in TDP-43. Inhibition of the UPS leads to increased levels of phosphorylated TDP-43 aggregates in cultured cells (Winton et al., 2008). Moreover, disruption of the UPS might contribute to increased levels of ubiquitinated TDP-43 in ALS and FTLD-TDP (reviewed in Lee et al., 2011).

1.4.3.2.3 C-Terminal fragments of TDP-43

25 and 35 kDa C-terminal TDP-43 fragments lacking NLS, are detected in the neurons of ALS patients and are normally absent from neurons from non-ALS cases (Igaz et al., 2011). It has been shown that these fragments are unable to regain access to the nucleus, contributing to their accumulation in the cytoplasm (reviewed in Lee et al., 2011). It has been suggested that these fragments are produced by proteolytic cleavage and derive from the activation of caspase-dependent cleavage (Zhang et al., 2007). In cell lines and primary rat neuronal cultures, the introduction of tandem repeats carrying the C-terminal Gln/Asn-rich region (residues 321-366) of TDP-43 can trigger the formation of phosphorylated and ubiquitinated aggregates (Budini et

al., 2013)

1.4.3.3 TDP-43 in AD

While TDP-43 pathology was first described in ALS and FTLD-TDP, it has now been detected in a number of other neurodegenerative diseases, such as AD (reviewed in Cook et al., 2008; Wilson et al., 2011). TDP-43 neuronal and glial inclusions have been estimated to occur in approximately 25-30% of sporadic AD cases (Uryu et al., 2008; Amador-Ortiz et al., 2007b; Kadokura et al., 2009), but perhaps lower (14%) in familial AD and Down's syndrome (Lippa et al., 2009). Pathologic forms of TDP-43, such as abnormal phospho-epitopes (Arai et al., 2009) or carboxyl-terminal epitopes, were detected in limbic regions of the brain, including the hippocampus, amygdala and adjacent cortices of AD patients (Amador-Ortiz et al., 2007a; Amador-Ortiz et al., 2007b; Uryu et al., 2008).

1.4.4 Overexpression and loss of TDP-43

It has been reported that the mRNA and protein expression of TDP-43 and NF-κB p65 are higher in the spinal cords of ALS patients than healthy individuals (Swarup et al., 2011b). Overexpression of the normal human TDP-43 gene has been shown to cause neurodegeneration in transgenic organisms from flies to mice (Li et al., 2010). This implies that aberrant accumulation of TDP-43 is toxic to vulnerable neurons and can cause ALS-like phenotypes at the cellular and organismal level (Johnson et al., 2009; Wegorzewska et al., 2009). Recent studies have identified several new molecular constituents of ALS-linked cellular aggregates, including FUS, TDP-43, OPTN, UBQLN2 and the translational product of intronic repeats in the gene

C9ORF72 (Blokhuis et al., 2013). Additionally, overexpression of WT or mutant TDP-43 in transgenic mice also can cause a neural degeneration of motor neurons without cytoplasmic TDP-43 aggregates (Wegorzewska et al., 2009; Stallings et al., 2010; Wils et al., 2010; Xu et al., 2010), which suggests an up-regulation of TDP-43 without TDP-43 cytoplasmic aggregates also can contribute to neurodegeneration by triggering pathogenic pathways via NF-κB activation (Swarup et al., 2011b).

Depletion of mouse TDP-43 in motor neurons also leads to an ALS-like neurodegenerative phenotype (Wu et al., 2010). In addition, overexpression and knockdown of TDP-43 can cause swimming defects in zebrafish (Kabashi et al., 2010). Both gain and loss of drosophila TDP-43 (dTDP-43) resulted in pupal lethality and reduced adult viability, impaired larval locomotor activity, axonal loss, and altered synaptic boutons (Feiguin et al., 2009; Li et al., 2010; Ritson et al., 2010; Lin et al., 2011; Wang et al., 2011). Both up- and down-regulated dTDP-43 directly and dramatically increased the expression of the neuronal MAP (Map205), resulting in cytoplasmic accumulations of the ecdysteroid receptor and a failure to switch Ecdysteroid receptor-dependent gene programs from a pupal to adult pattern (Vanden Broeck et al., 2013).

As decribed above, the loss-of-function and overexpression genotypes of TDP-43 were generated to study their effect on the transcriptome of the CNS, by using Drosophila melanogaster as a model. Using massively parallel sequencing, it was found that loss of TDP-43 results in widespread gene activation and altered splicing (Hazelett et al. 2012). Conversely, overexpression of TDP-43 resulted in decreased gene expression–a finding contrary to previous studies that indicated both loss-of-

function and over expression may cause ALS (Hazelett et al., 2012). Abnormal TDP-43 deposits have been found in the brains of cognitively normal elderly subjects (Arnold et al., 2013b). Additionally, NF disorganizations have been found in TDP-43 G348C mutant mice (Swarup et al., 2011a). However, It remains unclear if NF pathological alterations can also cause TDP-43 abnormalities and how this is affected by ageing.

1.5 Myelination

1.5.1 General introduction to myelination

Myelination is one of the fundamental biological processes in the development of vertebrate nervous system (Morell, 1984). Early ultrastructural investigations demonstrated that myelinated fibers develop stereotyped ratios between axon caliber, myelin thickness, and internodal distances (reviewed in Bradl and Lassmann, 2010). Myelination is associated with increases in axonal caliber, the latter which is important functionally as a determinant of neuronal conduction velocity (Arbuthnott et al., 1980). With increasing axon calibers, myelin sheaths are proportionally thicker and longer. That means, as axons increase in diameter, there is a correlated increase in sheath thickness (Windebank et al., 1985). G-ratio (axon diameter/fibre diameter; Rushton, 1951) is widely utilized as a functional and structural index of optimal axonal myelination (Chomiak and Hu, 2009). Myelin thickeness and node spacing is highly regulated and thought to be cotrolled by signalling beteween the axon and the oligodendrocytes (reviewed in Chrast et al., 2011). However, it is unclear how decreased axon calibre, which is found in many diseases, affects myelination.

Phosphorylation of NF is regulated by myelination (Starr et al., 1996). This is evidenced by the observations that NF phosphorylation is decreased in dysmyelinating mutant Trembler mice (de Waegh et al., 1992). In addition, axonal caliber is influenced by NF number (Hoffman and Griffin, 1992; Ohara et al., 1993; Eyer and Peterson, 1994) and NF spacing (Friede and Samorajski, 1970; Hoffman and Griffin, 1992). Disturbance of myelination is found to be associated with progression in many neurological diseases (Lazzarini, 2004). However, it is not clear

how this relates to NF alterations and changes in the axon.

1.5.2 Functions of myelination

The myelin sheath is an electrically insulating layer and helps to increase the speed by which information travels along the nerve (Lazzarini, 2004). Myelin sheath facilitates conduction while conserving space and energy (Waxman and Bangalore, 2004). It increases the transmission speed of the axons and also reduces ongoing energy consumption. Demyelinated axons have increased numbers of active mitochondria, suggesting higher energy consumption (Andrews et al., 2006; Campbell et al., 2011). In additon, myelination plays important roles in axonal transport (Edgar et al. 2004) and microtubule stability (Kirkpatrick et al., 2001). For example, the stability of MTs is drastically reduced in shiverer mice, a mouse line with a deletion in the myelin basic protein (MBP) gene (Kirkpatrick et al., 2001).

Myelinating oligodendrocytes are crucial for long-term axonal survival by providing metabolic support to the axons (Lee et al., 2012). Glucose is the primary energy source in the adult brain, however, when glucose levels are low, lactate from the oligodendrocytes can support the energy needs of neurons (Funfschilling et al. 2012; Lee et al. 2012). Monocarboxylate transporter 1 (MCT1), the most abundant lactate transporter in the CNS, is highly enriched in the oligodendrocytes (Funfschilling et al., 2012). Disruption of this transporter produces axon damage and neuron loss in animal and cell culture models (Lee et al., 2012). Reduced MBP and MCT1 expression are found in the ALS mouse model (Philips et al., 2013). Reduced expression of MCTs is one mechanism by which oligodendrocytes produce

neurotoxicity in patients and mouse models of ALS (Lee et al., 2012).

Demyelination can cause axonal atrophy. For example, mice with a null mutation of the myelin-associated glycoprotein (MAG) gene have a chronic atrophy of myelinated PNS axons that results in paranodal myelin tomaculi and axonal degeneration (Yin et al., 1998). However, loss of the structural proteins of compact PNS myelin-MBP does not lead to axonal atrophy (Yin et al., 1998).

1.5.3 Structure of myelin

In both CNS and PNS, myelination is a complex process in which glial cells extend processes that enwrap axons and generate compact myelin (Lazzarini, 2004). Oligodendrocytes are the glial cells that produce myelin by wrapping their process-extension of the plasma membrane around 6–10 different axons in the CNS (reviewed in Baumann and Pham-Dinh, 2001). In the CNS, myelination is characterized by proliferation and differentiation of oligodendrocyte precursors and accumulation of myelin-associated proteins and lipids (reviewed in Laule et al., 2007). In the PNS, Schwann cells enwrap single axons around segments of the axon, leaving small gaps in-between called nodes of Ranvier (Lazzarini, 2004). CNS and PNS myelin serve comparable functions and are superficially similar, but they differ in embryonic origin, genetics, composition, and ultrastructure (reviewed in Chrast et al., 2011).

1.5.4 Characteristic composition of myelin

Both CNS and PNS myelin is composed of 40% water, lipids (70-85% of the dry

mass) and protein (15-30% of the dry mass) (Martenson, 1992). The accepted view of membrane structure is that of a lipid bilayer with integral membrane proteins embedded in the bilayer and other extrinsic proteins attached to one surface or the other by weaker linkages (Martenson, 1992). Proteins and lipids are asymmetrically distributed in this bilayer, with only partial asymmetry of the lipids (reviewed in Laule et al., 2007). Figure 1.6 is the proposed molecular architecture of the layered membranes of compact myelin (reviewed in Laule et al., 2007).

1.5.4.1 Myelin basic protein (MBP) and proteolipid protein (PLP)

MBP and PLP are the two principle proteins in compact myelin of the CNS (Quarles et al., 2006). As an essential component of CNS myelin, MBP plays important roles in myelination in the CNS (Campagnoni et al., 2001). MBP comprises up to 40% of oligodendrocyte protein synthesis but is much lower in PNS (Quarles et al., 2006). The gene for MBP is on human chromosome 18 (Campagnoni et al., 2001). MBP genes from a number of species are highly conserved, and the gene can be alternatively spliced (Campagnoni et al., 2004). The MBP gene has seven exons, with the full length MBP (21.5 kDa) containing all seven exons, although this protein is one of the minor MBP proteins in myelin (Campagnoni et al., 2004). Exons 2, 5B and 6 are present or absent in four other MBP proteins found in myelin (Campagnoni et al., 2004). The most abundant MBP in human myelin contains exons 1B, 3, 4, 6 and 7 (18.5 kDa MBP), whereas, in rodent myelin, both the 18.5 kDa MBP and a 14 kDa MBP containing exons 1B, 3, 4, 5 and 7 are the most abundant (Quarles et al., 2006). Two different minor MBPs of approximately 17 kDa exist, which are encoded by exons 1B, 2, 3, 4, 5B and 7 or 1B, 3, 4, 6 and 7 respectively (Aruga et al., 1991).

Figure 1.6 The CNS myelin sheath surrounding an axon with inset depicting close up of bilayer, including myelin basic protein (MBP), PLP (proteolipid protein), 2', 3'-cyclic nucleotide 3'-phosphodiesterase (CNPase), and MAG (adapted from Laule et al, 2007, review).

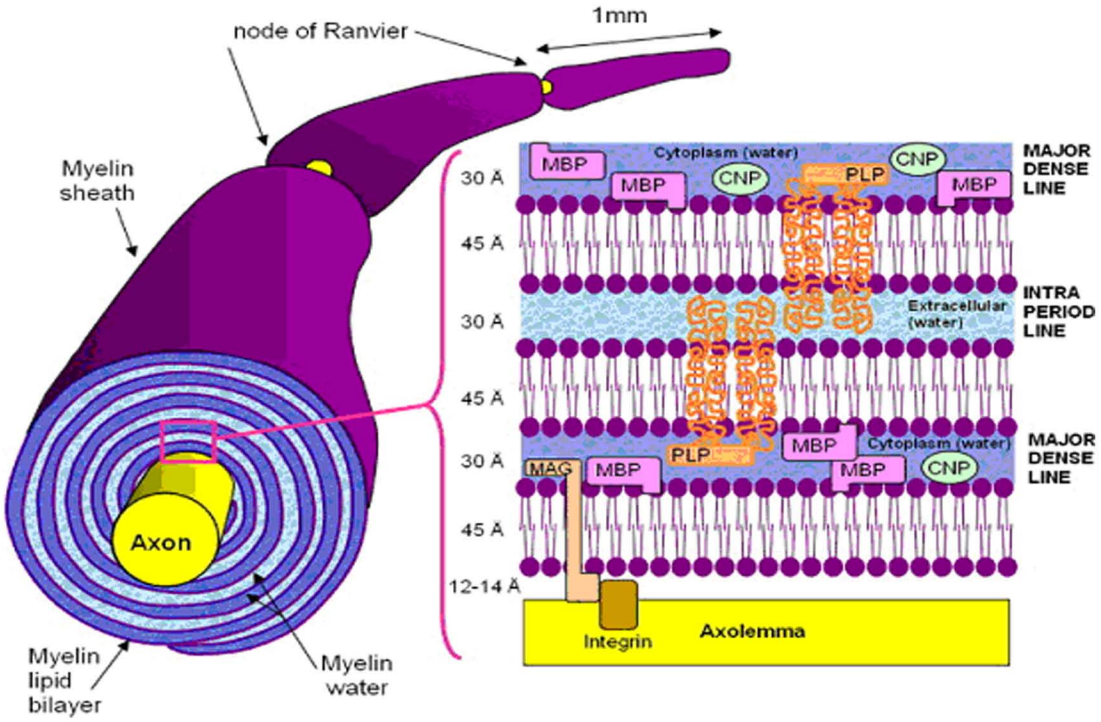
node of Ranvier
1mm
Myelin sheath
Axon
Myelin lipid bilayer
Myelin water
30 Å
45 Å
30 Å
45 Å
30 Å
45 Å
12-14 Å
Cytoplasm (water)
MBP
MBP
CNP
PLP
CNP
MBP
MAJOR DENSE LINE
Extracellular (water)
INTRA PERIOD LINE
MBP
Cytoplasm (water)
PLP
MAG
MBP
MBP
CNP
MAJOR DENSE LINE
Integrin
Axolemma

A diagrammatic representation of some of these alternative splicing schemes is presented in Figure 1.7 (Quarles et al., 2006). The ratio of the MBP changes with development, with more 14 kDa MBP found in mature rodent tissue (Campagnoni et al., 2004). MBP KO mice have showed markedly reduced MBP levels and incomplete CNS myelin sheath formation, leading to a progressive disorder characterized by tremors, seizures, and early death (Rosenbluth, 1980; Shen et al., 1985; Seiwa et al., 2002; Martin et al., 2006).

PLP is an integral membrane protein with four trans-membrane domains, comprising 50% of total myelin proteins (Lazzarini, 2004). PLP plays an important role in the formation or maintenance of the multilamellar structure of myelin (Quarles et al., 2006). Moreover, PLP is an insulator which greatly increases the velocity of axonal impulse conduction (Lazzarini, 2004). Oligodendrocytes lacking PLP are still capable of myelinating axons, although physical stability of myelin decreases, as PLP is responsible for the compaction of myelin sheaths (Boison et al., 1995). In human, point mutations in PLP are the cause of Pelizaeus-Merzbacher disease, a neurologic disorder of myelin metabolism (reviewed in Koeppen and Robitaille, 2002).

PLP and MBP differ greatly in character and sites of synthesis (reviewed in Kalwy and Smith, 1994). PLP is synthesized at the rough endoplasmic reticulum, transported to the Golgi by vesicular traffic, processed through the Golgi apparatus, and then transported to the myelin membrane. It is not entirely clear how PLP reaches its final destination, the myelin sheath (Lazzarini, 2004). MBP mRNA is, however, directly translocated to the ends of the cell processes, where it is translated

Figure 1.7 The amino acid sequences corresponding to the various mouse MBPs are encoded by a gene containing at least 11 exons (separated by introns – DNA regions whose base sequence does not code directly for proteins) (adapted from Quarles et al., 2006).

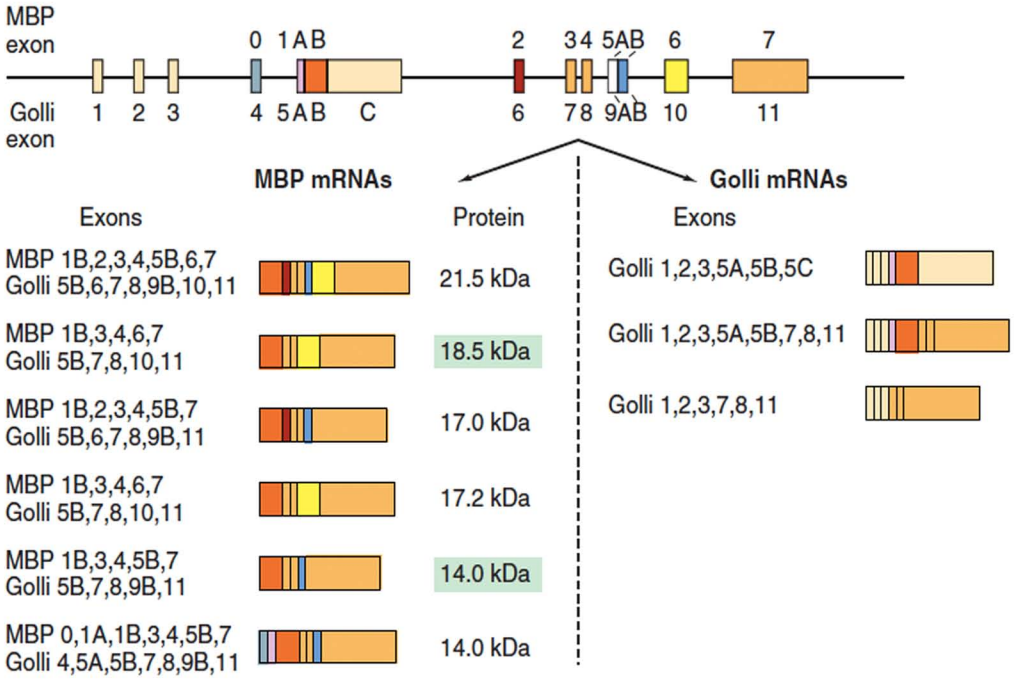
MBP exon
0 1A B
2
3 4 5AB
6
7
Golli exon
1 2 3
4 5A B C
6
7 8 9AB
10
11
MBP mRNAs
Golli mRNAs
Exons
Protein
Exons
MBP 1B,2,3,4,5B,6,7
Golli 5B,6,7,8,9B,10,11
21.5 kDa
MBP 1B,3,4,6,7
Golli 5B,7,8,10,11
18.5 kDa
MBP 1B,2,3,4,5B,7
Golli 5B,6,7,8,9B,11
17.0 kDa
MBP 1B,3,4,6,7
Golli 5B,7,8,10,11
17.2 kDa
MBP 1B,3,4,5B,7
Golli 5B,7,8,9B,11
14.0 kDa
MBP 0,1A,1B,3,4,5B,7
Golli 4,5A,5B,7,8,9B,11
14.0 kDa
Golli 1,2,3,5A,5B,5C
Golli 1,2,3,5A,5B,7,8,11
Golli 1,2,3,7,8,11

on free ribosomes and incorporated into the membrane (Brophy et al., 1993).

Although proteins responsible for compaction of CNS and PNS myelin are well characterized, less is known about proteins mediating axon–glial cell interactions in either CNS or PNS.

1.5.4.2 2', 3'-cyclic nucleotide 3'-phosphodiesterase (CNPase)

As an abundant protein in both CNS and PNS myelin, CNPase is found exclusively in the cytoplasm of oligodendrocytes and Schwann cells (Braun et al. 2004). The enzyme is distributed in single and double loose wraps of non-compact myelin (Quarles et al., 2006). Developmentally, this enzyme appears early in oligodendrocytes, earlier than most other myelin proteins (Kursula, 2008). CNPase continues to be expressed at high levels in oligodendrocytes and Schwann cells of adult animals. In various diseases, neurological mutants, and in experimental conditions in which myelin is reduced, CNPase is one of the earlier proteins to be severely reduced from the myelin (Braun et al., 2004). The enzyme itself exists in two forms in most species (three in mouse) with molecular weights of 48 and 46 kDa on Sulfate-polyacrylamide gel electrophoresis (SDS-PAGE), referred to as CNP2 and CNP1, respectively (Braun et al., 2004).

1.5.4.3 Myelin-associated glycoprotein (MAG)

MAG is a member of the I-type lectin subgroup of the Ig gene superfamily (Arquint et al., 1987; Lai et al., 1987; Salzer et al., 1987). In the CNS, MAG is present in the periaxonal membranes of myelin-forming oligodendrocytes, but it is also present in

the Schwann cell membranes of the Schmidt–Lanterman incisures, paranodal loops and the outer mesaxon (reviewed in Quarles, 2002; Georgiou et al., 2004). MAG was initially considered a potential receptor for an axonal ligand important to the initiation and progression of myelination (reviewed in Trapp, 1990). MAG is one of several neural proteins that inhibit neurite outgrowth in tissue culture and axonal regeneration *in vivo* (McKerracher et al., 1994; Mukhopadhyay et al., 1994). 60% of axonal growth cones of postnatal day 1 hippocampal neurons collapsed when they encountered polystyrene beads coated with recombinant MAG (rMAG) (Li et al., 1996). Mice with a null mutation of the MAG gene have a chronic atrophy of myelinated PNS axons that results in paranodal myelin tomaculi and axonal degeneration (Yin et al., 1998). These data suggest that MAG directly or indirectly modulates the axonal cytoskeleton and structural integrity.

1.5.5 Myelination and NFs

Although it has been well documented that NFs are essential for axons to achieve normal calibers (Cleveland et al., 1991) and that NFs are highly phosphorylated in myelinated domains (de Waegh et al., 1992; Mata et al., 1992; Garcia et al., 2003; Rao et al., 2003), the effects of altered axonal NF on myelin thickness, structure and composition remain unclear.

In HM-DKO mice, which lack genes encoding NF-H and NF-M subunits, NF content of large myelinated axons of the CNS was decreased in the absence of changes in myelin thickness and volume (Jacomy et al., 1999). In addition, mice null for NF-H achieved normal axonal calibers but conducted action potentials at

relatively reduced speeds (Rao et al., 1998; Zhu et al., 1998). In shiverer mutant mice, which lack functional MBP, CNS myelin sheath formation was markedly reduced but NF content was normal (Dyakin et al., 2010). Absence of MAG was correlated with reduced axonal calibers, decreased NF spacing, and reduced NF phosphorylation (Yin et al., 1998). These results show that although NFs play a fundamental role in axon radial growth, they do not act alone to determine the final caliber of axons (Kriz et al., 2000).

NF-L protein is important for the maintenance of normal morphology of myelinated axons. Morphological distortion and degeneration in myelinated axons were observed in the white matter region of spinal cord in 2- and 6-month old NF-L KO mice (Wu et al., 2008). The diameter of axons of upper motor neurons of NF-L KO mice decreased significantly while the thickness of their myelin sheath increases remarkably (Wu et al., 2008).

1.6 NF transgenic mice

To clarify the role of NFs in neurodegenerative diseases, the genes encoding the major NF proteins have been knocked out in mice as well as over-expressed (Table 1.1).

Table 1.1 Transgenic mouse models for NF subunit knockout or overexpression (adapted from reviewed in Liu et al., 2004a).

	NF-L –/–	NF-M –/–	NF-H –/–	NF-M/H –/–	NF-L over-expression (~4-fold)	NF-M over-expression (~2-fold)	NF-H over-expression (~1.2–4.5-fold)
Phenotype	no	no (limb show impaired, may paralyze later)	no	paralysis in hind limb	mice died before 3 weeks, motor neuron disease	no	no
Neuron degeneration, loss	no	no	no	–	yes	no	no
NF inclusion	yes, in cell body	yes	no	no	yes, massive	yes, both in cell body and axon	yes, both in cell body and axon
Axonal caliber changes	no large axons	decrease in ventral roots; 4 month decrease 35% and 2 years decrease >70%	no; smaller at the beginning but normal in adult	no large axons	increase in mediate level of NF-L; decrease in higher level	decrease 50%	decrease 50%
Axonal NF change	no NF; ~5% of normal level of NF-M/H left	<50% of NF ↓; NF-L decrease; NF-H and PO_4-NF-H increase, α-internexin decrease	NF ↓ no change; NF-M and PO_4-NF-M increase, α-internexin decrease	almost no NF; NF-L decrease to ~20% of normal level	NF accumulation	NF-H decrease	NF-M decrease
Axonal IF change	MT and GAP-43 increase	MT increase a little (1.35-fold)	MT increase ~2 fold; Tau increase; actin decrease	MT increase to 2 fold; α-internexin decrease	–	–	no
Axonal transport velocity of NF	–	increase to 2-fold	increase	increase to 2-fold	–	–	decrease >2–3-fold
Conduction velocity	decrease 70%	decrease 40%	decrease 40%	–	–	–	–
Indication	NF-L is responsible for NF formation	NF-M is more critical in axonal caliber than NF-H	NF-H is the key factor to interact with MT and actin	NF-M/H are needed for NF assembly in vivo and other key factors needed to form long-range interaction	NF-L 4-fold overexpression caused ALS-like disease; NF accumulation can cause ND directly	NF-M overexpres-sion did not cause neuron degenera-tion	NF-H 4.5-fold overexpression did not cause ND, so the slowing of transport only is not the reason for ND

1.6.1 NF knockout (KO) mice

Mice lacking NF proteins exhibit various degrees of reductions in axonal caliber and changes in spacing between the NFs (reviewed in Liem and Messing, 2009). None of the KO mouse models for NF genes developed gross developmental defects of the nervous system, which indicates that NFs are generally not required for axogenesis, or that other cytoskeletal elements may compensate for the absence of NFs. However, it is noteworthy that substantial loss of motor axons was detected in mice lacking NF-L, NF-M, or both NF-M and NF-H proteins (Zhu et al., 1997; Elder et al., 1998a, b, 1999a, b; Jacomy et al., 1999).

1.6.1.1 NF-L KO mice

Zhu et al. (1997) was the first group to generate NF-L KO mice, by using the technique of homologous recombination in embryonic stem cells in C57BL/6 mouse genetic backgrounds (Zhu et al., 1997). The NF-L KO mice developed normally and did not exhibit overt phenotypes (Zhu et al., 1997). However, NF-L KO mice have mild sensorimotor dysfunction and spatial memory deficits, but without overt signs of paresis at 6 months of age (Dubois et al., 2005). In the spinal cord of NF-L KO mice, there was decreased axon caliber, abnormal axon conductance and delayed maturation of regenerating myelinated axons (Zhu et al., 1997). Myelinated axons in NF-L KO mice exhibited a reduction of up to 50% in conduction velocity (Kriz et al., 2000). NF-L KO mice had a scarcity of IF structures and exhibited axonal hypotrophy (Zhu et al., 1997), confirming the importance of NF-L in IF assembly and in regulating axonal calibre (reviewed in Julien et al., 1999). By deleting NF-L, onset and progression of disease caused by familial ALS-linked SOD1 mutant G85R

are significantly slowed, while levels of NF-M and NF-H are markedly reduced in axons but are elevated in motor neuron cell bodies (Williamson et al., 1998). These results would be consistent with a requirement for heterodimerization of NF-L to NF-M or NF-H subunits to achieve efficient translocation into the axonal compartment (Zhu et al., 1997). In the mutant quiver quail model, the absence of NF-L leads to the "quivering" phenotype (Toyoshima et al., 2000). Recently, the first human case of a homozygous recessive mutation in NF-L has been shown to result in a severe, early-onset peripheral neuropathy with reduced numbers of myelinated fibers (Yum et al., 2009).

1.6.1.2 NF-H KO mice

Only a slight reduction in the caliber of myelinated axons has been found in the ventral roots of NF-H KO mice (Rao et al., 1998; Zhu et al. 1998), whereas the NF-H KO mice described by Elder et al. (Elder et al.1998b) exhibited a more pronounced reduction in the caliber of axons. These discrepancies may possibly be attributable to differences in the mouse genetic backgrounds. The mice from the Rao group (Rao et al., 1998) and from Julien's group (Zhu et al., 1998) were on a C57BL/6 background, whereas Elder et al. (Elder et al., 1998b) analyzed NF-H KO mice on a 129J background. However, the combined results suggest a relationship between the radial growth of axons lacking NF-H and the degree of compensatory changes in levels and/or phosphorylation of NF-L and NF-M subunits (reviewed in Julien et al., 1999).

1.6.1.3 NF-M KO mice

The lack of NF-M has a more severe effect than disruption of NF-H on the radial growth of large myelinated axons (Elder et al., 1998a, 1999a, b; Jacomy et al., 1999), which indicates that NF-M protein is more important than NF-H as mediator of axonal growth. The absence of NF-M did not cause any phenotypic changes in mice but caused an increase in NF-H level and a decrease in NF-L level (Elder et al., 1998a). The decrease of NF-L levels in NF-M KO mouse caused axonal NF content decrease of more than 50%, resulting in axonal atrophy (Elder et al., 1998a; 1999a). However, the axonal atrophy in skeletal muscles was not accompanied by significant axonal loss or anterior horn cell pathology (Elder et al., 1999a).

1.6.1.4 Double or triple NF KO mice

NF-M and NF-H double KO mice developed atrophy in ventral and dorsal roots as well as a hind limb paralysis with aging (Jacomy et al., 1999). Moreover, the disruption of both NF-M and NF-H subunits caused the sequestering of unassembled NF-L proteins in neuronal perikarya resulting in a reduction of axonal caliber equivalent to NF-L KO mice (reviewed in Lariviere and Julien, 2004).

A decrease of NF content in triple heterozygous KO mice (NF-L KO; NF-M KO; NF-H KO) shifted the calibers of large L5 ventral root axons from 5–9 to 1–5 μm (Nguyen et al., 2000).

1.6.2 Overexpression of NF in mouse models

Overexpression of NFTPs in mice can lead to neuronal dysfunction. NF inclusions, which are major hallmarks of a number of different neurodegenerative diseases, can be induced by over expression of mouse and human NFTPs in transgenic mice. Levels of expression may be important in determining the severity of the phenotypes (reviewed in Liem and Messing, 2009). NF accumulations in these mouse models can be reduced by an increase of NF-L levels (Kong et al., 1998; reviewed in Julien et al., 1998). Increasing the ratio of NF-L to NF-H and NF-M can restore the radial growth of axons (Marszalek et al., 1996; Julien et al., 1998) and normal dendritic trees in motor neurons (Kong et al., 1998). These studies prove the importance of subunit stoichiometry for correct NF protein assembly and transport (reviewed in Julien et al., 1999).

1.6.2.1 NF-L overexpressing mice

Four-fold overexpression of mouse NF-L causes striking ALS-like pathology, including intensive NF aggregation, neuronal degeneration and severe muscle atrophy (Xu et al., 1993). In addition, most of the mice died before 3 weeks post-natally with only 1/3 to 2/3 the body weight of normal mice (Xu et al., 1993). These studies confirm that NF aggregation in mice could directly cause abnormality of motor neurons (reviewed in Liu et al., 2004a).

1.6.2.2 NF-M overexpressing mice

With ~2-fold increase in expression of NF-M level in the mice, accumulations of

NFs, due to a block of transport of NFs into the axon, have been found in cell bodies and axons of ventral horn motor neurons, accompanied by decreased axonal caliber, but without neuronal degeneration and an overt functional phenotype (Cote et al., 1993; Collard et al., 1995).

1.6.2.3 NF-H over expressing mice

Overexpression of NF-H not only impairs NF transport into the axon resulting in severe perikaryal accumulation of NFs and proximal axonal swellings in motor neurons (Marszalek et al., 1996), but also inhibits dendritic arborization (Kong et al., 1998). However, NF-H over expression does not result in any overt phenotype, or neuron degeneration/loss (Marszalek et al., 1996).

In summary, these mouse models provide solid evidence for NF function: expression of NF-L is responsible for NF assembly, and NF-M/H subunits are required for NF assembly *in vivo*; NF-M is more critical for axonal growth than NF-H, and the latter may be working as a key factor for NF interaction with other cytoskeletal polymers. Transgenic mice such as NF-L KO mice, NF-H KO mice and NF-M or NF-H overexpression mice, appear to be able to survive without a substantial overt phenotype although alterations in NF can lead to cytoskeletal pathological changes similar to that seen in a number of neurodegenerative diseases (Table 1.1). However, little is known about how alterations to NFs are affected during ageing. In addition, links between NF alterations and other pathological features of neurodegenerative disease are unclear.

1.7 Project Aims

Despite an accumulating literature regarding the structure and function of NFs, the roles of NFs in neurodegenerative disease are currently poorly understood. Many studies modeling NF abnormalities in mice have been reported, in order to investigate the contribution to pathology associated with neurodegenerative disease. However, few of these studies have looked at the role of NFs with respectto apdaptive changes in the neuronal cytoskeleton, as well as in relation to myelination and NF RNA-binding proteins, in ageing or related neurodegenerative diseases. Therefore, this thesis will seek to determine the consequences of the absence of NFs on the adaptive capacity of the neuronal cytoskeleton in adulthood and ageing, the consequences on myelination and also on NF RNA-binding proteins that have been implicated in a number of neurodegenerative diseases.

AIM 1: To investigate the consequences of the absence of NF-L on the adaptive capacity of the neuronal cytoskeleton in adulthood and ageing

The NF-L subunit is considered as an obligate subunit polymer for the assembly of NFTPs into neuronal IFs (Carter et al., 1997). These triplet subunits are co-expressed in a subset of neurons throughout the brain, including a subgroup of neo-cortical pyramidal cells in many species (Vickers and Costa, 1992; Sampson et al., 1997; Kirkcaldie et al., 2002; Paulussen et al., 2011). Previous studies have shown that deletion of NF-L substantially reduced axonal NFs and resulted in NF accumulation which have been described in human neurodegenerative disease (Zhu et al., 1997; Wong et al., 2000;). However, the consequences of the absence of NFs on the adaptive capacity of the neuronal cytoskeleton in adulthood and ageing are not

known. To better understand this, this thesis has examined cytoskeletal proteins expression including phosphorylated and dephosphorylated NFs, NF-M and INT, actin, MAP2 and tubulin in the CTX of NF-L KO mice in adulthood and ageing. Additionally, this thesis has examed the density or cytoarchitectural of calretinin(CR)-immunolabelled non-pyramidal cells in the CTX of NF-L KO mice.

AIM 2: To determine the consequences of the absence of NF-L on NF RNA-binding protein--TDP-43

Recently, TDP-43, an NF-L mRNA binding protein (Strong et al., 2007), has been pathologically associated with a number of neurodegenerative diseases of ageing, such as ALS and AD (Wilson et al., 2011; Lee et al., 2012). However, mechanisms of TDP-43 pathogenesis are unknown. As TDP-43 is known to bind to NF-L mRNA, this thesis has investigated the consequences of the deficiency of NFs on TDP-43 protein. Therefore, immunohistochemical and quantitative Western blot approaches have been used to examine the changes of TDP-43 expression and distribution in the brains and spinal cords of NF-L KO mice at 10 weeks and 12 months. Additionally, this thesis has examed the the expression of phosphorylated TDP-43 in the brains and spinal cords of aged NF-L KO mice.

AIM 3 : To determine the consequences of the deletion of NF-L on myelination

NFs have a critical role in myelination by regulating axonal diameter. Additionally, MBP and PLP are important in the process of myelination of nerves in the CNS (Lazzarini 2004). Increasing evidences indicates that disturbance of myelination is found to be associated with progression of many neurological diseases (Philips et al.,

2013). However, the consequences of the deletion of NF on myelination is unclear. Therefore, this thesis has investigated the changes to myelin proteins such as MBP and PLP in the CNS of aging NF-L KO mice by using quantitative Western blot. In addition, immunofluorescence has been used to study the localization of MBP and PLP protein in the brains of aged NF-L KO mice.

Chapter 2: Materials and methods

These are the general techniques used across chapters, with specific details in individual experimental chapters.

2.1 Animals

All experiments were approved by the University of Tasmania Animal Ethics Committee, which was in accordance with the Australian Code of Practice for the Care and Use of Animals for Scientific Purposes. The mouse model used in this study was a NF-L KO mouse (Zhu et al., 1997), which was a kind gift from Dr Jean-Pierre Julien (Laval University, Canada) via the colony maintained at the Nathan Kline Institute (New York) by Dr Mala Rao. The mouse was bred on a C57Bl/6 background, which raised the interesting issue as to why the KO has a white colour rather than being black. The C57Bl/6 background of NF-L KO mice has been confirmed by genotype. The WT control mice were from a separate C57Bl/6 mouse colony and not littermates. Male mice were used at postnatal day 4 (P4), 10 weeks, 4-5 months and 12 months of age.

2.2 Immunohistochemistry and staining of mouse tissue sections

2.2.1 Transcardial perfusion and preparation of of tissue sections

Mice were anaesthetised with sodium pentobarbitone (200mg/kg, IP), and transcardially perfused with 4% paraformaldehyde (PFA) in phosphate buffer (PBS; 0.01 M, pH 7.2). The brains and spinal cords were removed and post-fixed in 4%

PFA overnight at 4°C.

Tissues were cryoprotected with 18% sucrose in PBS for 24 hours and 30% sucrose in PBS for another 24 hours at 4 °C. 40 μm coronal cryostat sections were serially collected in PBS with 0.01% NaN_3 at 4 °C.

2.2.2 Antigen retrieval

Tissue cryosections were loaded in two folded pieces of filter paper, sandwiched between two foam pads, which had been soaked in 0.01 M citrate buffer (pH 6.0). These layers were then placed in the embedding cassettes. The cassettes with tissue sections were heated on high power for six minutes in a pressure cooker (Nordic Ware, United States), then for four minutes on medium power. The tissue sections were cooled to room temperature in citrate buffer before being transferred back into 0.01 M PBS. Tissue sections were then removed from the tissue cassettes and washed three times with 0.01 M PBS for 10 minutes each at room temperature on an orbital shaker.

2.2.3 Immunofluorescence

40 μm brain or spinal cords cryostat sections were washed with 0.01 M PBS before non-specific binding sites were blocked in Serum-Free Protein Block solution (Dako, Denmark) for 20 minutes at room temperature. Primary antibodies, which recognize and bind to specific epitopes of proteins, were applied to the sections at appropriate concentrations (Table 2.1), diluted in a diluent solution (0.3% Triton-X in 0.01 M PBS), which is used to permeabilise cell membranes. Optimum concentrations were

individually determined for each antibody and control experiments, omitting primary antibodies, eliminated all immunoreactivity. Tissue sections were incubated in primary antibodies on an orbital shaker for overnight at room temperature or 4°C, followed by three 0.01M PBS washes. Species and isotype specific AlexaFluor fluorescent secondary antibodies (Molecular Probes, United States; Table 2.2) were applied at appropriate concentrations and incubated in the dark, on an orbital shaker for 2 hours at room temperature. Sections were washed three times with 0.01 M PBS, and mounted onto microscope slides and coverslipped with fluorescence mounting medium (Dako, Denmark).

Table 2.1 Primary Antibodies

Antibody	Immunogen	Source/supplier details	Working dilution		Characterization
			WB	IF	
INT	Purified recombinant rat alpha-internexin	Novus Biologicals Rabbit polyclonal NB300-139	1:5000	1:1000	Blizzard et al., 2009
NFM	Highly purified primate neurofilament proteins	AbD Serotec Rabbit polyclonal AHP246	1:5000	1:1000	Jones et al., 2008
SMI32	Homogenised hypothalami of rat dephosphorylated neurofilaments	Sternberger Mouse monoclonal SMI-32R	1:1000	1:1000	Sternberger and Sternberge, 1983
SMI312	Homogenised hypothalami of rat phosphorylated neurofilaments	Sternberger Mouse monoclonal SMI-312R	1:1000	1:1000	Woodhouse et al., 2009
CR	Purified recombinant human calretinin	Swant Rabbit polyclonal 18299	1:1000	1:1000	Schwaller et al., 1994
MAP2A and 2B	Bovine brain microtubule protein	Chemicon Mouse monoclonal MAB3418	1:1000	1:1000	Matsunaga et al., 1999
actin	N-terminal actin peptide (amino acid residues 20-33)	Sigma Rabbit polyclonal A5060	1:1000	1:1000	Haase et al., 2009
TDP-43	Purified TAR DNA binding protein	Proteintech Rabbit polyclonal 10782-2-AP	1:1000	1:500	Huang et al., 2010

pTDP-43	Purified phosphoserine 403/404 TAR DNA binding protein	Cosmo Bio Co Rabbit polyclonal TIP-PTD-P05	1:1000	1:300	Hasegawa et al., 2008
MBP	Synthetic peptide corresponding to residues 102-116 of human Myelin Basic Protein	Sigma Rabbit polyclonal M3821	1:1000	1:200	Encinas and Enikolopov, 2008
PLP	Synthetic peptide corresponding to C terminal amino acids 269-276 of mouse myelin PLP	Abcam Rabbit polyclonal ab28488	1:1000	1:1000	Karim et al., 2007
CNPase	Human purified full length native CNPase protein	Abcam Mouse monoclonal ab 6319-100	1:1000	1:1000	Wu et al., 2012
GAPDH	Purified GAPDH from skeletal muscle	Millipore Mouse monoclonal MAB374	1:10000		Evdokimovskaya et al., 2012

WB: Western blot; IF: Immunofluorecence

Table 2.2 Second antibodies

Antibody	Source	Working dilution	
		WB	IF
Goat Anti-Mouse IgG, Horseradish Peroxidase-Conjugated	Dako Goat polyclonal P0447	1:5000	
Goat Anti-rabbit IgG, Horseradish Peroxidase-Conjugated	Dako Goat polyclonal P0448	1:5000	
Alexa Fluor 488 goat anti-mouse IgG (H+L)	Molecular Probes Goat polyclonal A11029		1:1000
Alexa Fluor 546 goat anti-mouse IgG (H+L)	Molecular Probes Goat polyclonal A11030		1:1000
Alexa Fluor 488 goat anti-rabbit IgG (H+L)	Molecular Probes Goat polyclonal A11034		1:1000
Alexa Fluor 546 goat anti-rabbit IgG (H+L)	Molecular Probes Goat polyclonal A11035		1:1000
Biotinylated goat anti- mouse IgG (H+L)	VECTOR Goat polyclonal P1126		1:1000
Biotinylated goat anti-rabbit IgG (H+L)	VECTOR Goat polyclonal K0325		1:1000

2.2.4 4', 6-diamidino-2-phenylindole (DAPI) staining

Tissue sections were incubated in the dark with 0.3mM DAPI (Molecular Probes, Invitrogen, United States) in 0.01 M PBS for 20 minutes, at room temperature on an orbital shaker. Then, tissue sections were washed three times with 0.01M PBS for 10 minutes each, at room temperature in the dark on an orbital shaker.

2.2.5 3, 3'-Diaminobenzidine (DAB)- avidin-biotin complex (ABC) staining

Tissue sections were washed two times with 0.01M PBS for 10 minutes each, at room temperature on an orbital shaker. Then, tissue sections were incubated in 3% H_2O_2 in methanol for 20 minutes at room temperature. After three 0.01M PBS washes, sections were incubated in Serum-Free Protein Block solution (Dako, Denmark) for 30 minutes. Then, blocking solution was removed and sections were incubated in primary antibodies at appropriate concentrations (Table 2.1) or control overnight at room temperature, followed by four 0.01M PBS washes. Rabbit or mouse sera were used as control. Sections were incubated in species and isotype specific biotinylated second antibodies at appropriate concentrations (VECTOR Laboratories, United States; Table 2.2) on an orbital shaker for 2 hours at room temperature, followed by four 0.01M PBS washes. The Vectastain ABC Kit (VECTOR Laboratories, United States) was used for biotin amplification, according to manufacturer's instructions. After three 0.01M PBS washes, the DAB substrate kit for peroxidase (VECTOR Laboratories, United States) was used for DAB staining, according to manufacturer's instructions. DAB staining was applied for 2-10 minutes

until adequate staining intensity was obtained. After washing in water for 5 minutes, sections were post-stained with haematoxylin to label nuclei for 3 minutes. Sections were then incubated in ammoniated water for 3 minutes, followed by a water wash. After 30 minutes in xylene at room temperature, the tissue sections were coverslipped with DPX (Di-N-Butyle Phthalate in Xylene) mounting media (Sigma-Aldrich, United States).

2.3 Western blot analysis

2.3.1 Tissue preparation

WT and NF-L KO mice (n=3 or 5/group) were anaesthetized with sodium pentobarbitone (140 mg/kg sodium pentobarbitone, i.p. Virbac, Australia) and decapitated. The tissues were dissected and frozen in liquid nitrogen followed by storage at -80 °C.

2.3.2 Protein sample preparation

Proteins from the tissues of NF-L KO mice and WT controls were extracted as described previously (Klugmann et al., 1997). The protein concentration of samples was determined with Bio-Rad DC protein assay (Bio-Rad Laboratories, United States) using bovine serum albumin (BSA) as a standard. Samples were processed in triplicate.

2.3.3 Western blot

Western blots were performed as described previously (Liu et al., 2004b; Staal et al.,

2011) with modifications. Samples were separated by SDS-PAGE (15µg protein/lane; Precise 4-20% or 10% SDS Tris-Glycine gels, Thermo Fisher Scientific, United States) according to Laemmli (1970), by using the XCell SureLock™ Mini-Cell gel electrophoresis system (Invitrogen, United States). Broad range pre-stained molecular protein standards (PageRuler™ Plus; Thermo Fisher Scientific, United States) were also run on each gel to allow protein size determination. Protein gels were transferred to a polyvinylidene fluoride (PVDF) membrane (Bio-Rad Laboratories, United States), and membranes were blocked for 2 hours in 5% commercial skim milk powder dissolved in Tris-buffered saline with 0.1% Tween-20 (TBST) at room temperature on an orbital shaker. Blocked membranes were incubated overnight at 4°C in primary antibodies diluted in TBST (Table 2.1). Membranes were then washed three times in TBST at room temperature on an orbital shaker. Species-appropriate goat anti-mouse or anti-rabbit IgG coupled to horseradish peroxidase secondary antibodies (Dako, Denmark; Table 2.2) were applied and visualized with a chemiluminescent peroxidase substrate kit (Millipore, United States). Images were acquired with a Chemi-Smart 5000 Imaging System (Vilber Lourmat, Australia) equipped with Chemi-Capt 5000 software. Band intensity was measured as the sum optical density by using ImageJ software (version1.43u; NIH) and normalized to glyceraldehyde 3-phosphate dehydrogenase (GADPH).

2.4 Microscopy

Confocal images of fluorescence-labelled slides were acquired on a Zeiss LSM 510 META confocal microscope (Carl Zeiss, Germany) with Zeiss 10X (N.A. 1.0), Zeiss

20X (N.A. 1.0) and 63X (N.A. 1.0) objectives. Observation of sections labeled with Alexa Fluor 488 secondary antibody was achieved by laser excitation at a 488-nm line from an argon laser with emission detected through a 522/35-nm bandpass filter. Visualization of sections labeled with Alexa Fluor 546 secondary antibody was achieved by laser excitation at a 546-nm line from a helium neon laser with emissions detected through a 580/32-nm bandpass filter. The two fluorescence images were acquired individually by using the ZE2008 software (Carl Zeiss, Germany). Images were acquired using the same acquisition parameters for all samples and saved as 8-bit TIFF files for analysis with ImageJ software (version1.43u; NIH). For analyses, images were acquired at identical exposure settings and adjusted in an identical manner. Images for figures were prepared using Adobe Photoshop (CS5).

2.5 Motor function analysis

Motor function is mediated by several structures, starting in the CTX, brain stem and spinal cord, and terminating in skeletal muscle. To assess the locomotion function of transgenic mice, this thesis performed gait analysis, which was based on the analysis of foot prints-a very good indicator of walking stability and body balance.

Footprint test was performed as described previously (Carter et al., 1999) with modifications. Nontoxic BodyArt body/face paint (Global Colours, Australia), diluted to a thin consistency with water, was placed on the front (red) and hind (blue) paws of a restrained mouse. The mouse then walked along a 7 x 60cm strip of white paper bounded on each side by 10cm-high plastic barriers, leaving a trail of paw

prints from which various measures could be recorded. The mouse's feet were rinsed in water and dried in a tissue-lined cage; the mouse was then returned to its home cage. If the initial walk did not yield a clear set of prints, the procedure was repeated once more, and the most consistent pattern from the two attempts was used for measurement. Footprint performances were evaluated as described above with three trials per day on three consecutive days.

Parameters measured from the stride pattern test were stride length (distance between consecutive rear paw prints on the same side), hind-base width (distance between right and left hind paws), front-base width (distance between right and left front paws) and uniformity measurement (difference in placement of the hind paw compared with that of the front paw from the previous step) (Figure 2.1). From each stride pattern test strip, stride length and uniformity were measured for 3-5 consistently-spaced steps on the right and the left sides, and hind-base width and front-base width were measured for 3-5 consistently-spaced steps.

2.6 Statistical analysis

For all experiments, a minimum of three mice were utilized for quantitative analysis. Graphs were prepared in Microsoft Excel (Office 2011) or Prism (version 5.0b). Error bars represent standard errors of the mean (SEM). Significance was determined by ANOVA or t-test, and $p<0.05$ was considered as significant.

Figure 2.1 Parameters measured from footprints were stride length, hind-base width, front-base width and uniformity (adapted from Carter et al., 1999).

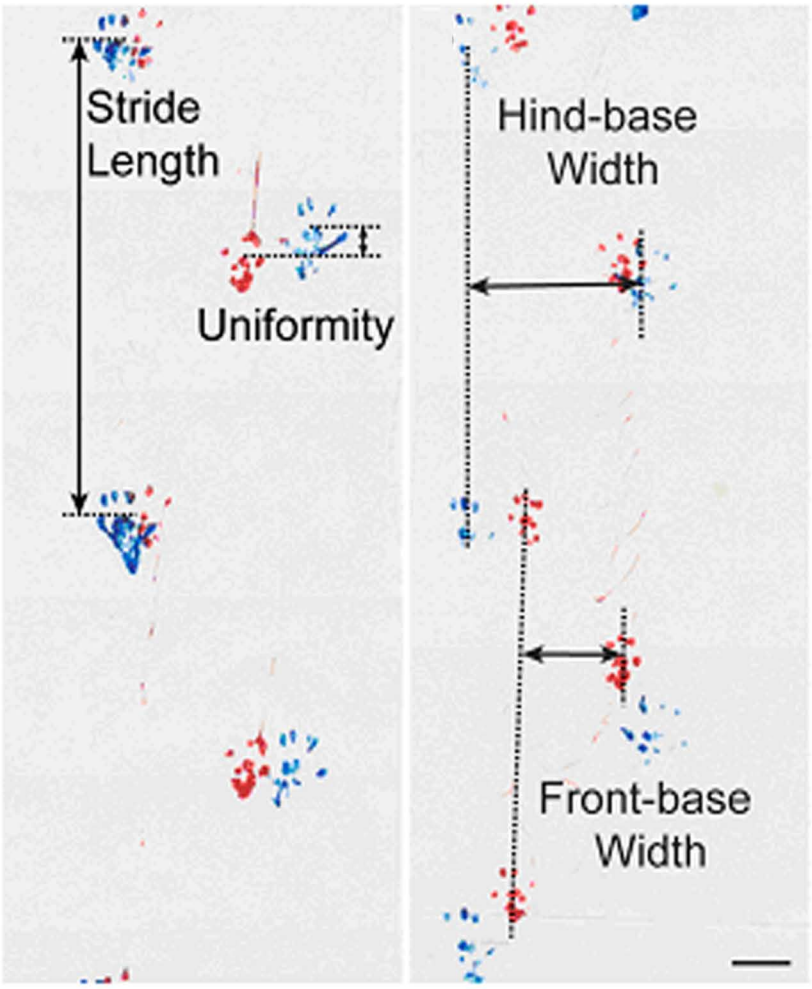
Stride
Length
Uniformity
Hind-base
Width
Front-base
Width

Chapter 3: Cytoskeletal changes during development and ageing in the CTX of NF-L KO mice

3.1 Introduction

As noted in Chapter 1, NFs play an important role in the structural integrity of neurons and in neuronal development. The mammalian NF triplet is composed of three subunit proteins: NF-H (180 to 200 kDa), NF-M (130 to 170 kDa) and NF-L (60 to 70 kDa) (Fliegner and Liem, 1991; Lee et al., 1996). These triplet subunits are co-expressed in a subset of neurons throughout the brain, including a subgroup of neocortical pyramidal cells in many species (Vickers and Costa, 1992; Sampson et al., 1997; Kirkcaldie et al., 2002; Paulussen et al., 2011). The NF triplet is also present in a subset of non-pyramidal and multipolar cortical neurons in humans (Sampson et al., 1997) and mice (Van der Gucht et al., 2007; Paulussen et al., 2011).

NF-L is the first NF triplet protein expressed during development (Benson et al., 1996), and has been purported to play a critical role in the formation of NFs by acting as the backbone on which NF-M and NF-H co-polymerise to form IFs (Carter et al., 1997).

Previous studies in the spinal cord have shown that genetic deletion of NF-L protein resulted in inhibition of dendritic growth, most dramatically in large motor neurons, mildly in medium neurons, but with no effect on small neurons (Zhang et al., 2002). From as early as 6 months of age, NF-L KO mice are characterized by mild sensorimotor dysfunction and spatial memory deficits, but without overt signs of

paresis (Dubois et al., 2005). In addition, formation of protein aggregates in motor neurons in the spinal cord has been reported in NF-L KO mice from 1 to 6 months of age (Li et al., 2006). Moreover, NF-L KO mice have been shown to mimic the reduced NF-L mRNA levels seen in ALS resulting in perikaryal accumulation of NF proteins and axonal hypotrophy in motoneurons (Wong et al., 2000). Recently, the first human case of a homozygous recessive mutation in NF-L has been shown to result in a severe, early-onset peripheral neuropathy with reduced numbers of myelinated fibers (Yum et al., 2009).

The absence of NF-L protein has been reported to result in significant reduction in levels of NF-M and NF-H proteins and increases in the levels of alpha-tubulin and GAP-43 in the CTX and sciatic nerve of adult NF-L KO mice (Zhu et al., 1997). In this thesis, relative levels and localization of cytoskeletal proteins were determined, especially NF proteins and their modified forms, in the CTX of NF-L KO mice relative to WT mice (C57Bl/6) through early postnatal development (P4), in mature animals (5 months), as well as aged mice (12 months). The effect of NF-L deletion on both cortical pyramidal and non-pyramidal cells, were investigated, the latter including a subset of cortical interneurons that are labeled for CR but lack NFTPs.

3.2 Materials and methods

3.2.1 Animals

NF-L KO mice were maintained on a C57Bl/6 background (Zhu et al., 1997). For the purposes of this study, NF-L KO mice were compared to WT mice (C57Bl/6). The control mice were from a separate C57Bl/6 mouse colony and not littermates. Male mice were used at P4, 5 months and 12 months of age, selected to be representative of young (early postnatal development), mature and aged animals. All experiments were approved by the University of Tasmania Animal Ethics Committee.

3.2.2 Tissue preparation

For Western blot studies, WT and NF-L KO mice at P4, 5 months and 12 months of age (n=5/group) were anaesthetized and decapitated as described in Section 2.3.1. Both hemispheres of the neocortex above the rhinal fissure were dissected and frozen in liquid nitrogen followed by storage at -80 °C.

For immunofluorescence studies, WT and NF-L KO mice at 5 months of age (n=5/group) were anaesthetized and transcardially perfused with 0.01M pH 7.4 PBS, followed by 4% PFA as described in Section 2.2.1. Brains were dissected and processed for 40 μm coronal cryostat sections of mouse brain, as described in Section 2.2.1.

3.2.3 Antibody characterization

The detailed information for antibodies used in this study is listed in Table 2.1.

3.2.4 Western blot

Proteins from the CTX of P4, 5 month-old and 12 month-old NF-L KO mice and WT controls (n=5 /group) were extracted as described previously (Klugmann et al., 1997). Protein concentration was determined with Protein Assay (Bio-Rad Laboratories, United States) using BSA as a standard. Proteins (15 µg) were separated by 4-20% or 10% SDS-PAGE and blotted onto a PVDF membrane (Bio-Rad Laboratories, United States) as described in Section 2.3.3. Primary antibody (Table 2.1) binding was visualized by goat anti-mouse or anti-rabbit IgG coupled to horseradish peroxidase (Dako, Denmark; Table 2.2). Immunoreactive bands were visualized and measured as described in Section 2.3.3.

3.2.5 Immunofluorescence

Free-floating 40µm brain cryostat sections were incubated overnight at 4°C with primary antibodies (Table 2.1) in diluent (0.3% Triton X-100, 0.01M PBS) as described in Section 2.2.3. Sections were then washed with 0.01M PBS and incubated with Alexa Fluor 546 conjugated to goat anti-mouse, or Alexa Fluor 488 conjugated to goat anti-rabbit IgG (Molecular Probes, United States) (Table 2.2) as described in Section 2.2.3. Sections were washed with PBS before mounting onto Fisher Super Frost Plus slides using fluorescent mounting medium (Dako, Denmark), and air-dried in the dark.

3.2.6 Image acquisition

Fluorescence-labeled sections were viewed with a Zeiss LSM 510 META confocal microscope (Carl Zeiss, Germany) and images acquired using ZEN software (Carl Zeiss, Germany) as described in Section 2.4. Digital images were compiled in Adobe Photoshop CS4 (Adobe, United States).

3.2.7 Analysis of effect of NFL deletion on non-pyramidal neurons

For analyses of calretinin immunolabelled interneurons and their laminar distribution, sections of different cortical regions (motor and sensory CTX) labeled in the same experiment, were viewed with an upright Leica fluorescent microscope (Leica Microsystems GmbH, Germany) and an Olympus digital camera (Olympus Corporation, Japan). Images were imported into Adobe Photoshop CS4 (Adobe, United States) and analyzed with ImageJ. Cortical layers were delineated based on labeling with red FluoroNissl (Molecular Probes, United States). Interneurons, immunolabelled for CR, were counted across all the layers of the motor (M1, M2) and sensory CTX (S1BF, 4 images/region/mouse, 5 NF-L KO and 3 WT mice, 5 months of age).

3.2.8 Statistical Analysis

For all experiments, a minimum of three mice was utilized for quantitative analysis. Error bars represent SEM. Significance was determined by two-way ANOVA, with Bonferroni corrections made for multiple comparisons within a single experiment. $p<0.05$ was considered significant.

3.3 Results

3.3.1 Changes to expression of intermediate filament protein expression during development

Western blot analysis of the expression of IFs in WT and NF-L KO mice showed that protein levels differed significantly between genotypes. In this experiment, each protein was analyzed using a separate 2-way ANOVA with genotype and age as factors.

• SMI 32

This antibody labels dephosphorylated epitopes of medium and heavy NF triplet, and is expressed in perikarya, dendrites, and developing axons. In CTX, WT animals showed low levels at P4, a peak at 5m and low levels at 12m; KO mice showed very low levels at all ages, significantly less than WT at P4 and 5m (Figure 3.1 A).

• SMI 312

This monoclonal antibody labels phosphorylated epitopes of medium and heavy NF triplet, and is expressed in mature axons. In WT CTX, SMI 312 labeling was complementary to SMI 32: high levels at P4, low levels at 5m and high at 12m. KO mice levels were lower at all ages: moderate levels were present at P4 and then virtually absent at 5m and 12m. The WT-KO difference was significant at P4 and 12m, but not at 5m (Figure 3.1 B).

Figure 3.1 Changes of cytoskeletal protein expression in the CTX of NF-L KO mice and their WT controls at P4, 5 months and 12 months of age (n=3). Equal amounts of brain tissue were separated on a gel and labeled with the following antibodies: SMI 32(A), SMI 312 (B), NFM (C) and INT (D). The changes of target proteins in NF-L KO mice are expressed as percentages relative to WT controls (*$p<0.001$). GAPDH served as a loading control.

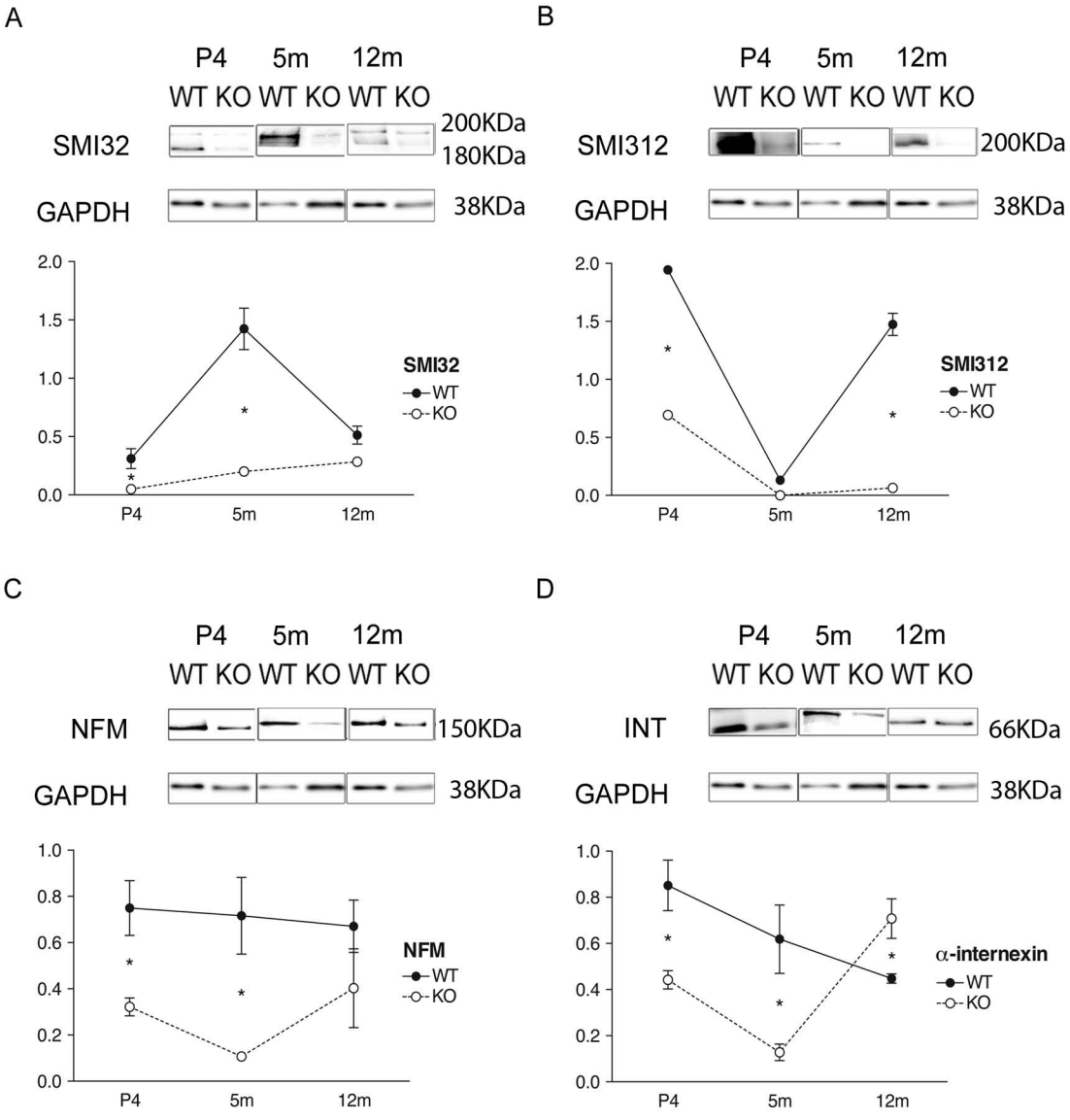
A
P4 5m 12m
WT KO WT KO WT KO
SMI32
200KDa
180KDa
GAPDH
38KDa
SMI32
WT
KO
B
P4 5m 12m
WT KO WT KO WT KO
SMI312
200KDa
GAPDH
38KDa
SMI312
WT
KO
C
P4 5m 12m
WT KO WT KO WT KO
NFM
150KDa
GAPDH
38KDa
NFM
WT
KO
D
P4 5m 12m
WT KO WT KO WT KO
INT
66KDa
GAPDH
38KDa
α-internexin
WT
KO

• NFM

This antibody labels the medium weight NF triplet regardless of phosphorylation. In the CTX of WT mice, levels were similar at P4, 5m and 12m, whereas in the KO mice levels were significantly less at P4 and 5m, but similar at 12m (Figure 3.1 C).

• INT

This antibody labels INT, a class IV neuronal intermediate filament, which has the capacity to form IFs as a homo-polymer but can also co-polymerise with NF triplet protein (Cui et al., 1995). In WT animals, INT levels declined steadily from P4 to 12m, whereas in KO mice, INT levels were significantly less at P4 and 5m, then significantly greater at 12m (Figure 3.1 D).

3.3.2 Alterations in localization of neurofilament proteins in cortical neurons of NF-L KO mice

To determine whether significant changes in total amounts of each cytoskeletal component could translate into altered processing, transport and distribution within the cell, confocal analysis of INT, NFM, phosphorylated and dephosphorylated NF (NF-P and NF-DP) immunolabeling in the sensory CTX (S1BF) of WT and NF-L KO mice at 5 months of age was undertaken. The somatosensory CTX at 5 months was selected for this study as it has been reported that, from as early as 6 months of age, NF-L KO mice were characterized by mild sensorimotor dysfunction (Dubois et al., 2005).

SMI 312 immunolabeling of nerve fibers was present in axons of cortical neurons in WT control mice (Figure 3.2 A), but substantially reduced in layer 2/3 of the CTX of NF-L KO mice (Figure 3.2 B). SMI 312 labeling was absent from cell bodies and dendrites in WT mice (Figure 3.2 A). In contrast, SMI 312 immunolabeling was occasionally localized to perikarya of cortical pyramidal neurons in layer 2/3 of the CTX of NF-L KO mice (Figure 3.2 B).There were, likewise, relatively fewer NF-M labeled neurites in layer 2/3 of the CTX of NF-L KO mice (Figure 3.3 B, D) relative to WT animals (Figure 3.3 A, C). INT-immunoreactive nerve fibers were present in the layer 2/3 of CTX of WT controls (Figure 3.4 A) and that of NF-L KO mice (Figure 3.4 B). The density of INT labeled fibers was lower in the NF-L KO mice as compared to WT control mice (Figure 3.4 A, B). SMI 32 immunolabeling was localized to cell bodies, dendrites and some thick axons in WT mice (Figure 3.5 A). However, SMI 32 immunolabeling demonstrated abnormal accumulation in the cell bodies of pyramidal neurons in layer 2/3 (data not shown) and layer 5 of the CTX of NF-L KO mice (Figure 3.5 B).

3.3.3 Changes to expression of other cytoskeletal proteins in the CTX of NF-L KO mice

Expression of other cytoskeletal proteins, such as MAP2, neuron-specific class III beta-tubulin and beta-actin, were investigated in the CTX of NF-L KO relative to WT mice by Western blot analysis (Figure 3.6 A). The expression level of MAP2 (Figure 3.6 B) and type III beta-tubulin protein (Figure 3.6 C) was significantly ($P<0.05$) increased in the CTX of NF-L KO mice at P4, 5 months and 12 months of age, as compared with WT animals. In addition, the levels of beta-actin protein

Figure 3.2 Immunofluorescence labeling for phosphorylated NFs (SMI 312) in layer 2-4 of the CTX of WT (A) and NF-L KO (B) mice at 5 months of age. Arrows indicate examples of cell bodies of pyramidal neurons. Scale bar, 50 μm.

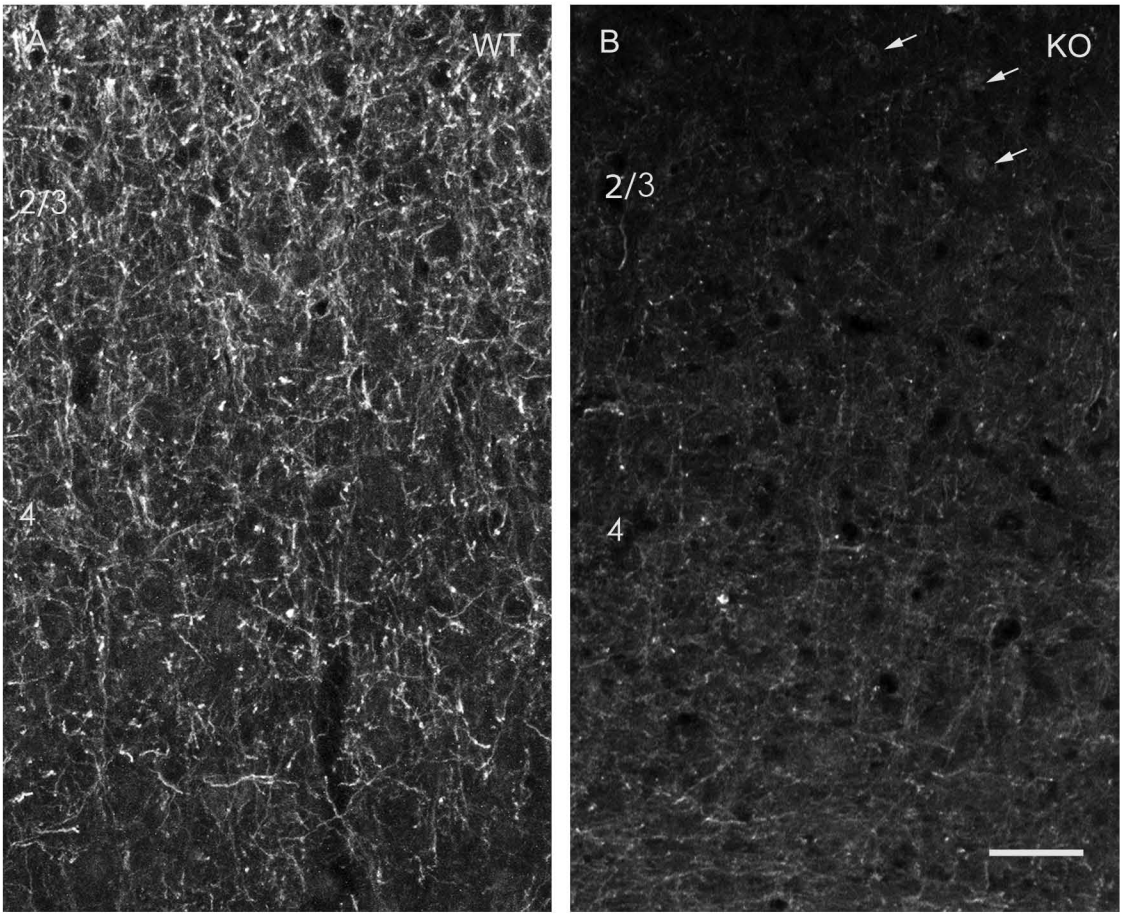
A
WT
2/3
4
B
KO
2/3
4

Figure 3.3 NFM immunolabeling in layer 2-4 (A, B) and layer 2/3 (C, D) in the CTX of WT (A, C) and NF-L KO (B, D) mice at 5 months of age. Arrows indicate examples of cell bodies of pyramidal neurons. Scale bars, A, B 50μm; C, D 20 μm.

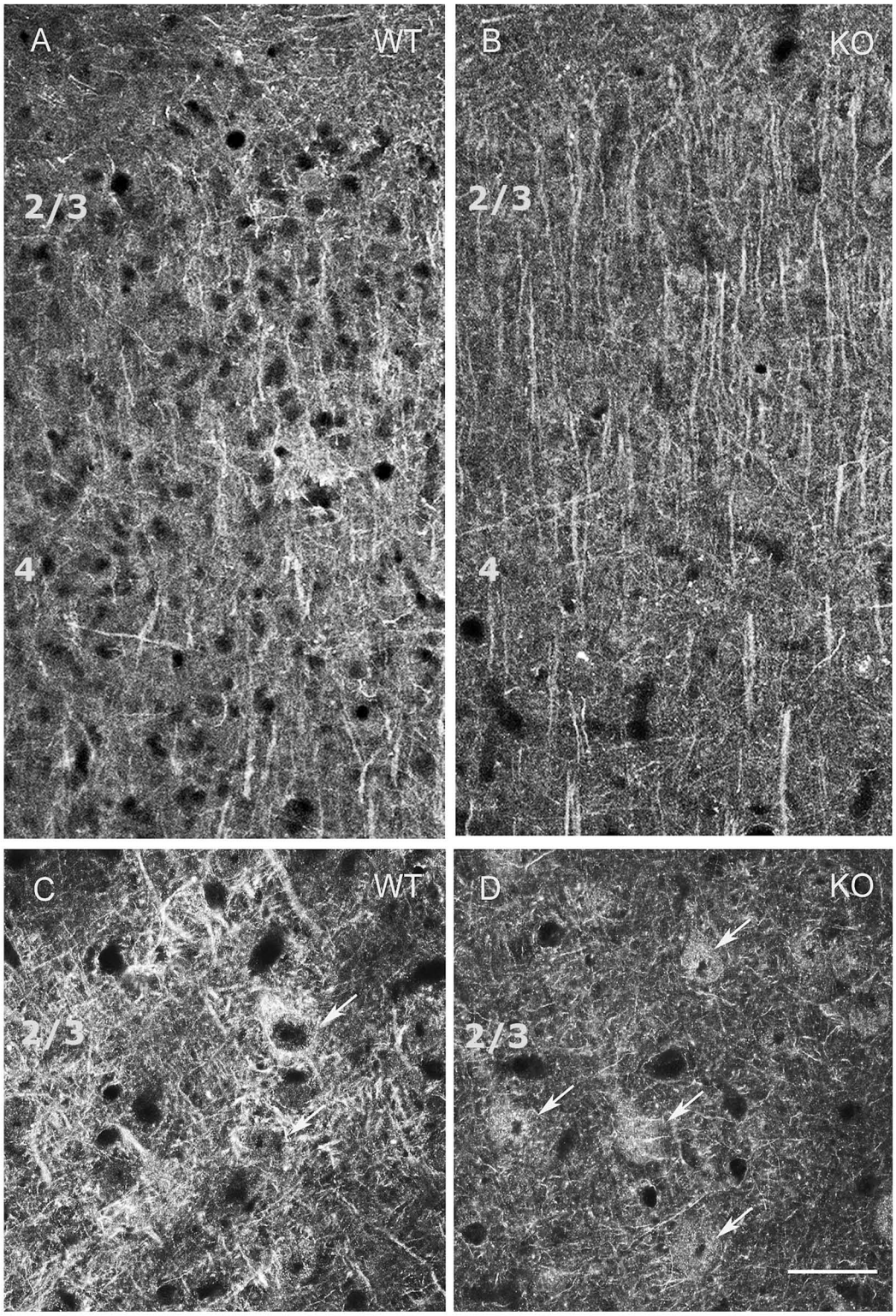
A
WT
2/3
4
B
KO
2/3
4
C
WT
2/3
D
KO
2/3

Figure 3.4 Confocal microscope images of INT labeling in layer 2-4 of the CTX from NF-L KO (B) and WT control mice (A) at 5 months of age. Scale bar, 50 μm.

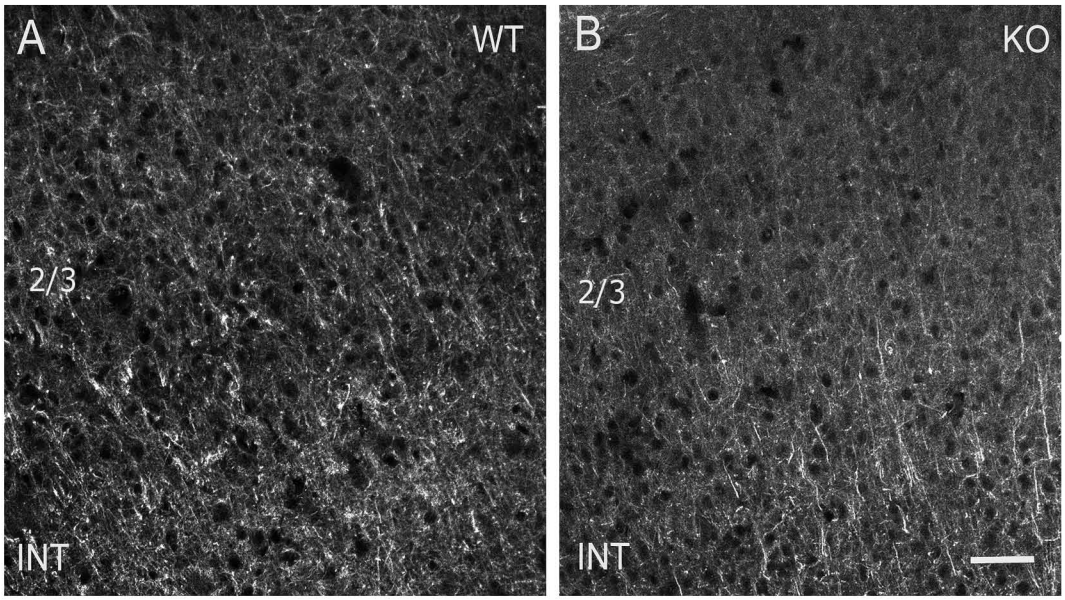
A
WT
2/3
INT
B
KO
2/3
INT

Figure 3.5 Confocal microscope images of layer 5 of the CTX immunolabeled for SMI 32 in WT (A) and NF-L KO (B) mice at 5 months of age. Arrows point to examples of cell bodies of pyramidal neurons. Scale bar, 20 μm.

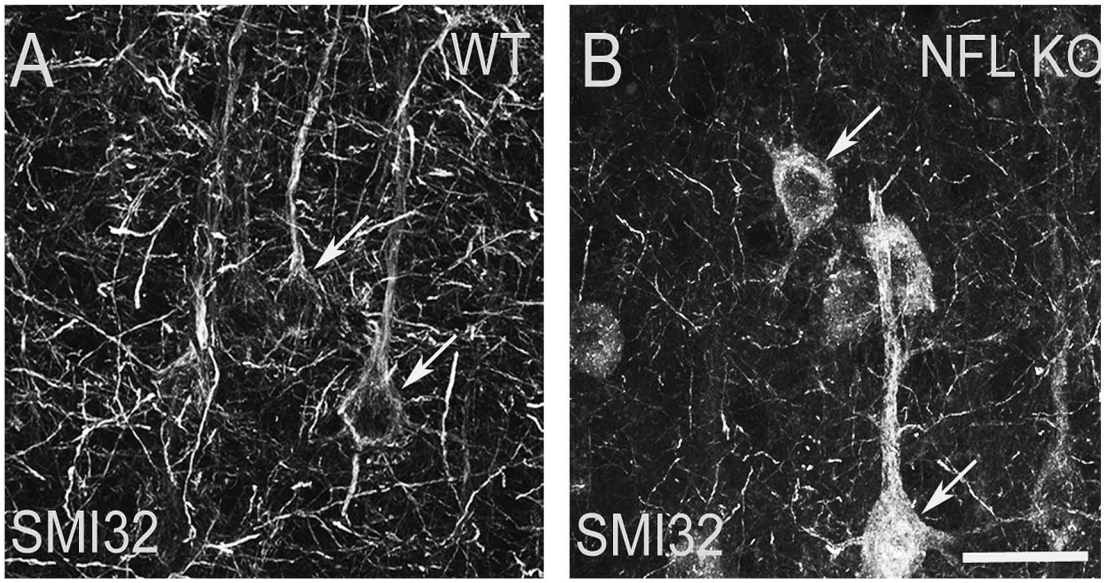
A
WT
SMI32
B
NFL KO
SMI32

Figure 3.6 Changes in MAP2, class III beta-tubulin and beta-actin expression in the cortex of NF-L KO mice compared to WT mice at P4, 5 months and 12 months of age (n=3). A: Western blot analysis of MAP2, class III beta-tubulin and beta-actin. B-D: Relative amount of the protein expression of MAP2 (B), class III beta-tubulin (C) and beta-actin (D) normalized with GAPDH respectively (*$p<0.001$). GAPDH served as a loading control.

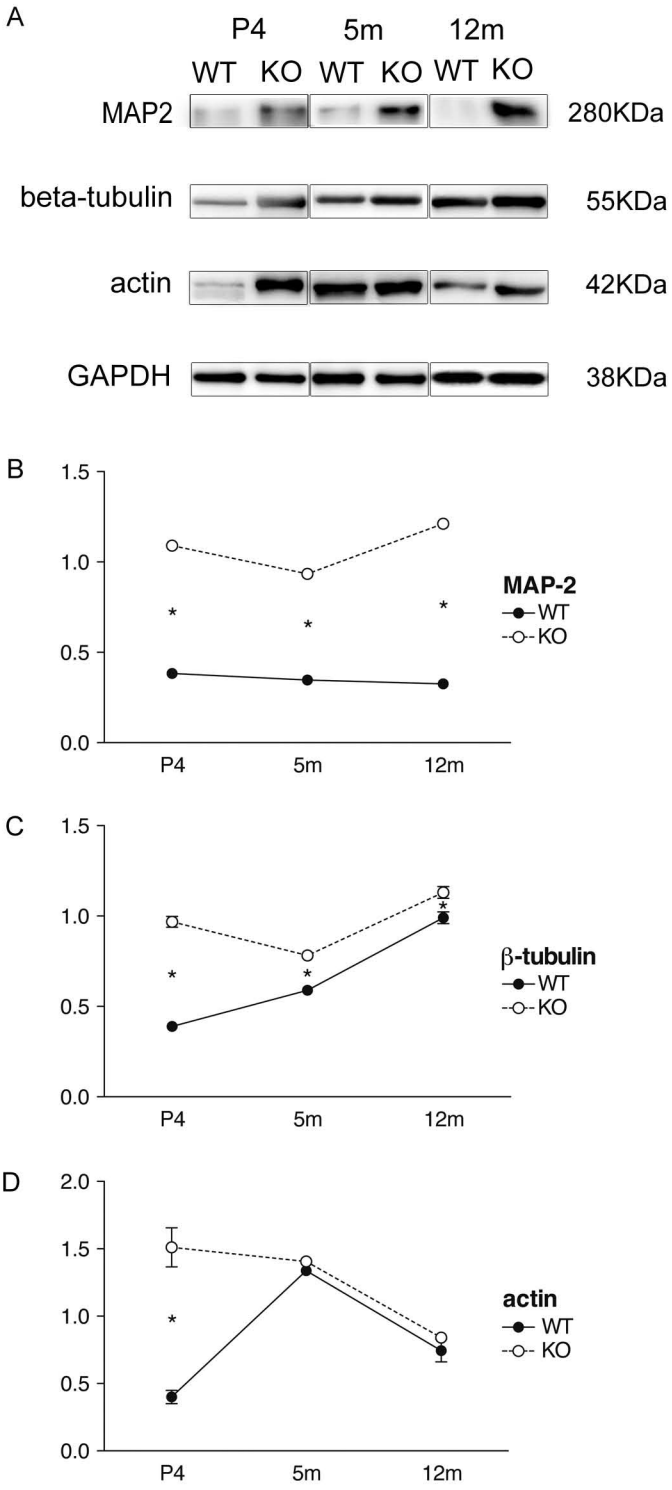
A
P4
5m
12m
WT KO WT KO WT KO
MAP2
280KDa
beta-tubulin
55KDa
actin
42KDa
GAPDH
38KDa
B
1.5
1.0
0.5
0.0
P4
5m
12m
MAP-2
WT
KO
C
β-tubulin
D
2.0
actin

(Figure 3.6 D) were significantly ($P<0.05$) increased in the CTX of NF-L KO mice at P4.

3.3.4 Analysis of the effect of NF-L deletion on non-pyramidal neurons

To investigate the effect of NF-L deletion on non-pyramidal cells, CR labeling was used to identify a subset of inhibitory neurons (interneurons) that do not contain NFTPs. The distribution of CR labeled neurons was also used to assess broad cytoarchitectural changes with respect to cell location between WT and NF-L KO mice.

First, the expression of CR in the CTX of NF-L KO mice was analyzed by Western blotting (Figure 3.7 A, B). Compared with WT controls, CR protein levels in NF-L KO mice were significantly reduced at both P4 and 12 months of age ($p<0.01$ and $P<0.001$, respectively; Figure 3.7 B).

The distribution of CR-positive neurons across cortical layers at 5 months was investigated to assess whether the distribution of non-NF triplet-containing neurons was altered by the cytoskeletal changes observed. S1BF and M1/M2 were chosen for analysis because they are adjacent to each other in the CTX, but differ noticeably in their NF triplet-labeling pattern (Paulussen et al., 2011), suggesting that any architectonic effects of NF-L deletion would differ between them. Counts of CR-positive neurons in each cortical layer for S1BF (sensory CTX) and M1/M2 (motor CTX) were analyzed using two-way ANOVA. For both regions, the counts of CR-positive neurons differed significantly between cortical layers ($p < 0.0001$; Figure

Figure 3.7: Analysis of effect of NF-L deletion on non-pyramidal neurons. A: Western blot analysis of calretinin protein in the cortex from NF-L KO mice and their WT controls at P4, 5 months and 12 months of age (n=3). GAPDH served as a loading control. B: Relative changes in CR protein in NF-L KO mice compared with WT controls (*$p<0.01$). C, D: Distribution of interneuron population with CR marker in adult motor (C) and sensory cortex (D) of NF-L KO mice and their WT controls at 5 months of age. Y-axis represents mean numbers of cortical neurons labeled with the CR per mm2. E, F: CR immunolabeling in layer 2/3 of the cortex in WT (E) and NF-L KO (F) mice at 5 months of age. Scale bar, 50 μm.

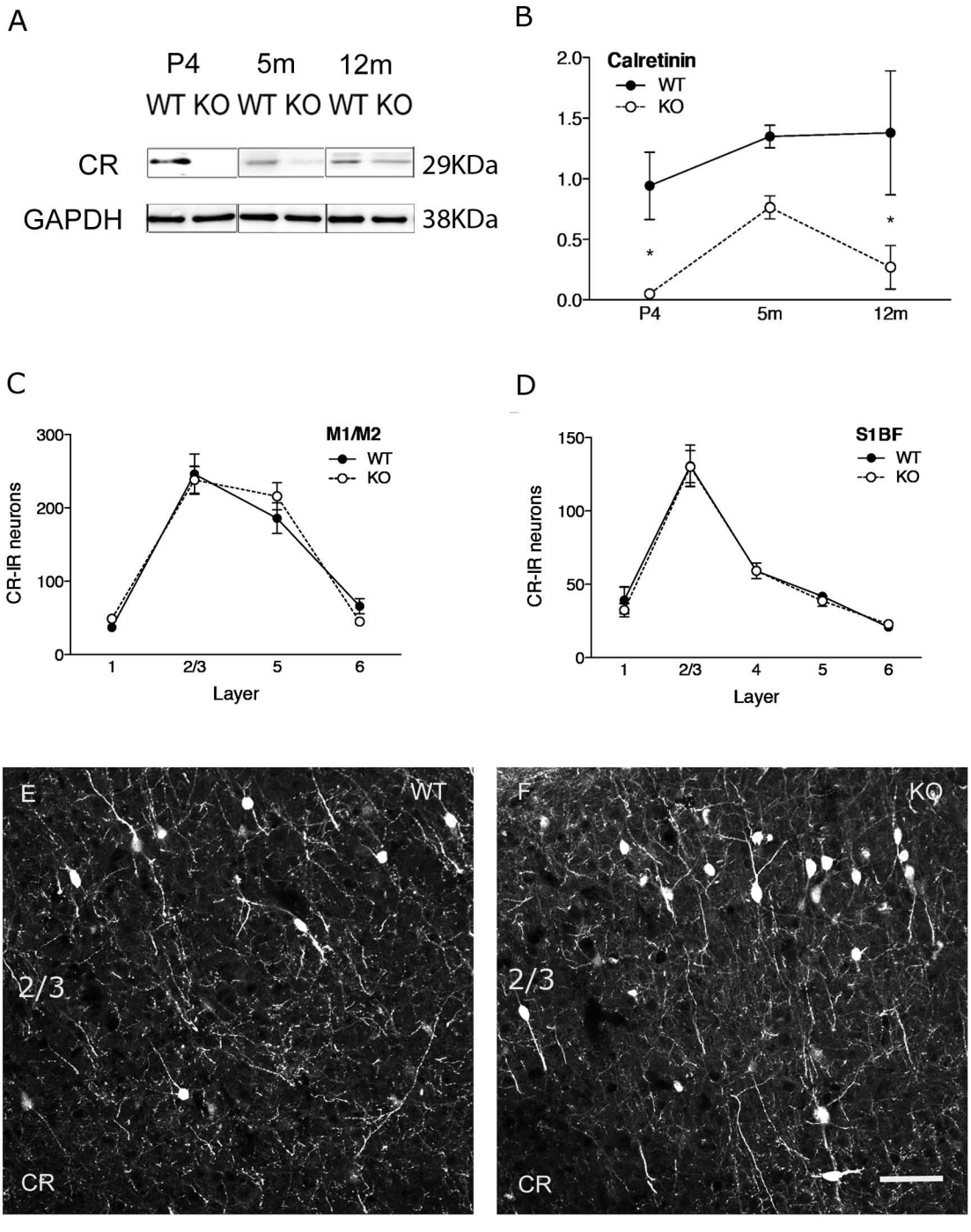
A
P4
5m
12m
WT KO WT KO WT KO
CR
29KDa
GAPDH
38KDa
B
Calretinin
WT
KO
2.0
1.5
1.0
0.5
0.0
P4
5m
12m
C
M1/M2
WT
KO
CR-IR neurons
300
200
100
0
1
2/3
5
6
Layer
D
S1BF
WT
KO
CR-IR neurons
150
100
50
0
1
2/3
4
5
6
Layer
E
WT
2/3
CR
F
KO
2/3
CR

3.7 C, D), but there was no overall effect of genotype, and no interaction between genotype and layer (meaning that the same laminar distribution was observed for all layers of the WT and KO mice). The "hump" in the M1/M2 graph (Figure 3.7 C) reflects the absence of layer 4 in this area, resulting in increased numbers of CR-positive neurons in the enlarged layer 5. In summary, there were no significant differences in the laminar distribution of CR neurons in either region or the total number of labeled cells in the NF-L KO mice compared to the WT animals.

In addition, confocal images of CR labeled neurons in layer 2/3 of adult CTX at 5 months showed no observable change of CR labeling distribution within the different compartments of the labeled neurons (Figure 3.7 E, F).

3.4 Discussion

Deletion of NF-L protein in mice significantly altered the expression of other neuronal intermediate filament proteins in the CTX at various ages, as assayed by Western blotting. The differing profiles of NF subunits and phosphorylation states (Fig 3.1A-D) presumably reflect altered NF assembly and phosphorylation, beginning at P4 when all of the markers of IFs are significantly reduced in KO animals. WT animals showed a great increase in NF-P labeling between 5 and 12 months, with a corresponding reduction in NF-DP labeling suggesting that widespread phosphorylation is taking place, masking the NF-DP epitope. NF-L KO mice were low in expression for both NF-DP and NF-P at these ages, indicating a lack of the normal NF forms, which these antibodies detect. In WT animals, INT labeling was initially high but decreased steadily as the CNS matured, whereas NF-L KO resulted in reduced INT expression at P4 and 5 months, but with a marked increase from 5 to 12 months. This may reflect a partially successful compensatory response in which INT substituted for NF-L to assemble NFs. If this was the case, the resultant filaments were not detected by SMI 32 or SMI 312, presumably due to a lack of recognizable epitopes. This scenario is consistent with the data from this thesis on the expression of NF-M, consistent at all ages in WT animals, but initially lower in the NF-L KO mice, then increasing at the time INT demonstrated increased expression. Although previous studies have found that, in the absence of NF-L, NF-M and NF-H subunits are not able to assemble into 10 nm filaments alone (Carter et al., 1997), the data present in this thesis suggest that INT could potentially compensate for an absent in NF-L because of its type IV neuronal IF similarities (Yuan et al., 2006b).

These changes of NF-DP proteins detected by Western blotting were also associated with changes found by immunohistochemistry in the typical cellular localization of NF-DP proteins in cortical neurons of 5-month-old NF-L KO mice. Moreover, the deletion of NF-L resulted in reduced CR protein expression without affecting the distribution of cortical interneurons labeled for this protein. In addition, increased expression of MAP2 and neuron-specific class III beta-tubulin were found at P4, 5 months and 12 months of age. These findings suggest that the deletion of NF-L may be compensated for by alterations in other cytoskeletal proteins without necessarily disrupting cortical structure or connectivity.

Mice lacking NF-L exhibit a scarcity, but not a complete absence, of neuronal IF structures associated with a reduction in adult cortical levels of NF-M and NF-H (Zhu et al., 1997). Combined with the current findings, this suggests that NF-L is a critical backbone protein to which NF-M and NF-H co-polymerize to form NFs (Carter et al., 1997), which can only partially be compensated for by increased INT expression.

In WT rodent brains, NF proteins and INT are enriched in a subset of cortical pyramidal cells (Kirkcaldie et al., 2002; Dickson et al., 2005; King et al., 2006; Paulussen et al., 2011). Although it has been demonstrated that NF-L KO disrupts filament expression and localization, there is little apparent effect on overall cortical structure. The observed abnormalities in, for example, NF-DP labeling of soma, are probably due to defective NF assembly as well as the transport of these proteins into axons. When NF-L expression is disrupted in Japanese quail, axonal transport of NF

proteins is impaired, with subsequent accumulation of NF-H and NF-M in the cell body of motor neurons, similar to that seen in ALS (Toyoshima et al., 2000).

The compensatory increases in expression of other cytoskeletal components may explain why the NF-L KO mouse does not exhibit a major neurological/behavioral phenotype. NF-L KO mice have mild sensorimotor dysfunction and spatial memory deficits, but no severe symptoms such as overt signs of paresis (Dubois et al., 2005). This may indicate a lack of functional disruption, or that the neocortex is relatively unimportant in mouse behavior (Kirkcaldie, 2012). The adaptive changes in other cytoskeletal proteins underlines the inter-relationship of NFs, MTs and MFs in maintaining neuronal structure and function (reviewed in Julien et al., 2000).

To assess whether these changes affected other cells, interneurons labeled for CR were examined, that typically lack the NFTPs (Sampson et al., 1997; Blizzard et al., 2011). CR is a calcium-binding protein, which helps to buffer calcium within neurons (Sampson et al., 1997) and may modulate excitability in the neurons which express it (Camp and Wijesinghe, 2009). There was no difference in total cell number or laminar distribution of CR positive neurons in the NF-L KO CTX in either the motor (M1, M2) or sensory (S1BF) regions in the adult CTX (Fig. 3.7E, F), in accordance with the existing literature (Conde et al., 1994; DeFelipe et al., 1999; Park et al., 2000; Yamashita et al., 2003). However, the amount of cortical CR protein was reduced in the NF-L KO mice, which may imply functional changes in these interneurons, which typically synapse onto pyramidal neurons affected by the reduced NF levels (Kirkcaldie, 2012).

In conclusion, these findings indicate that there are compensatory changes in expression and distribution of cytoskeletal components in central nervous system neurons which lack NF-L, and that the lack of NF proteins does not affect the structure and cytoarchitecture of the adult CTX. These results indicate a close and dynamic inter-relationship between cytoskeletal proteins in the maintenance of the structure and function of the neuronal cytoskeleton, and a resilience of cortical structure to changes imposed by cytoskeletal disruption.

Chapter 4: Changes to TDP-43 expression in ageing NF-L KO mice

4.1 Introduction

TDP-43 is a 414 amino-acid hnRNP encoded by the TARDBP gene (Ou et al., 1995), which was identified as a transcriptional repressor that binds to both DNA and RNA with multiple functions such as transcriptional repression, pre-mRNA splicing and translational regulation (reviewed in Buratti and Baralle, 2008; Wang et al., 2008). TDP-43 is also a NF-L mRNA binding protein, acting to stabilize mRNA transcription and also with a role in NF mRNA metabolism and transport (Strong et al., 2007).

Normally, TDP-43 is localized to the nucleus. However, pathologic TDP-43, (cytosolic aggregation, ubiquitination, abnormal phosphorylation and proteolytically cleaved C-terminal fragments of TDP-43) becomes localised to the cytoplasm (Neumann et al., 2006; Winton et al., 2008). TDP-43 mislocalization is associated with a reduction in NF-L mRNA levels (Caccamo et al., 2009). Pathologic TDP-43 is a primary component of ubiquitin-positive and alpha-synuclein-negative inclusions in affected brain and spinal cord regions of patients with FTLD-TDP and ALS, known as TDP-43 proteinopathies (Neumann et al., 2006; Armstrong et al., 2013). In addition, TDP-43 pathology has also been detected in PD, dementia with Lewy bodies and AD cases (Amador-Ortiz et al., 2007b; Higashi et al., 2007; Bigio, 2008; Uryu et al., 2008; Wilson et al., 2011). The reason for the abnormal cytoplasmic localization of TDP-43 in these neurodegenerative diseases is unknown. One

possible mechanism may relate to dysfunction of cellular apoptosis susceptibility, which is deficient in FTLD and ALS patients (Nishimura et al., 2010). A recent study has described Rho guanine nucleotide exchange factor as an NF-L mRNA destabilizing factor that forms cytoplasmic inclusions in ALS (Droppelmann et al., 2013). Hence, alterations in RNA metabolism in motor neurons may explain the development of protein inclusions, including the neurofilamentous aggregates, observed in ALS pathology (Droppelmann et al., 2013).

Pathogenic mutations in the TDP-43 gene have been identified in sporadic and familial ALS (Gitcho et al., 2008; Sreedharan et al., 2008; Yokoseki et al., 2008). In addition, an A90V mutation has been identified in a FTLD patient with a family history of dementia (Winton et al., 2008). Recently, a mutation in the TDP-43 gene has been detected in a family presenting with PD, who later develop ALS and FTLD (Mosca et al., 2012). Collectively, this suggests a direct link between TDP-43 abnormalities and neurodegeneration across a range of conditions.

TDP-43 has been reported to be upregulated in the cerebrospinal fluid of patients with ALS (Kasai et al., 2009) and in peripheral blood lymphocytes from ALS patients (Mougeot et al., 2011; Nardo et al., 2011). Overexpression of the normal human TDP-43 gene causes neurodegeneration in transgenic animals such as Drosophila, monkey and rat (Li et al., 2010; Uchida et al., 2012).

The finding that TDP-43 regulates NF-L mRNA may provide a potential link to ALS in which NF-L mRNA expression is decreased and pathologic TDP-43 is present (Caccamo et al., 2009). In addition, NF-L KO mice have been shown to mimic the

reduced NF-L mRNA levels seen in ALS resulting in perikaryal accumulation of NF proteins and axonal hypotrophy in motoneurons (Wong et al., 2000). However, causes and effects are unclear. Hence, this chapter investigated whether alteration in NF-L expression affected TDP-43. In order to determine whether deficiency of NF-L protein resulted in pathologic TDP-43, the relative levels and localization of TDP-43 were investigated in the CTX and spinal cord of young (10 weeks) and aged (12 months) NF-L KO mice, relative to age-matched WT mice (C57Bl/6). This study demonstrated that lack of NF-L protein or mRNA expression can affect the expression levels of TDP-43 in the CTX and spinal cord, and was associated with motor dysfunction, however, this does not result in pathologic accumulations of TDP-43.

4.2 Methods and materials

4.2.1 Animals

As described in Section 2.1, NF-L KO mice were maintained on a C57Bl/6 background (Zhu et al., 1997). For the purposes of this study, NF-L KO mice were compared to WT mice (C57Bl/6). Male mice were used at 10 weeks, 4 months and 12 months of age. All experiments were approved by the University of Tasmania Animal Ethics Committee.

4.2.2 Body weight

The body weights of four NF-L KO mice and four WT mice at 12 months of age were measured.

4.2.3 Footprint test

The footprint test (Carter et al., 1999) was used to compare the gaits of NF-L KO mice with that of WT control mice. Three NF-L KO mice and 5 WT mice at 4 months of age, 4 NF-L KO mice and 4 WT mice at 12 months of age were tested as described in Section 2.5. Parameters of footprint including the stride length (mm), base width (mm) and uniformity (mm) were measured.

4.2.4 Tissue preparation

For Western blot studies, WT and NF-L KO mice at 10 weeks and 12 months of age (n=3/group) were anaesthetized and decapitated as described in Section 2.3.1. Tissue

samples of CTX, HIP and corpus callosum (CC) and cervical spinal cord (SC-C), thoracic spinal cord (SC-T) and lumbar spinal cord (SC-L) were dissected and frozen in liquid nitrogen followed by storage at -80 °C.

For immunohistochemistry and immunofluorescence studies, WT and NF-L KO mice at 10 weeks and 12 months of age (n=3/group) were anaesthetized and transcardially perfused as described in Section 2.2.1. Sections of brains and lumbar spinal cords were prepared as described in Section 2.2.1.

4.2.5 Western blot

Western blots were performed as described in Section 2.3 with modifications. Proteins from the CTX, HIP, CC, SC-C, SC-T and SC-L of 10-week old and 12-month old NF-L KO mice and WT controls (n=3 each) were extracted as described in Section 2.3.2. Protein concentration was determined with Protein Assay (Bio-Rad) using BSA as a standard. Proteins (15µg) were separated by 4-20% SDS-PAGE and blotted onto a PVDF membrane as described in Section 2.3.3. Primary antibody (Table 2.1) binding was visualized by goat anti-mouse or anti-rabbit IgG coupled to horseradish peroxidase (Dako, Denmark; Table 2.2). Immunoreactive bands were visualized and measured as described in Section 2.3.3.

4.2.6 Immunohistochemistry and Immunofluorescence

40 µm brain or spinal cord cryostat sections were treated with antigen retrieval as described in Section 2.2.2. Then non-specific binding sites of the sections were blocked in Protein Block, Serum-Free (Dako, Denmark) solution for 20 minutes at

room temperature. Following blocking, the sections were washed with 0.01 M PBS, they were then incubated overnight at 4°C with primary antibodies (Table 2.1) in 2x diluent (0.6% Triton X-100 in 0.01 M PBS). For immunoperoxidase labelling, primary antibodies were visualised using a DAB staining system (VECTOR Laboratories, United States) as described in Section 2.2.5. For immunofluorescence, sections were washed with 0.01M PBS and incubated with Alexa Fluor 488 conjugated to goat anti-mouse or Alexa Fluor 546 conjugated to goat anti-rabbit IgG (Molecular Probes, United States; Table 2.2). Sections were washed with PBS before mounting onto Fisher Super Frost Plus slides using fluorescent mounting medium (Dako, Denmark), and air-dried in the dark. Nuclei were counterstained with DAPI as described in Section 2.2.4.

4.2.7 Image acquisition

Fluorescence-labeled sections were viewed with a Zeiss LSM 510 META confocal microscope (Carl Zeiss, Germany) and images acquired as described in Section 2.4.

4.2.8 Statistical Analysis

Statistical analysis was undertaken as described in Section 2.6. For footprint analysis, a non-parametric t-test was used to determine differences on uniformity parameter. One-way ANOVA followed by a Tukey post-hoc was used to determine differences in the stride length (mm) and base width (mm) parameters, respectively.

4.3 Results

4.3.1 Reduced body weight in aged NF-L KO mice

To determine if lack of NF-L resulted in the change of body weight in aging NF-L KO mice, the body weight of 4 NF-L KO mice (Figure 4.1 B) and 4 WT mice (Figure 4.1 A) at 12 months of age was assessed. The body weight of NF-L KO mice at 12 months was 21% lower than that of age-matched WT mice (Figure 4.1 C), which was similar to a previous report that young NF-L KO mice (19 to 28 weeks) had a lower body weight than WT mice (Dubois et al., 2005). It was interesting that NF-L KO mice show white colour rather than being black as normal C57Bl/6 mice. However, the reason remained unknown.

4.3.2 Changes to TDP-43 expression in the brain and spinal cord of aged NF-L KO mice

To determine if the expression of TDP-43 was affected by ageing in NF-L KO mice, the expression of TDP-43 in the brain and spinal cord of NF-L KO relative to WT mice at 12 months was investigated by Western blot analysis. To determine whether there were regional alterations in the levels of TDP-43, studies of three regions of brain—CTX, HIP and CC and three regions of spinal cord—SC-C, SC-T and SC-L were undertaken. TDP-43 protein was significantly increased ($P<0.05$) in the CTX of NF-L KO mice at 12 months of age, as compared with WT animals (Figure 4.2). Furthermore, there was a significant increase ($P<0.05$) of the level of TDP-43 protein in the SC-L of 12-month old NF-L KO mice (Figure 4.3). However, TDP-43 expression in other regions of the brain and spinal cord of NF-L KO mice was not

Figure 4.1 Body weight of NF-L KO and WT (C57BL/6) mice at 12 months of age. (A) WT mouse at 12 months of age. (B) NF-L KO mouse at 12 months of age. (C) Body weight of NF-L KO mice at 12 months was significantly ($P<0.05$) lower than that of age-matched WT mice. All values are expressed as the mean ± SEM. Asterisk indicates $p<0.05$.

A

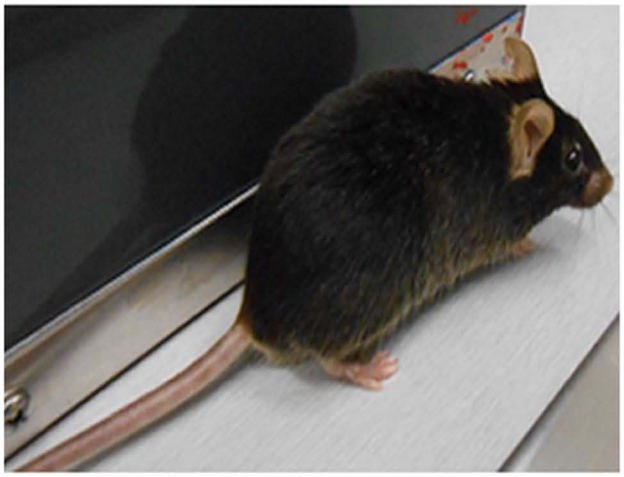

B

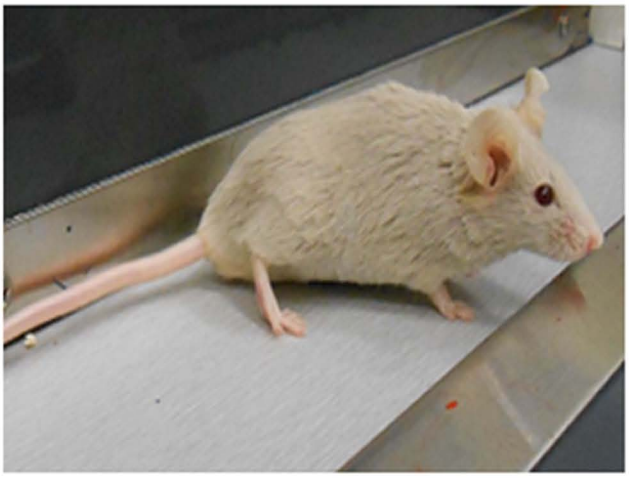

C

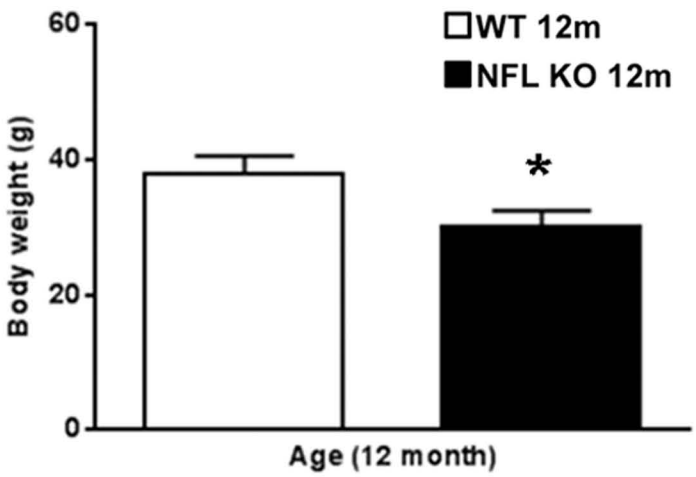

Figure 4.2 Western blot analysis of TDP-43 protein expression in the CTX, HIP and CC of NF-L KO mice and WT controls at 12 months of age (n=3/group). Equal amounts of brain tissue were separated on a gel and labeled with the TDP-43 antibody. Relative amounts of protein expression of TDP-43 were normalized with GAPDH (*$p<0.05$).

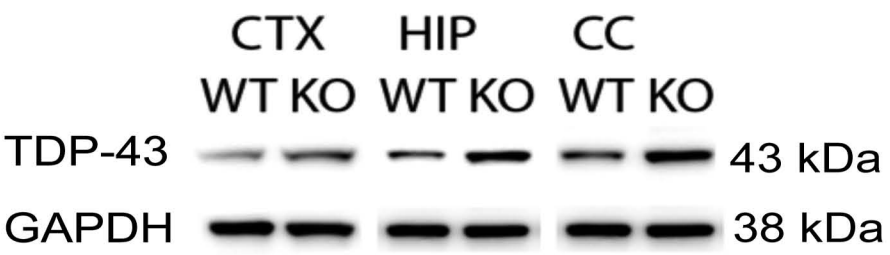
CTX
HIP
CC
WT KO WT KO WT KO
TDP-43
43 kDa
GAPDH
38 kDa

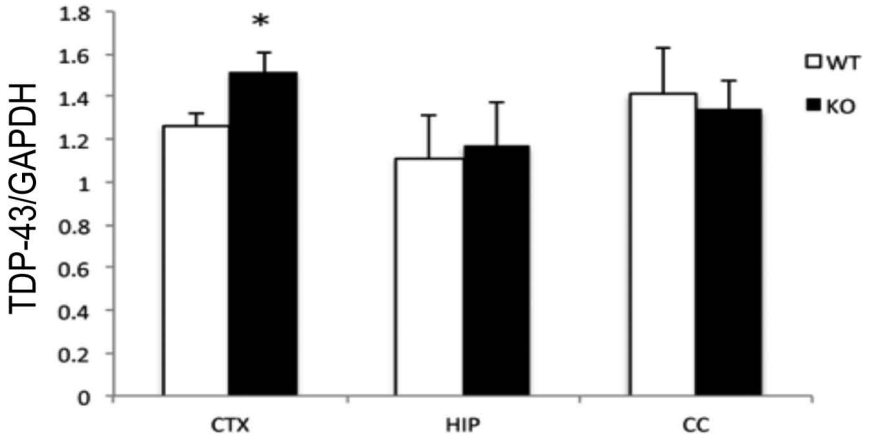
TDP-43/GAPDH
1.8
1.6
1.4
1.2
1
0.8
0.6
0.4
0.2
0
*
WT
KO
CTX
HIP
CC

Figure 4.3 Western blot of TDP-43 protein in the SC-C, SC-T, SC-L of NF-L KO mice and WT controls at 12 months of age (n=3/group). Equal amounts of tissue were separated on a gel and labeled with TDP-43 antibody. Relative amounts of the protein expression of TDP-43 were normalized with GAPDH (*$p<0.05$).

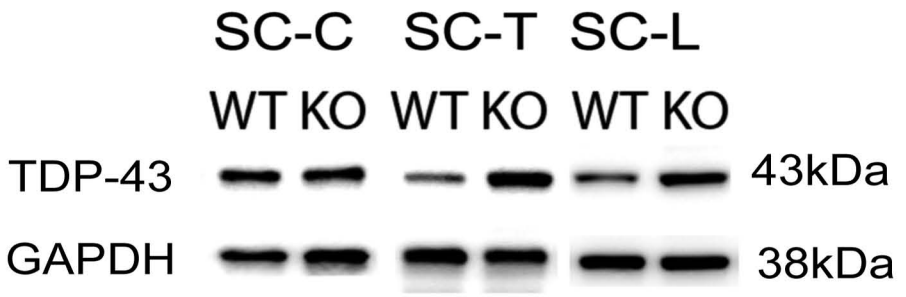
SC-C
SC-T
SC-L
WT KO WT KO WT KO
TDP-43
43kDa
GAPDH
38kDa

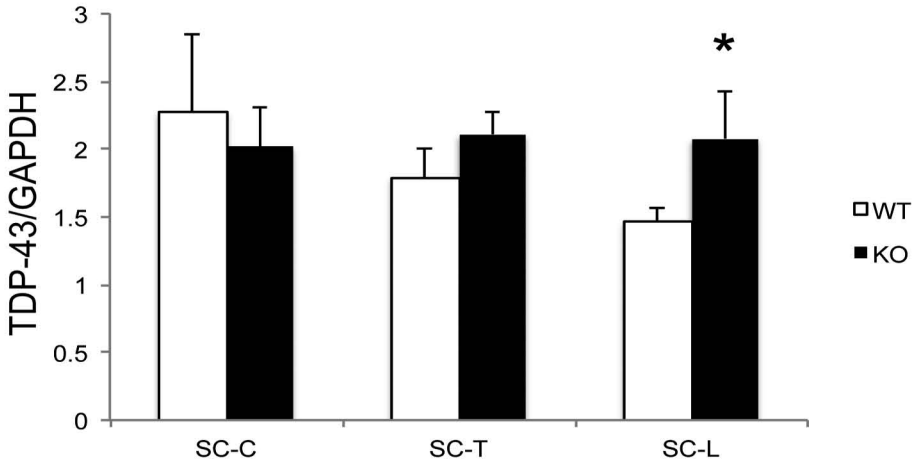
TDP-43/GAPDH
3
2.5
2
1.5
1
0.5
0
*
SC-C
SC-T
SC-L
WT
KO

significantly different to control animals.

4.3.3 Localization of TDP-43 in the brain and spinal cord of aged NF-L KO mice

As TDP-43 protein was significantly increased in the CTX and SC-L of 12-month old NF-L KO mice relative to WT animals, confocal microscopy was used to examine the brain and SC-L sections immunolabelled with antibodies to TDP-43. In order to investigate if the lack of NF-L resulted in alterations in the localization of TDP-43 in neurons, sections were also stained with DAPI. The merged images of TDP-43 (red) and DAPI (blue) showed that TDP-43 was increased in cortical neurons (Figure 4.4) and neurons in the ventral horn region of the SC-L (Figure 4.5) of NF-L KO mice at 12 months of age, compare to WT animals. However, no mislocalization of TDP-43 from the nucleus to the cytoplasm was observed. DAB staining confirmed that there were increased TDP-43 protein (brown) in the CTX of WT and NF-L KO mice at 12 months of age, without TDP-43 mislocalization, compared to WT animals (Figure 4.6).

4.3.4 Alterations in TDP-43 expression in the brain and spinal cord in 10-week old NF-L KO mice

To better understand whether the loss of NF-L gene altered TDP-43 expression in the brain and spinal cord in earlier life stages of NF-L KO mice, the expression levels of TDP-43 were investigated in NF-L KO and WT mice at 10 weeks of age. Western blotting showed that the expression levels of TDP-43 were significantly increased in all three regions of spinal cord, including SC-C ($p<0.001$), SC-T ($p<0.0001$) and SC-

Figure 4.4 Confocal microscope images of TDP-43 labelling (red) in the CTX from NF-L KO (D-F) and WT (A-C) control mice at 12 months of age. Nuclei were labelled with DAPI (blue). Note increased TDP-43 labelling (arrows) in NF-L KO mice. Scale bar, 20 μm.

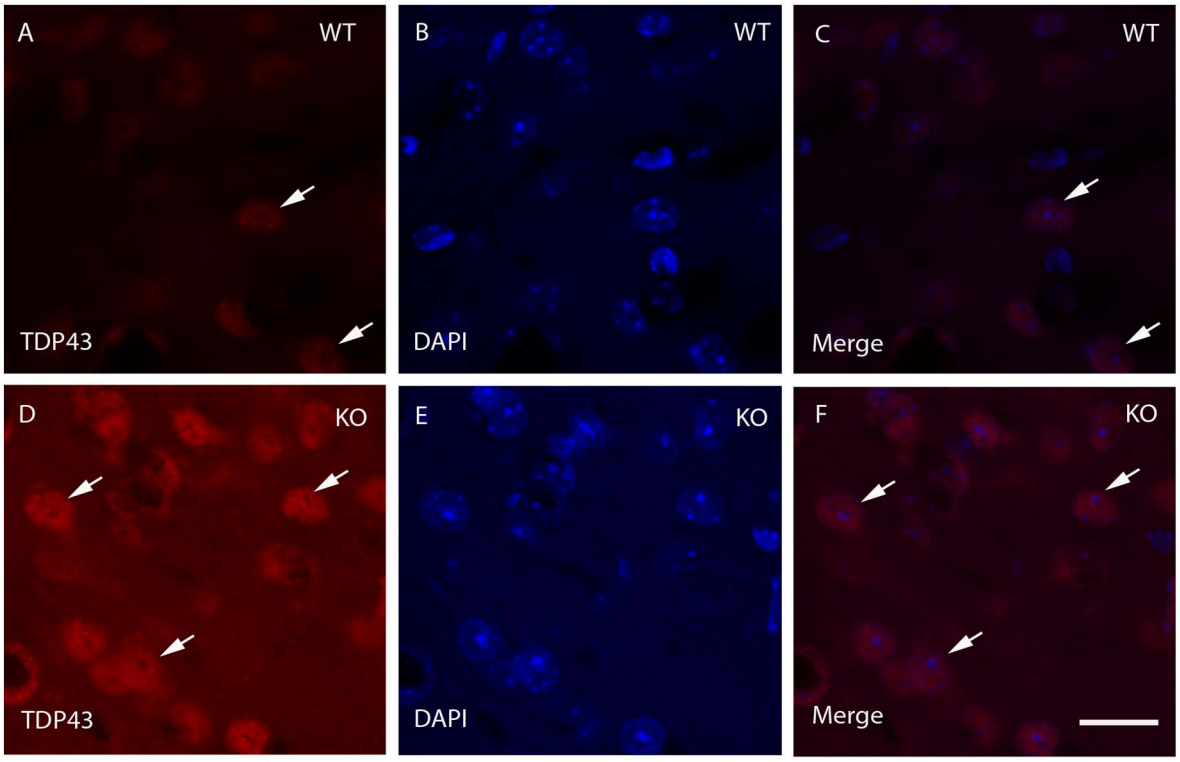
A
WT
TDP43
B
WT
DAPI
C
WT
Merge
D
KO
TDP43
E
KO
DAPI
F
KO
Merge

Figure 4.5 Confocal microscope images of the SC-L immunolabelled for TDP-43 (red) in WT (A-C) and NF-L KO mice (D-F) at 12 months of age. Nuclei were labelled with DAPI (blue). Note increased TDP-43 labelling (arrows) in NF-L KO mice. Scale bar, 20 μm.

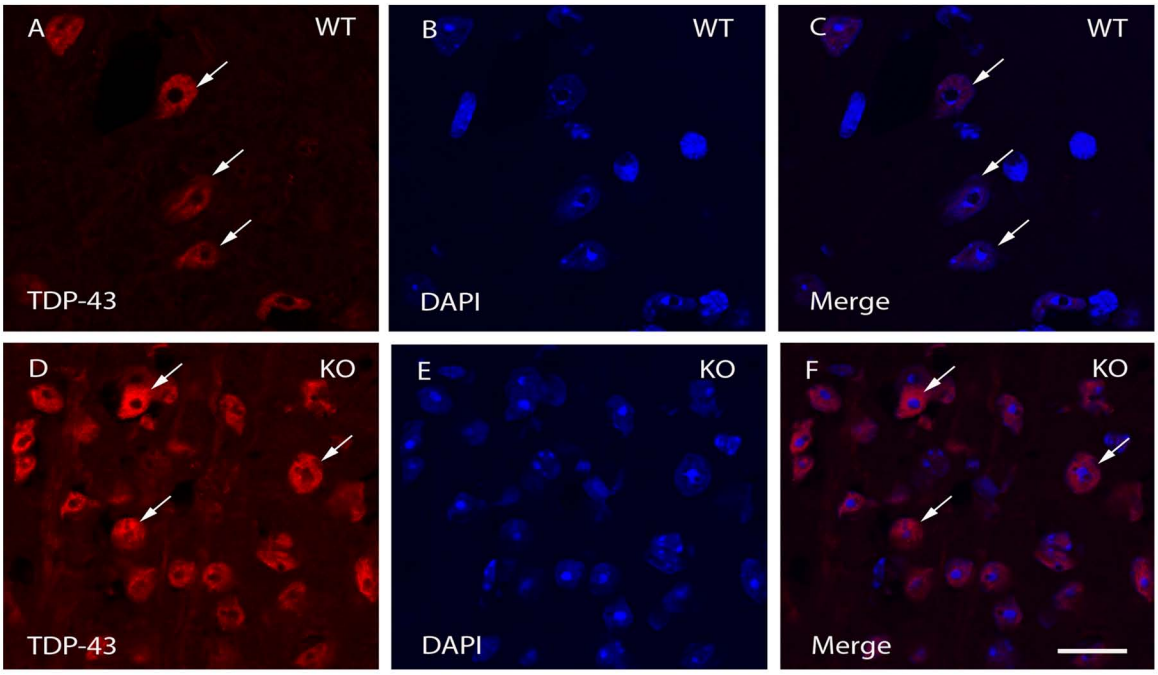
A
WT
TDP-43
B
WT
DAPI
C
WT
Merge
D
KO
TDP-43
E
KO
DAPI
F
KO
Merge

Figure 4.6 DAB staining (brown) for TDP-43 in the CTX of WT (A) and NF-L KO (B) mice at 12 months of age. Nuclei were post-stained with haematoxylin (blue). Scale bar, 30 μm.

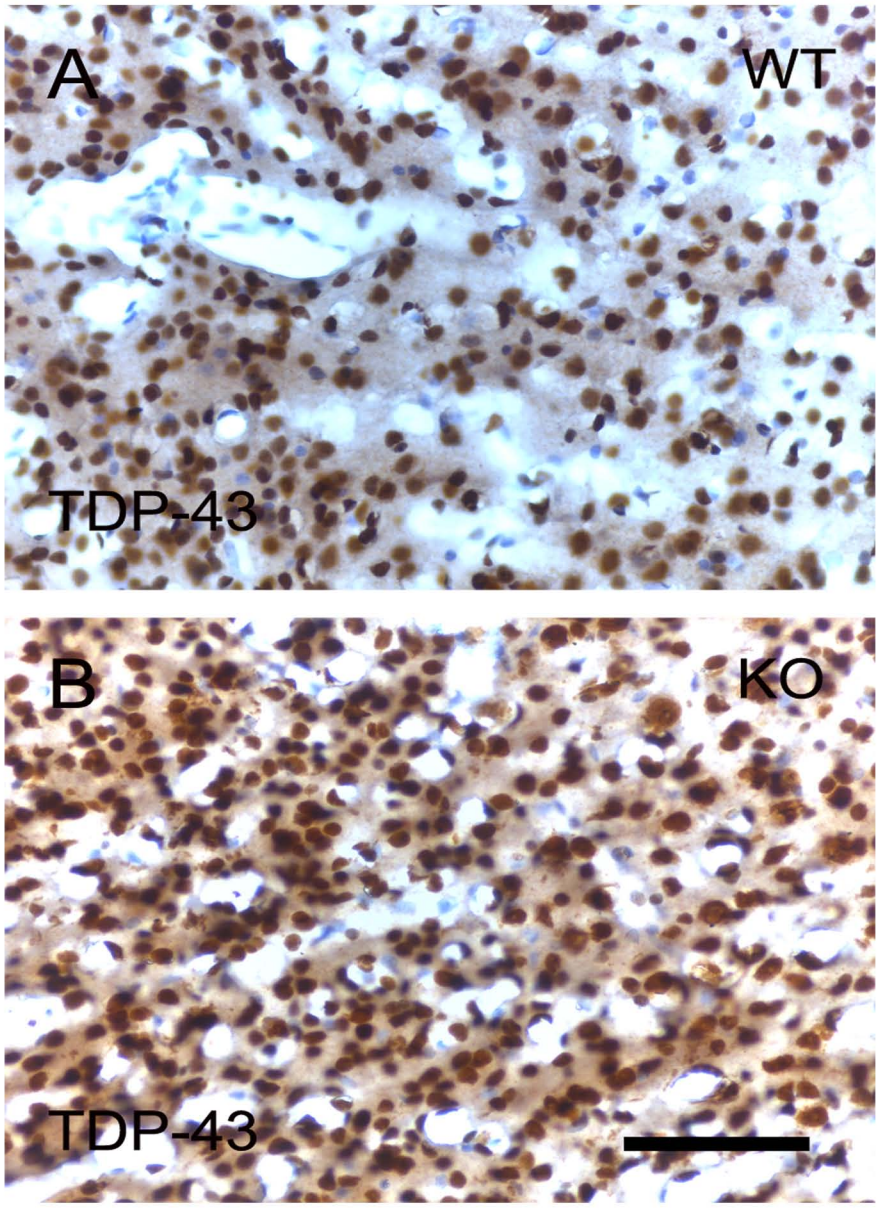
A
WT
TDP-43
B
KO
TDP-43

L ($p<0.05$) of 10-week-old NF-L KO mice, compared to WT mice (Figure 4.7). However, there was no significant change in TDP-43 protein abundance in the CTX, HIP and CC between NF-L KO and WT mice at 10 weeks of age (Figure 4.8).

In addition, TDP-43 immunolabelling was also increased in the ventral horn region of the spinal cord of NF-L KO mice relative to WT animals at 10 weeks of age (Figure 4.9).

4.3.5 Motor dysfunction in young and aged NF-L KO mice

Footprint analysis was carried out to determine if the increase of TDP-43 in the spinal cord correlated with motor dysfunction in young and aged NF-L KO mice. Footprint patterns of WT and NF-L KO mice at 4 months and 12 months of age are illustrated in Figure 4.10. WT mice at 12 months of age, walked in a straight line, with a regular even alternating gait (Figure 4.10). By contrast, NF-L KO mice had staggering movements, and a gait that lacked a uniform pattern (Figure 4.10).

The resulting footprint patterns were assessed quantitatively by four measurements: stride length of front and hind paws, base width of front and hind paws and uniformity (the distance from front footprint/hind footprint overlap) (Figure 4.10). At 4 and 12 months, NF-L mice exhibited a significantly ($p<0.05$) shorter stride length of front and hind paws (Figure 4.10), as compared with age-matched controls. In addition, at 4 months, NF-L KO mice displayed a significantly ($p<0.05$) greater uniformity compared with control mice (Figure 4.10), and this effect became more pronounced as the mice got older (12 months) (Figure 4.10). These data indicate that

Figure 4.7 Western blot analysis of TDP-43 protein expression in the SC-C, SC-T, SC-L of NF-L KO mice and WT controls at 10 weeks of age (n=3/group). Equal amounts of tissue were separated on a gel and labeled with TDP-43 antibody. Relative amounts of the protein expression of TDP-43 were normalized against GAPDH (*$p<0.05$, **$p<0.001$, ***$p<0.0001$).

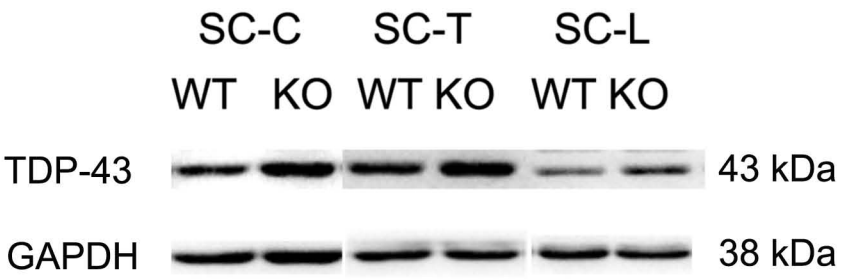
SC-C
SC-T
SC-L
WT KO WT KO WT KO
TDP-43
43 kDa
GAPDH
38 kDa

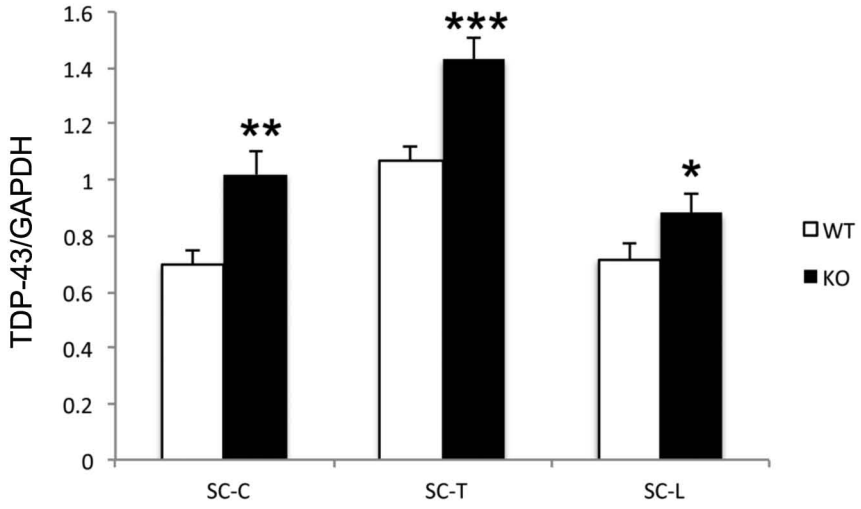
TDP-43/GAPDH
1.6
1.4
1.2
1
0.8
0.6
0.4
0.2
0
**
***
*
SC-C
SC-T
SC-L
WT
KO

Figure 4.8 Western blot analysis of TDP-43 protein expression in the CTX, HIP and CC of NF-L KO mice and WT controls at 10 weeks of age (n=3/group). Equal amounts of tissue were separated on a gel and labeled with TDP-43 antibody. Relative amounts of the protein expression of TDP-43 were normalized against GAPDH.

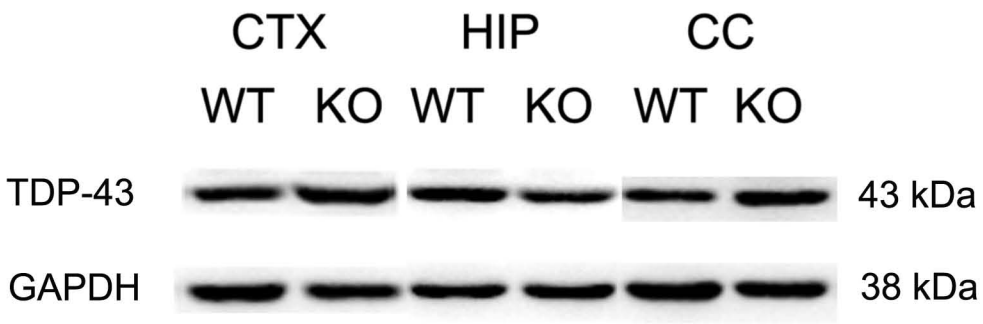
CTX
HIP
CC
WT KO WT KO WT KO
TDP-43
43 kDa
GAPDH
38 kDa

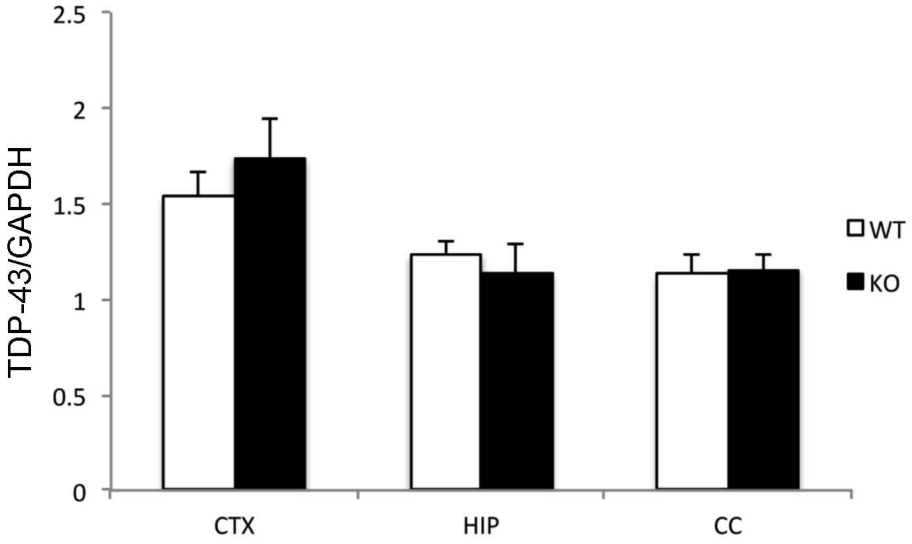
TDP-43/GAPDH
2.5
2
1.5
1
0.5
0
CTX
HIP
CC
WT
KO

Figure 4.9 Immunofluorescence labeling for TDP-43 in the ventral horn region of spinal cord of WT (A) and NF-L KO (B) mice at 10 weeks of age. Scale bars, 50 μm.

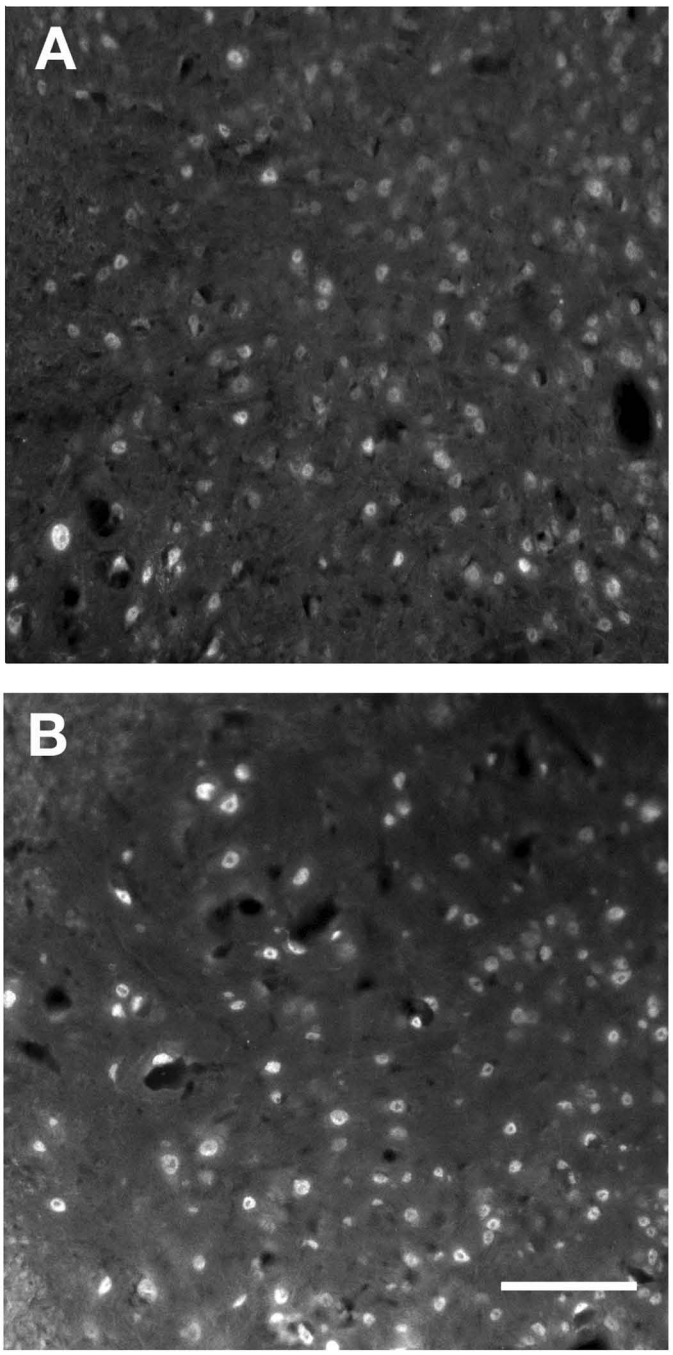
A
B

Figure 4.10 Footprint analysis of NF-L KO mice and WT controls at 4 and 12 months, respectively, including stride length, base width and uniformity measurement. All values are expressed as the mean ± SEM (* $p<0.05$).

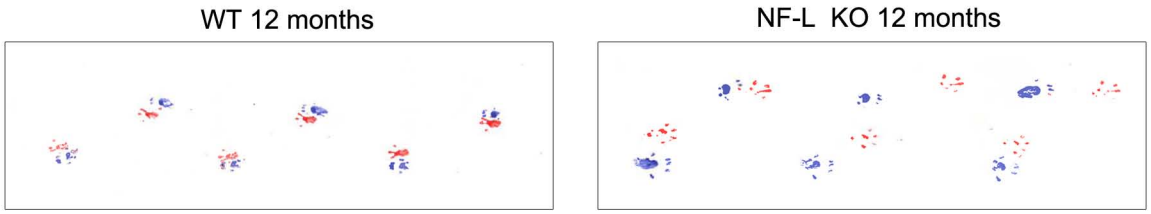
WT 12 months
NF-L KO 12 months

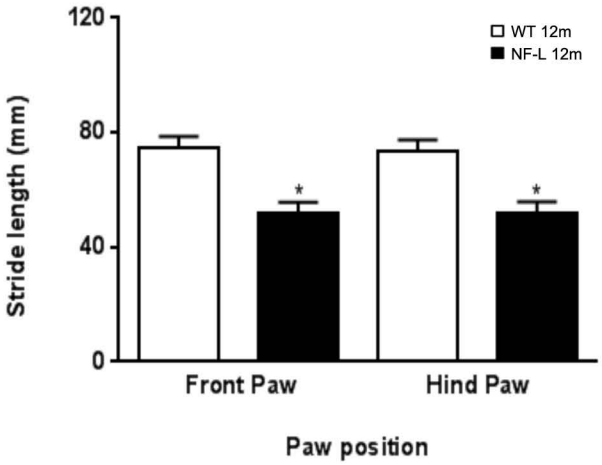
Stride length (mm)
120
80
40
0
WT 12m
NF-L 12m
*
*
Front Paw
Hind Paw
Paw position

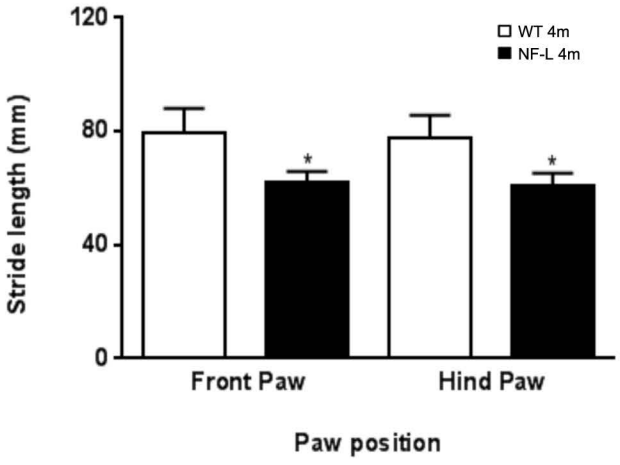
Stride length (mm)
120
80
40
0
WT 4m
NF-L 4m
*
*
Front Paw
Hind Paw
Paw position

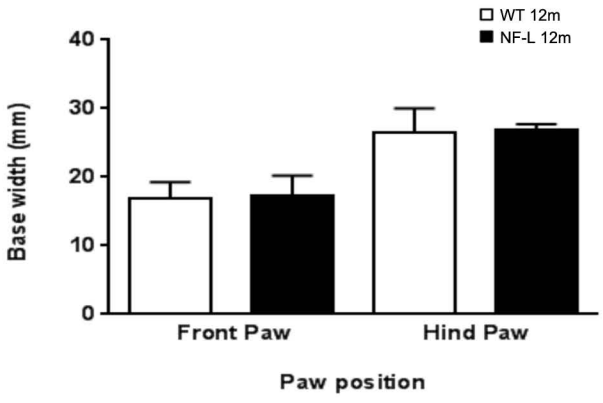
Base width (mm)
40
30
20
10
0
WT 12m
NF-L 12m
Front Paw
Hind Paw
Paw position

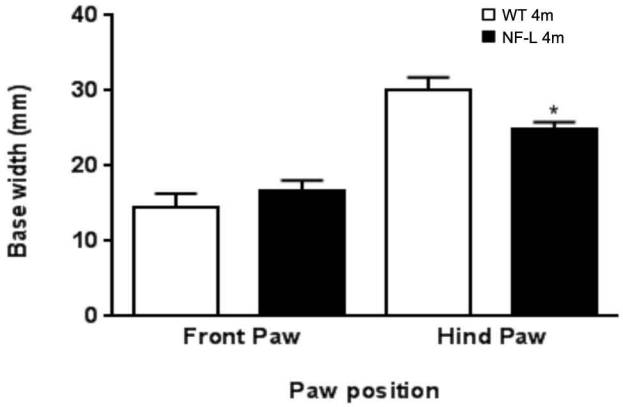
Base width (mm)
40
30
20
10
0
WT 4m
NF-L 4m
*
Front Paw
Hind Paw
Paw position

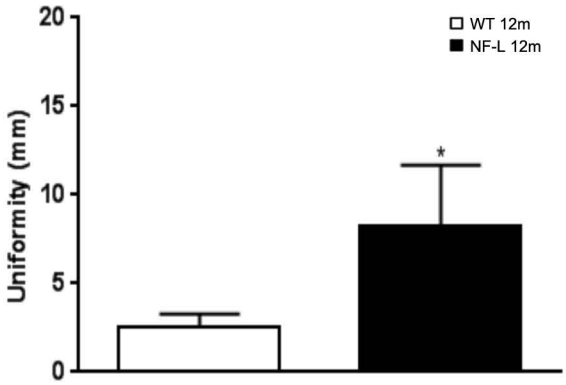
Uniformity (mm)
20
15
10
5
0
WT 12m
NF-L 12m
*

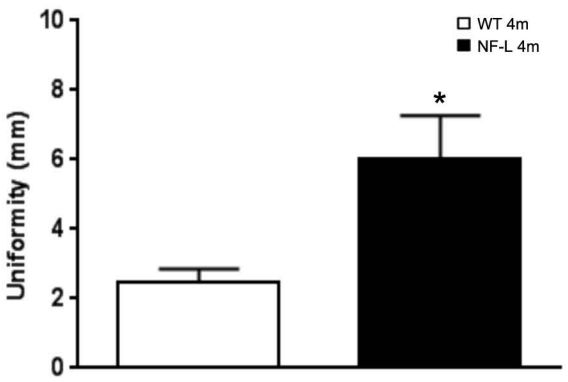
Uniformity (mm)
10
8
6
4
2
0
WT 4m
NF-L 4m
*

the NF-L animals show a motor deficit from early ages (4 months) and this motor deficit becomes worse with ageing (12 months).

4.3.6 Phosphorylation state of TDP-43 in the spinal cords of 10-week-old and 12-month-old NF-L KO mice

Levels of phosphorylated TDP-43, a marker of pathologic TDP-43, were assessed in the spinal cords of NF-L KO mice and WT controls by Western blotting. High molecular weight bands were not detected on the normal TDP-43 immunoblotting gel suggesting that the phosphorylation is at low levels in normal tissue. In both spinal cords of WT and NF-L KO mice, immunoblot of pTDP-43 (pS403/404) demonstrated two bands at 25 kDa and 45 kDa, with additional fragments. Labelling intensity of 45 KDa band is high at 10 weeks and low at 12 months in WT and NF-L KO mice. As determined by densitometric analysis of Western blot, the level of pTDP-43 protein was significantly ($p<0.05$) increased in the SC-T of 10-week-old NF-L KO mice (Figure 4.11), compared to WT controls. Moreover, an increase of pTDP-43 was detected in the SC-C of NF-L KO mouse at 12 months (Figure 4.12), compared to WT mice. These findings suggest that in the spinal cord of NF-L KO mice, there are subtle changes in amounts of pTDP-43, but the banding patterns are the same.

4.3.7 Change to pTDP-43 in the brains of NF-L KO mice at 10 weeks and 12 months of ages

To determine the phosphorylation state of TDP-43 in the brain of NF-L KO mice, Western blotting was used to measure the level of pTDP-43 in brains of 10-week old

Figure 4.11 pTDP-43 protein expression in the SC-C, SC-T, SC-L of NF-L KO mice and WT controls at 10 weeks of age (n=3/group). Equal amounts of tissue were separated on a gel and labeled with the pTDP-43 antibody. Relative amounts of the protein expression of pTDP-43 were normalized against GAPDH (*$p<0.05$).

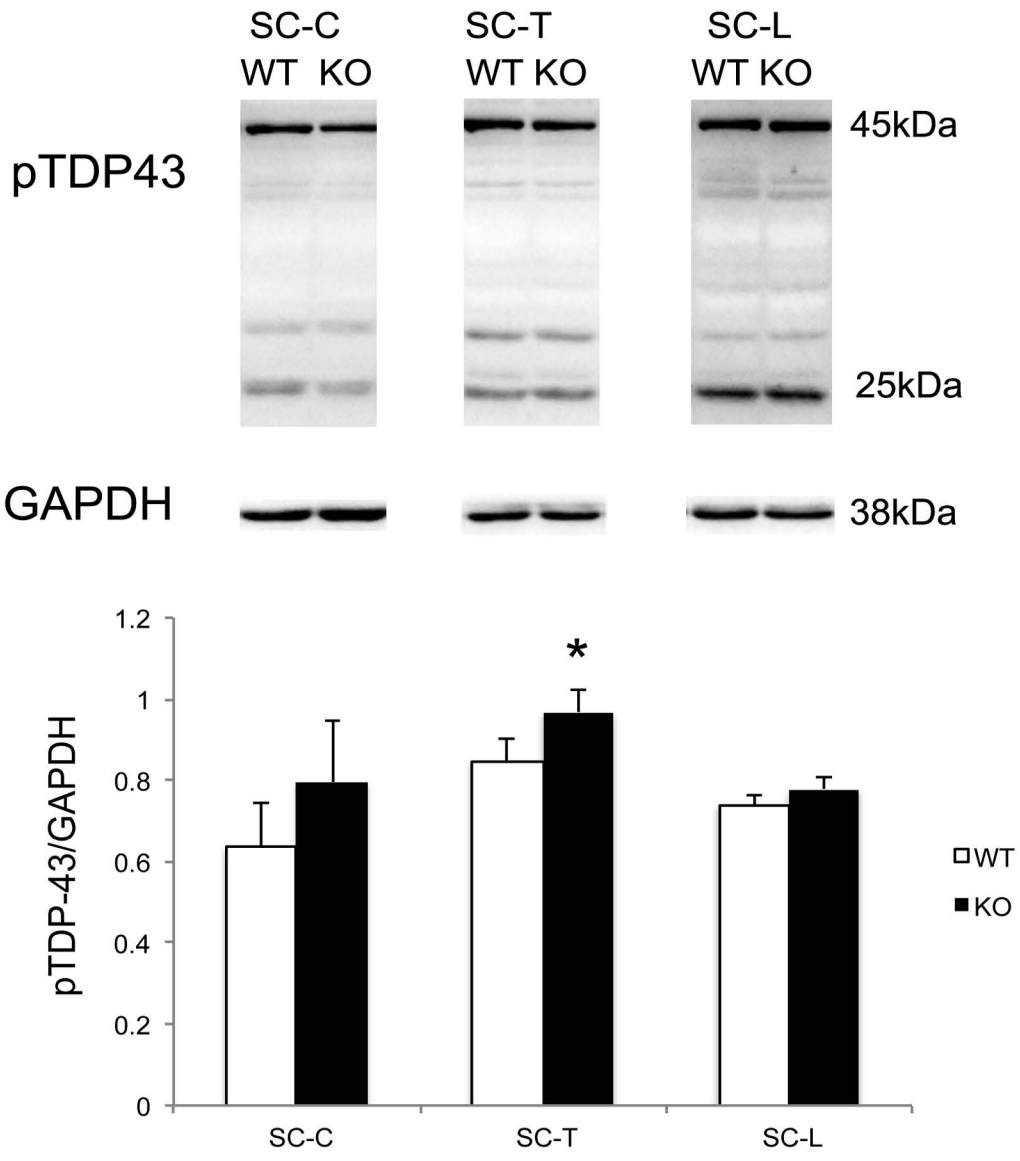
SC-C
WT KO
SC-T
WT KO
SC-L
WT KO
pTDP43
45kDa
25kDa
GAPDH
38kDa
pTDP-43/GAPDH
1.2
1
0.8
0.6
0.4
0.2
0
*
SC-C
SC-T
SC-L
WT
KO

Figure 4.12 pTDP-43 protein expression in the SC-C, SC-T, SC-L of NF-L KO mice and WT controls at 12 months of age (n=3/group). Equal amounts of tissue were separated on a gel and labeled with the pTDP-43 antibody. Relative amounts of the protein expression of pTDP-43 were normalized against GAPDH (*$p<0.05$).

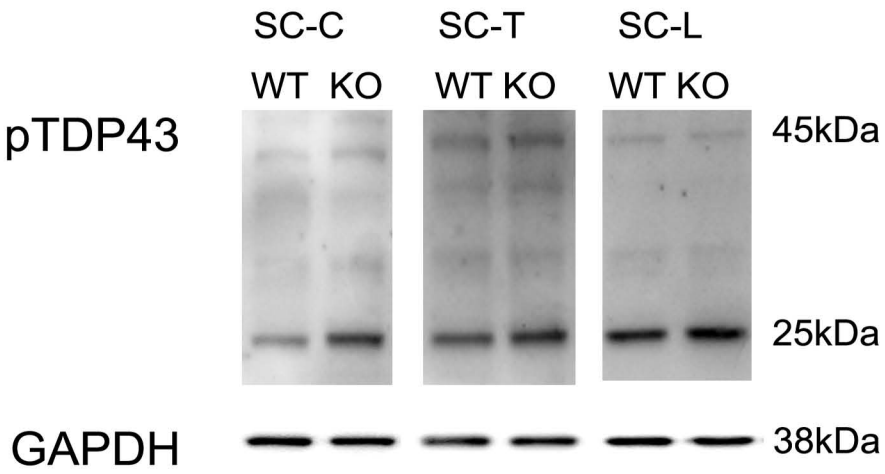
SC-C
SC-T
SC-L
WT KO
WT KO
WT KO
pTDP43
45kDa
25kDa
GAPDH
38kDa

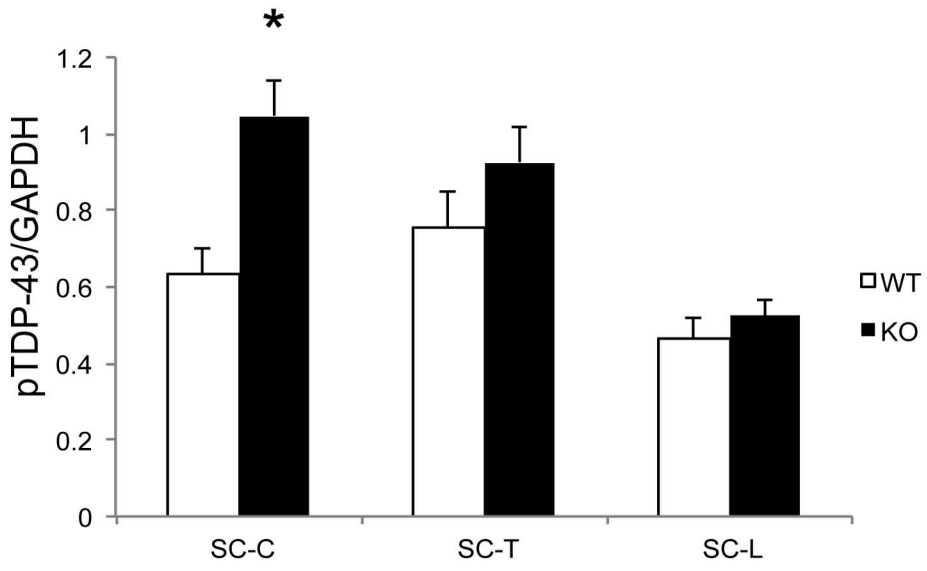
*
1.2
1
0.8
0.6
0.4
0.2
0
pTDP-43/GAPDH
SC-C
SC-T
SC-L
WT
KO

and 12-month old NF-L KO mice and age-matched WT mice, respectively. There was no signifcant ($p<0.05$) difference in pTDP-43 protein abundance in the CTX, HIP and CC of NF-L KO and WT mice at 10 weeks (Figure 4.13) and 12 months of age (Figure 4.14). However, in addition to two bands at 25 kDa and 45 kDa of pTDP-43 detected in CTX, HIP and CC of WT and NF-L KO mice at 10 weeks and 12 months, the CC of the ageing brain of WT and NF-L KO mice, has an unusual band at approximately 37 kDa (Figure 4.14), which was not observed in the CTX and HIP. These findings suggest that in CC of aged brain, there are some subtle changes in the banding patterns of pTDP-43 or postranslational modification of pTDP-43 species, without a change of the amount of pTDP-43 bewteen WT mice and NF-L mice.

Figure 4.13 Western blot analysis of pTDP-43 protein expression in the CTX, HIP and CC of NF-L KO mice and WT controls at 10 weeks of age (n=3/group). Equal amounts of tissue were separated on a gel and labeled with pTDP-43 antibody. Relative amounts of the protein expression of pTDP-43 were normalized against GAPDH.

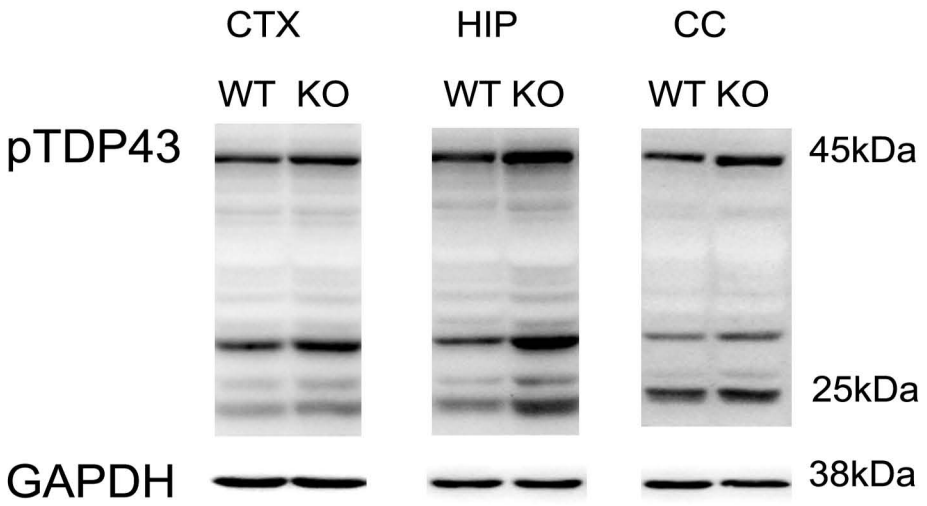
CTX
HIP
CC
WT KO
WT KO
WT KO
pTDP43
45kDa
25kDa
GAPDH
38kDa

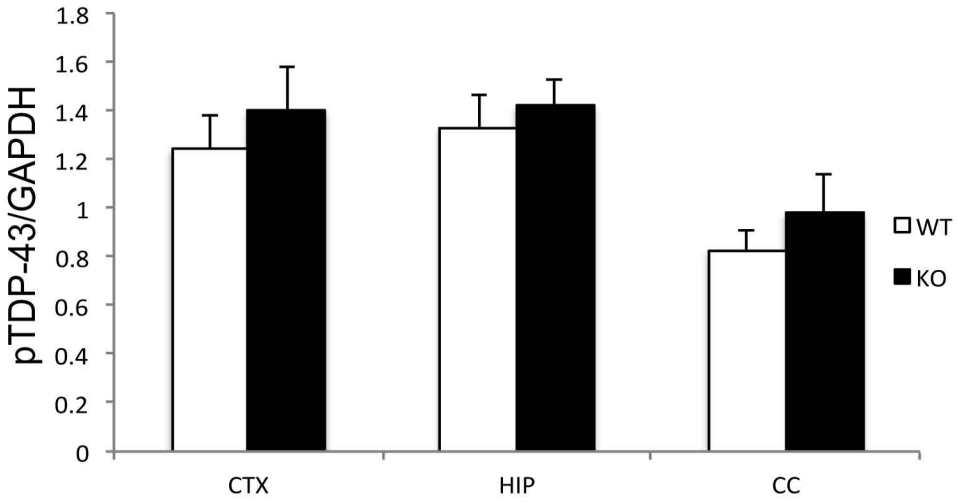
pTDP-43/GAPDH
1.8
1.6
1.4
1.2
1
0.8
0.6
0.4
0.2
0
CTX
HIP
CC
WT
KO

Figure 4.14 pTDP-43 protein expression in the CTX, HIP and CC of NF-L KO mice and WT controls at 12 months of age (n=3/group). Equal amounts of tissue were separated on a gel and labeled with pTDP-43 antibody. Relative amounts of the protein expression of pTDP-43 were normalized with GAPDH.

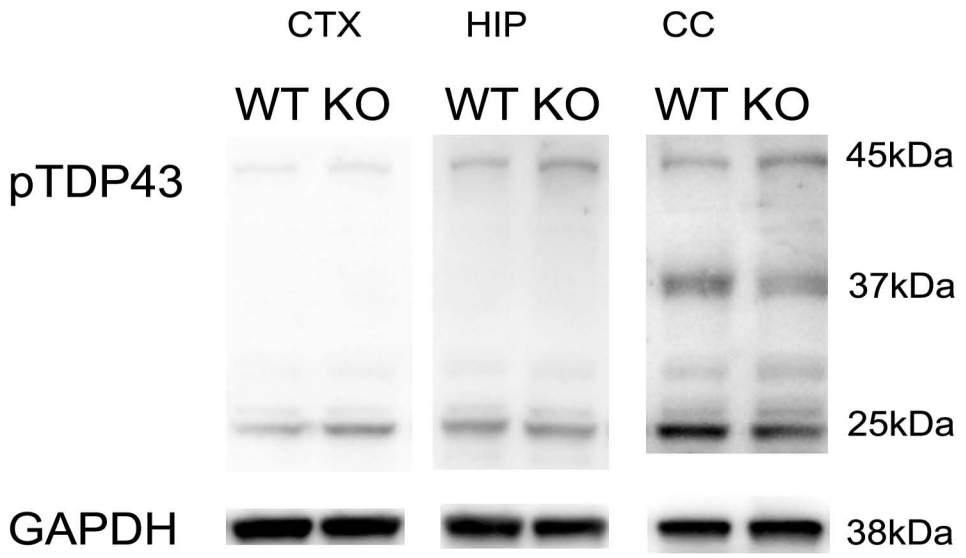
CTX
HIP
CC
WT KO
WT KO
WT KO
pTDP43
45kDa
37kDa
25kDa
GAPDH
38kDa

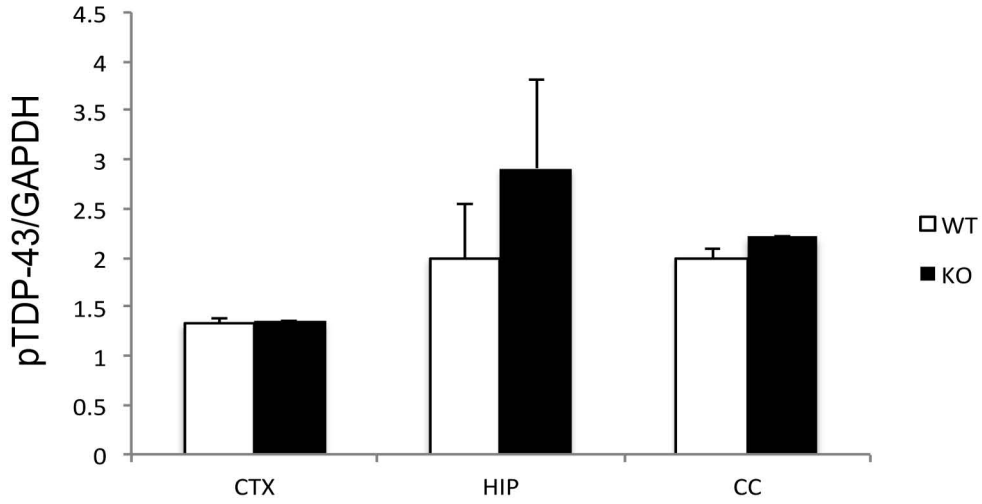
pTDP-43/GAPDH
4.5
4
3.5
3
2.5
2
1.5
1
0.5
0
CTX
HIP
CC
WT
KO

4.4 Discussion

TDP-43 is involved in nuclear-cytoplasmic shuttling of RNA granules including NF-L, NF-H and actin mRNAs to the neurites (Strong et al., 2007). In addition, TDP-43 can function as a NF-L mRNA 3'UTR binding protein, influencing the stability of NF-L transcripts (Strong et al., 2007). Moreover, the interaction of TDP-43 with the NF-L mRNA 3' UTR involves UG motifs present on stem loops of the 3'UTR as well as the RRM1 and RRM2 motifs of TDP-43 (Strong et al., 2010). However, the interaction between NF-L and TDP-43 during ageing remains undefined. Based on the previous findings that deficiency of NF-L protein results in significant alterations of the expression of other NF proteins and neurofilamentous aggregates in the CTX at various ages (Chapter 3), this chapter examined the relationship between NF-L and TDP-43 in young and aged NF-L KO mice. This chapter is the first report to demonstrate that the lack of NF-L was associated with increased expression of TDP-43 proteins in 10-week and 12-month old mice, strongly suggesting a close association between NF-L and TDP-43. In this regard, NF-L may be a negative regulator of TDP-43. This is consistent with a previous report showing increased TDP-43 proteins in injured young NF-L KO mice (Mossie et al., 2009), which indicated that, in the absence of NF-L mRNA, TDP-43 is free to interact with other mRNA substrates and TDP-43 can potentially act in a “dominant-negative” fashion to regulate NF-L mRNA stability (Mossie et al., 2009).

Overexpression of the human TDP-43 gene induces motor neuron degeneration in transgenic mice (Wils et al., 2010). In addition, increased expression of the TDP-43 gene has been reported to be neurotoxic to neurons and glia. Although the

mechanisms behind this are currently unclear toxicity may be due to both a hyperactive innate immune response resulting in toxicity on neuronal cells in addition to an increased vulnerability to a toxic environment (Kabashi et al., 2009; Wils et al., 2010). Neuronal sensitivity to TDP-43 overexpression is dependent on timing of induction (Cannon et al., 2012). In this thesis, it was found that the lack of NF-L leads to TDP-43 overexpression without cytoplasmic aggregates, which is consistent with the previous studies that neuronal overexpression of WT or mutant TDP-43 in transgenic mice did not cause cytoplasmic TDP-43 aggregates (Wegorzewska et al., 2009; Stallings et al., 2010; Wils et al., 2010; Xu et al., 2010), although it did cause a dose-dependant degeneration of cortical and spinal motor neurons. This raises the possibility that an up-regulation of TDP-43, rather than TDP-43 cytoplasmic aggregates, may contribute to neurodegeneration by triggering pathogenic pathways, eg, via NF-κB activation (Swarup et al., 2011b).

In this chapter, aged NF-L KO animals exhibited worse motor dysfunction than younger KO animals, suggesting that ageing is a risk factor in the NF-L KO mice. Interestingly cortical and lumbar regions were pathologically vulnerable to NF-L mRNA reduction during ageing, resulting in an increase of TDP-43. Whether the vulnerabillity of these regions to increased TDP-43 is correlated to the alterations in motor function remains to be determined.

Phosphorylation of TDP-43 is a consistent feature in all sporadic and familial forms of TDP-43 proteinopathies (Neumann et al., 2009). In this thesis, the band patten of the pTDP-43 immunoblot demonstrated two bands at 25 kDa and 45 kDa, with additional fragments. The labelling intensity of the 25 kDa band was higher than

45kDa band, which was similar to reports on TDP-43 in ALS/FTLD (Hasegawa et al., 2008). Phosphorylation of full-length TDP-43, resulting in a product of 45 kDa, was first observed in FTLD-U and ALS brains (Neumann et al., 2006). However, in this thesis, this 45 kDa band was not observed with the phosphorylation-independent TDP-43 antibody in the NF-L KO mice. In addition, cytoplasmic accumulation of phosphorylated TDP-43 was absent in neurons of NF-L KO mice. These data suggest that increases in TDP43 do not necessarily correlate with increased expression of pTDP-43 or abnormal cellular localisation. Interestingly, TDP-43 protein expression has been reported to be upregulated 1.5 times in ALS patients (Mishra et al. 2007; Gitcho et al. 2009). In the current study, the percentage of TDP-43 upregulation was approximately 20% in the CTX and 41% in the SC-L of NF-L KO mice, compared to WT controls. Upregulation of TDP-43 alone may not be sufficient to cause cytoplasmic accumulations and extensive phosphorylation.

The band pattens of pTDP-43 immunoblots were different in the CC of both WT and NFL-KO mice at 12 months of age, as compared to the CTX and HIP of age-matched WT and NF-L KO mice. The CC of the brain had an unusual band at 37 kDa, which was not detected in the CTX and HIP. This finding is similar to a previous report that there was a band of pTDP-43 at about 30 kDa in FTLD-U type 3 pathology case that is associated with cortical and spinal tract degeneration (Neumann et al., 2009).

In conclusion, the findings in this chapter indicate that the absence of NF-L results in a small but significant increase in TDP-43, without cytoplasmic accumulations in CNS and motor dysfuntion in young and ageing animals, supporting the proposal

that upregulation of TDP-43 alone may not be sufficient to cause cytoplasmic accumulations and extensive phosphorylation.

Chapter 5: Myelination is altered in young and aged NF-L KO mice

5.1 Introduction

Oligodendrocytes are the glial cells that produce myelin sheaths around axons in the CNS (reviewed in Baumann and Pham-Dinh, 2001). Increasing evidence indicates that disturbance of myelination is associated with disease progression in many neurological conditions (Lazzarini 2004; Mitew et al., 2010; Philips et al., 2013). In addition, it has been proposed that non-neuronal cells, such as oligodendrocytes, may play an important role in neurodegeneration (Lee et al., 2012). Recently, oligodendrocytes have been particularly implicated in ALS pathogenesis with studies in human patients showing degeneration of oligodendrocytes, particularly in the grey matter of the spinal cord, which is compensated by increased proliferation and differentiation of oligodendrocyte precursor cells (Philips et al., 2013). However, these newly differentiated oligodendrocytes demonstrated reduced MBP suggesting that they are dysfunctional (Philips et al., 2013). Moreover, it has been reported that aberrant localization of TDP-43 to the cytoplasm rather than the nucleus, which is a morphological hallmark of the neuropathology of sporadic ALS, is not limited to motor neurons, but also occurs in oligodendrocytes (Neumann et al., 2007).

Substanital evidence suggests a complex interplay of signalling between myelinating cells such as oligodendrocytes and the axon (reviewed in Nave et al., 2008; Brahic et al., 2009). Myelination (in the CNS and PNS) plays a critical role in expansion of

axonal diameter through its interation with structural proteins such as NFs (de Waegh et al., 1992), which is referred to as radial axonal growth (Ohara et al., 1993; Zhu et al., 1997). The modulation of axonal caliber by myelin appears to be linked to changes in the phosphorylation state and dynamic behavior of NFs (de Waegh et al., 1992). The C-terminal 426 amino acid tail of the NF-M subunit is a determinant of axonal diameter in large caliber myelinated axons (Garcia et al., 2003; Rao et al., 2003). In adddition, variations in the number of KSP repeats within the NF-M carboxy terminal tail may contribute to an increase in axonal caliber (Barry et al., 2010). In this regard, MAG is known to signal to the axon, locally influencing the expression and phosphorylation of axonal NFs and their associated kinases (Hsieh et al., 1994; Dashiell et al., 2002; Nguyen et al., 2009). MBP protein is essential for the formation and maintenance of myelin in the CNS, and also interacts with cytoskeletal and signaling proteins such as MAG (Lazzarini, 2004; Vassall et al., 2013).

The effect of axonal signals on myelination, however, is less clear, although it is known that myelination is more likely to occur in larger caliber axons (Lazzarini, 2004) and that a number of axonal signals are responsible for induction of myelination of small caliber axons (reviewed in Nave et al., 2008). Recent studies have identified biophysical and signalling based mechanisms that are involved in axonal selection and myelin sheath generation by oligodendrocytes (Simons et al., 2013). Although demyelination is thought to be able to cause axonal degeneration (in diseases such as multiple sclerosis (MS) (Lazzarini, 2004), it is currently unclear how axonal abnormalities affect myelination (Simons et al., 2013).

A previous study has reported that the diameter of axons of upper motor neurons in the spinal cord of 2- and 6-month-old NF-L KO mice was decreased significantly while the thickness of their myelin sheath increased substantially (Zhu et al., 1997; Wu et al., 2008), indicating that NFs play a key role in maintaining axonal caliber. However, the effect of axonal NF alterations on myelination in the brain is not known. Furthermore, it is unclear how age-related changes in cytoskeletal proteins affect the structure and integrity of the myelin sheath. This thesis used a mouse model (NF-L KO mice), to determine the effects of the lack of NF-L on myelin proteins, and how this may be affected by ageing.

Chapter 3 showed that the absence of the NF-L gene and related protein resulted in the accumulation of other NFs in ageing neurons. In order to determine whether deficiency of the NF-L protein and reduced NFs result in myelin alterations during brain maturation and ageing of the CNS, this chapter investigated the relative protein levels and localisation of MBP and PLP in three regions of brain including CTX, HIP and CC, and three regions of spinal cord including SC-C, SC-T and SC-L of 10-week-old and 12-month-old NF-L KO mice relative to age-matched WT mice (C57BL/6). This chapter also measured the expression of CNPase in the brain of aged NF-L KO mice. This Chapter demonstrates that protein levels of MBP in the CTX and PLP in the CC are significantly reduced in the young and aged NF-L KO mice, supporting the proposal that NF-L is critical for the normal development and regulation of myelination.

5.2 Materials and Methods

5.2.1 Tissue preparation

For Western blot studies, protein samples of CTX, HIP, CC, SC-C, SC-T and SC-L from WT and NF-L KO mice at 10 weeks and 12 months of ages (n=3/group) were prepared as described in Section 2.3.1. For immunofluorescence studies, 40 μm coronal cryostat sections of brain and spinal cord from WT and NF-L KO mice at 10 weeks and 12 months of age (n=3/group) were prepared as described in Section 2.2.1.

5.2.2 Western blot

Proteins from the tissue samples of 10-week and 12 month-old NF-L KO mice and WT controls (n=3 each) were extracted as described in Section 2.3.2. Proteins (15 μg) were separated by 4-20% SDS-PAGE and blotted onto a PVDF membrane as described in Section 2.3.3. Primary antibody (Table 2.1) binding was visualised by goat anti-mouse or anti-rabbit IgG coupled to horseradish peroxidase (Dako, Denmark; Table 2.2). Immunoreactive bands were visualized and measured as described in Section 2.3.3.

5.2.3 Immunofluorescence

40 μm brain or spinal cord cryostat sections were washed with 0.01M PBS, followed by antigen retrieval and blocking of non-specific binding sites as described in Section 2.2.2. Sections were then incubated overnight at 4°C with primary antibodies

(Table 2.1) in diluent (0.3% Triton X-100, 0.01M PBS) as described in Section 2.2.3. Sections were washed with 0.01M PBS and incubated with Alexa Fluor 546 conjugated to a goat anti-rabbit secondary antibody or Alexa Fluor 488 conjugated to goat anti-mouse IgG (Molecular Probes, United States; Table 2.2). Sections were washed with PBS before mounting onto Fisher Super Frost Plus slides using fluorescent mounting medium (Dako, Denmark), and air-dried in the dark.

5.2.4 Data Collection and Analyses

Fluorescence-labeled sections were viewed with a Zeiss LSM 510 META confocal microscope (Carl Zeiss, Germany) and images acquired as described in Section 2.4.

For all experiments, a minimum of three mice was utilized for quantitative analysis as described in Section 2.6. Significance was determined by ANOVA and $p<0.05$ was considered as significant.

5.3 Results

5.3.1 MBP expression in the brains and spinal cords of young NF-L KO and WT mice

MBP is involved in the development, compaction, and stabilization of the multilamellar myelin sheath, and also interacts with cytoskeletal proteins (Harauz et al., 2004; Lazzarini, 2004; Philips et al., 2013). To quantify changes in myelination in the early stage of NF-L KO mice development, this thesis first examined MBP protein levels of NF-L KO mice at 10 weeks of age, compared to age-matched WT mice, by Western blot analysis of brain and spinal cord lysates. To determine whether there were regional alterations in the levels of MBP, this thesis studied three regions of brain—CTX, HIP, CC and three regions of spinal cord—SC-C, SC-T and SC-L. Three major MBP bands (17, 21 and 33 kDa) were detected by Western blot in all samples. When the density of all three MBP bands was measured together for quantification, there was a significant decrease ($p<0.05$) of MBP protein in the CTX of 10-week old NF-L KO compared to WT controls (Figure 5.1), but no difference with respect to the HIP and CC samples. In addtion, MBP protein levels were significantly decreased ($p<0.05$) in SC-T samples, but not for the SC-C and SC-L, from NF-L KO mice as compared to WT mice at 10 weeks of age (Figure 5.2).

5.3.2 MBP expression in the brains and spinal cords of 12-month old NF-L KO and WT mice

To determine if the expression of MBP was affected by ageing in NF-L KO mice, this thesis studied the expression of MBP in the CTX, HIP, CC, SC-C, SC-T and SC-

Figure 5.1 Western blot analysis of MBP protein expression in the CTX, HIP and CC of NF-L KO mice and WT controls at 10 weeks of age (n=3/group). Equal amounts of tissue sample were separated on a gel and labeled for MBP. Relative amounts of the protein expression of MBP were normalized against GAPDH (*$p<0.05$).

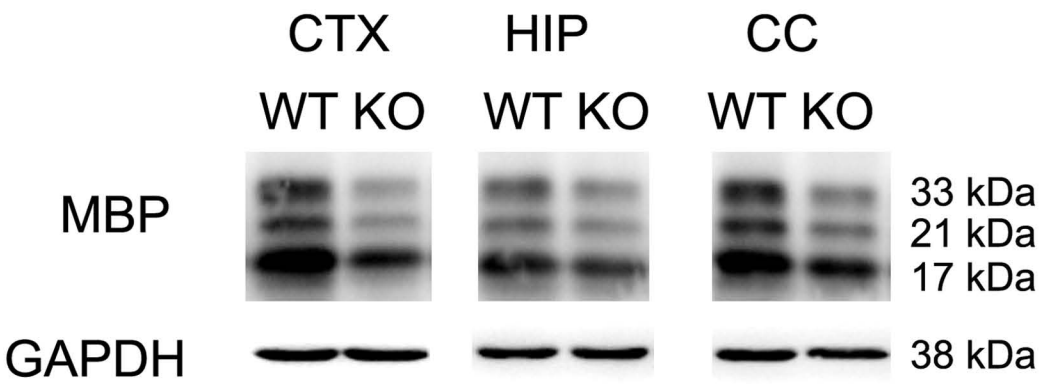
CTX
HIP
CC
WT KO
WT KO
WT KO
MBP
GAPDH
33 kDa
21 kDa
17 kDa
38 kDa

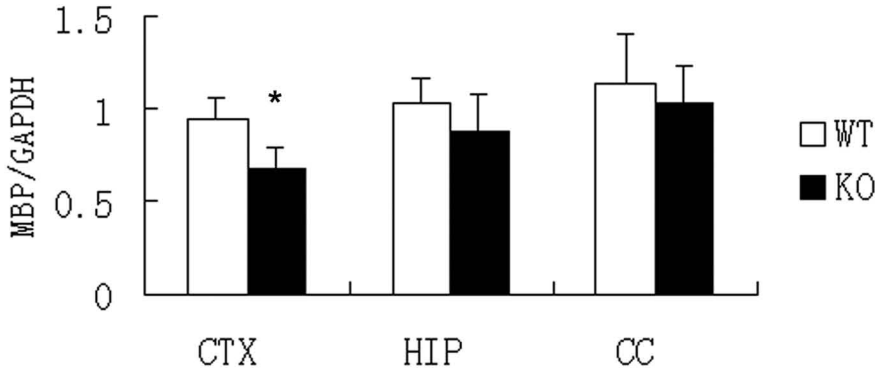
1.5
1
0.5
0
MBP/GAPDH
*
CTX
HIP
CC
WT
KO

Figure 5.2 Western blot analysis of MBP protein expression in the SC-C, SC-T, SC-L of NF-L KO mice and WT controls at 10 weeks of age (n=3/group). Equal amounts of tissue sample were separated on a gel and labeled with MBP. Relative amounts of the protein expression of MBP were normalized against GAPDH (*$p<0.05$).

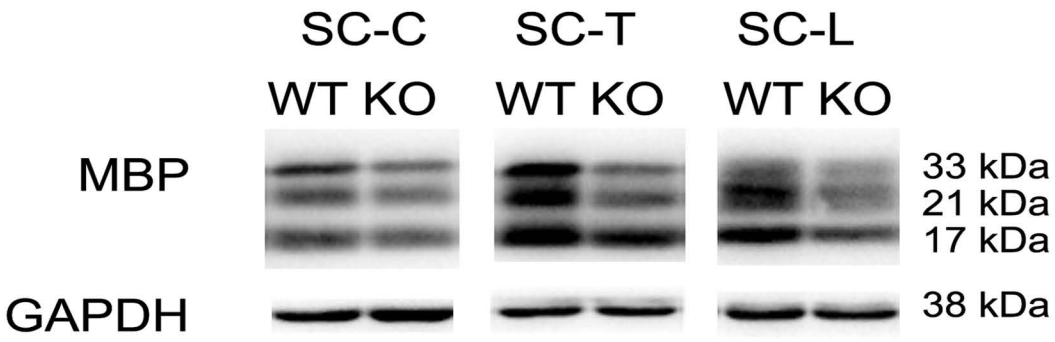
SC-C
SC-T
SC-L
WT KO
WT KO
WT KO
MBP
GAPDH
33 kDa
21 kDa
17 kDa
38 kDa

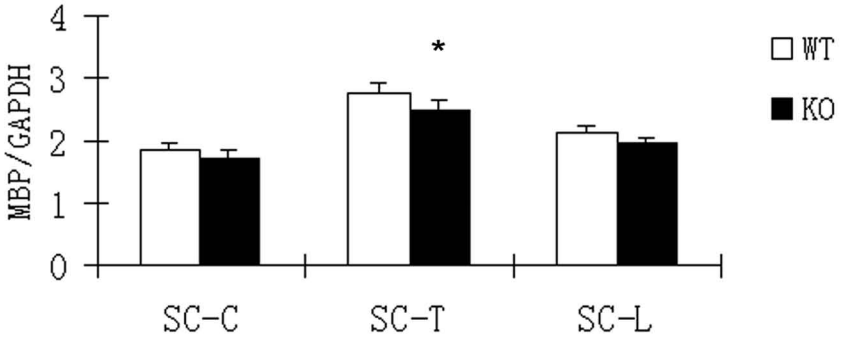
MBP/GAPDH
4
3
2
1
0
*
WT
KO
SC-C
SC-T
SC-L

L of NF-L KO animals relative to WT mice at 12 months of age by Western blot analysis. It was observed that, similar to young mice, the protein level of MBP was significantly reduced ($p<0.05$) in the CTX of 12-month-old NF-L KO mice, but not for the HIP and CC, compared with age-matched WT mice (Figure 5.3). In addtion, MBP protein levels were significantly decreased ($p<0.05$) in the SC-T of NF-L KO mice at 12 months of age, compared to WT controls, but there was no statistical difference with respect to the SC-C and SC-L samples. (Figure 5.4).

To further study the expression of MBP in the CTX of ageing NF-L KO mice, 40 μm brain sections from 12-month old NF-L KO mice and from age matched controls were immunolabelled with antibodies against MBP. MBP labelling was decreased in the CTX of NF-L KO mice (Figure 5.5 B) at 12 months of age, compared to WT mice (Figure 5.5 A).

5.3.3 PLP protein expression in the brains and spinal cords of WT and NF-L KO mice at 10 weeks of age

In addition to MBP, PLP is another major protein of membranes of the myelin sheath in the CNS (Lazzarini, 2004; Philips et al., 2013). To further quantify changes in myelination in early stage of NF-L KO mice, protein samples from the CTX, HIP, CC, SC-C, SC-T and SC-L of NF-L KO mice and WT controls at 10 weeks, were immunoblotted with an antibody to PLP. A single PLP band (30 kDa) was detected by Western analysis. PLP was significantly decreased ($p<0.05$) in the CC of NF-L KO mice at 10 weeks, but not for the CTX and HIP, compared with age-matched WT mice (Figure 5.6). In the SC-L of 10-week-old NF-L KO mice, PLP abundance

Figure 5.3 Western blot analysis of MBP protein expression in the CTX, HIP and CC of NF-L KO mice and WT controls at 12 months of age (n=3/group). Equal amounts of tissue sample were separated on a gel and labeled with MBP. Relative amounts of the protein expression of MBP were normalized against GAPDH (*$p<0.05$).

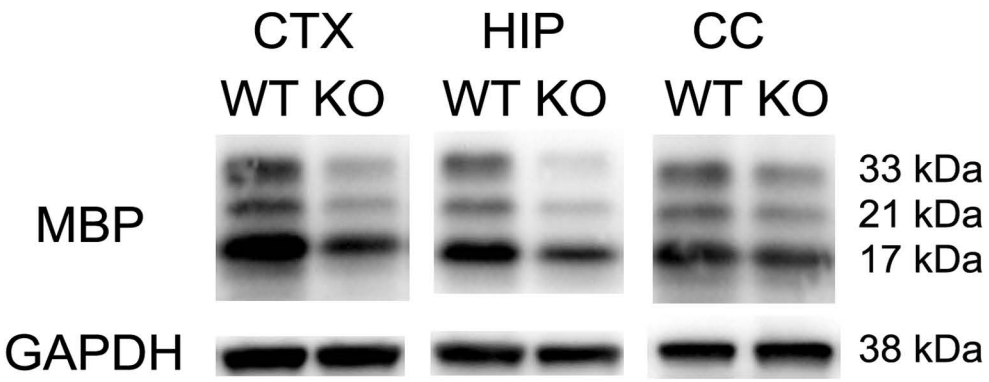
CTX
HIP
CC
WT KO
WT KO
WT KO
MBP
GAPDH
33 kDa
21 kDa
17 kDa
38 kDa

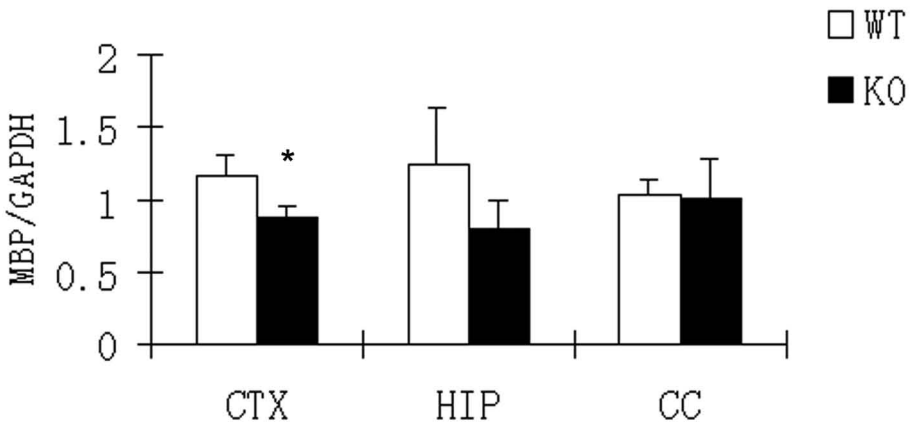
WT
KO
MBP/GAPDH
2
1.5
1
0.5
0
*
CTX
HIP
CC

Figure 5.4 Western blot analysis of MBP protein expression in the SC-C, SC-T, SC-L of NF-L KO mice and WT controls at 12 months of age (n=3/group). Equal amounts of tissue were separated on a gel and labeled with MBP. Relative amounts of the protein expression of MBP were normalized against GAPDH (*$p<0.05$).

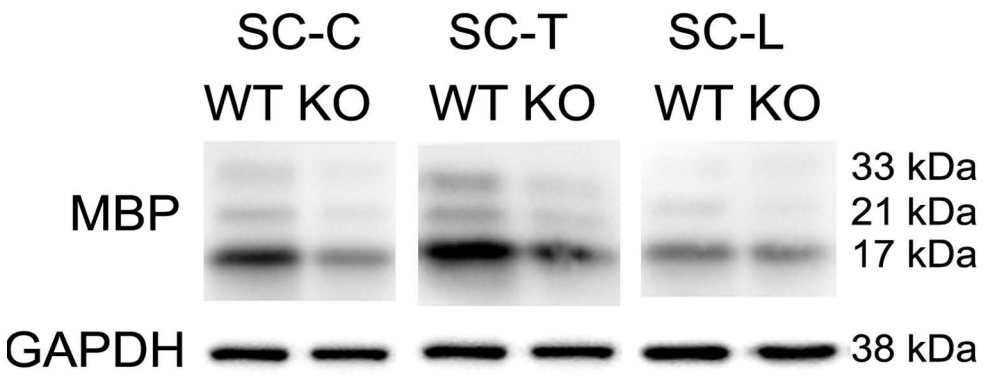
SC-C
SC-T
SC-L
WT KO
WT KO
WT KO
MBP
33 kDa
21 kDa
17 kDa
GAPDH
38 kDa

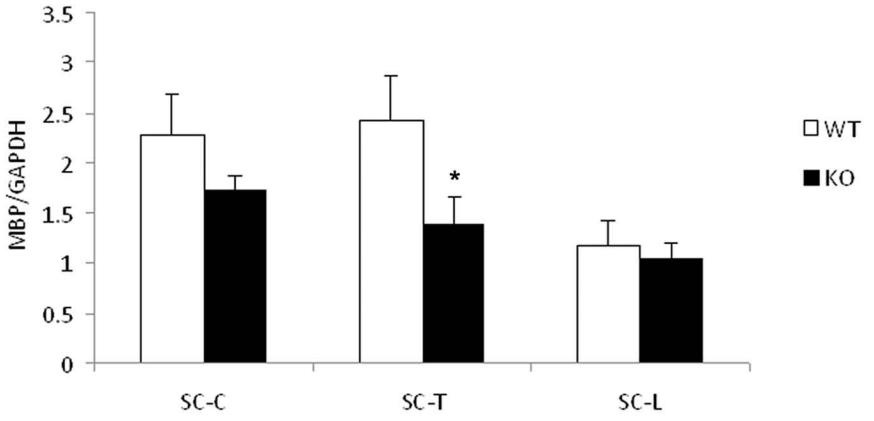
3.5
3
2.5
2
1.5
1
0.5
0
MBP/GAPDH
*
WT
KO
SC-C
SC-T
SC-L

Figure 5.5 Confocal images of MBP labeling in the CTX of WT (A) and NF-L KO (B) mice at 12 months of age. Scale bars, A, B 100 μm.

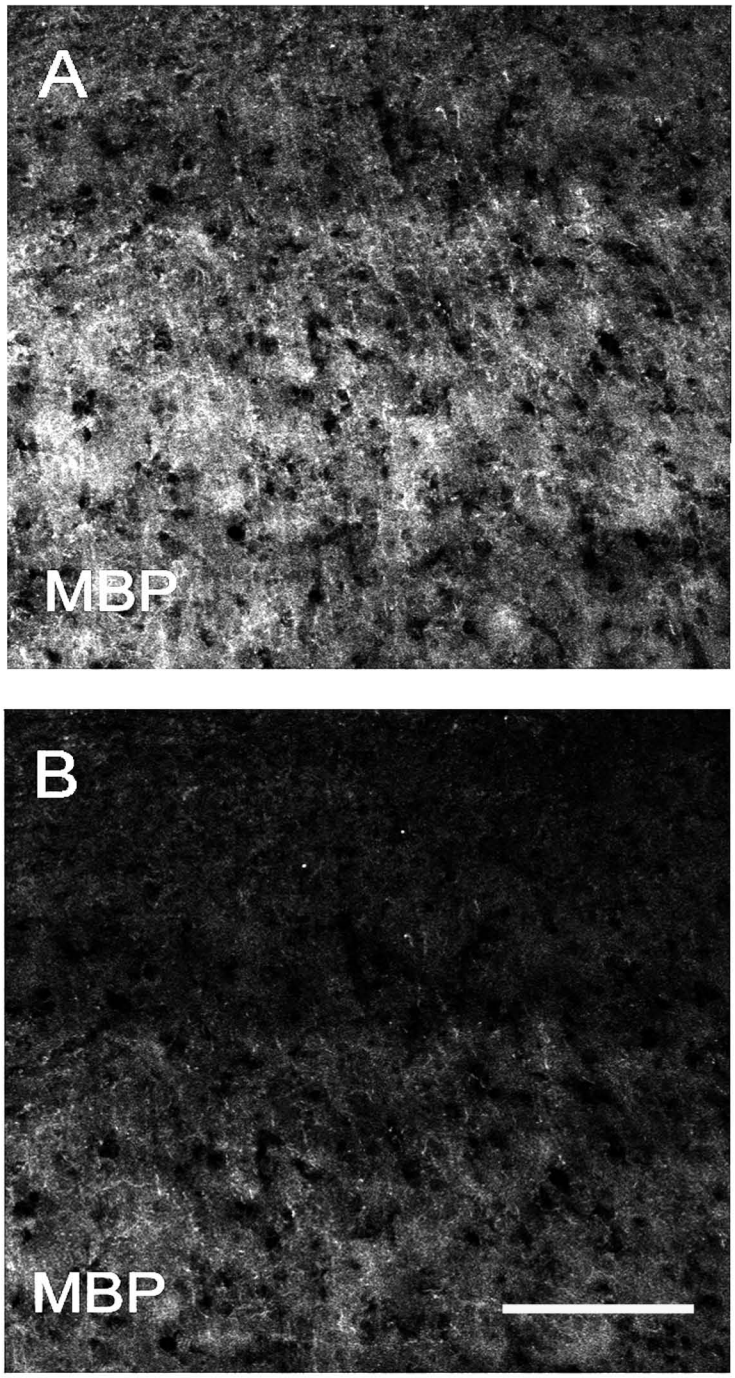
A
MBP
B
MBP

Figure 5.6 Western blot analysis of PLP protein expression in the CTX, HIP and CC of NF-L KO mice and WT controls at 10 weeks of age (n=3/group). Equal amounts of tissue sample were separated on a gel and labeled with PLP. Relative amounts of the protein expression of PLP were normalized against GAPDH (*$p<0.05$).

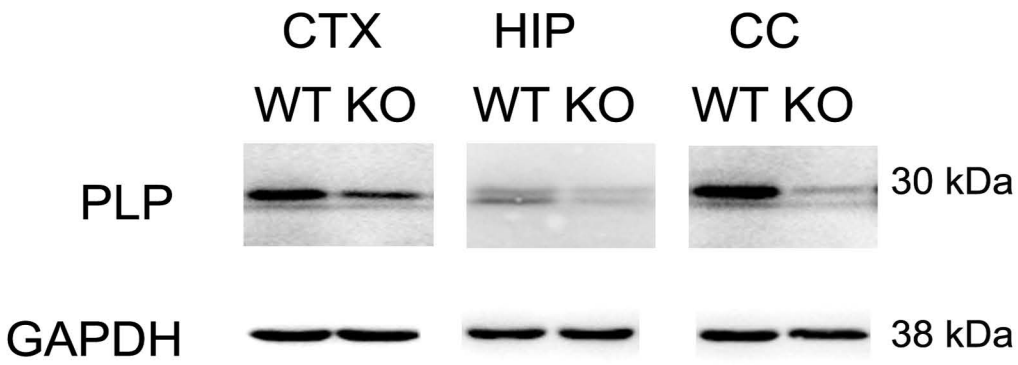
CTX
HIP
CC
WT KO
WT KO
WT KO
PLP
30 kDa
GAPDH
38 kDa

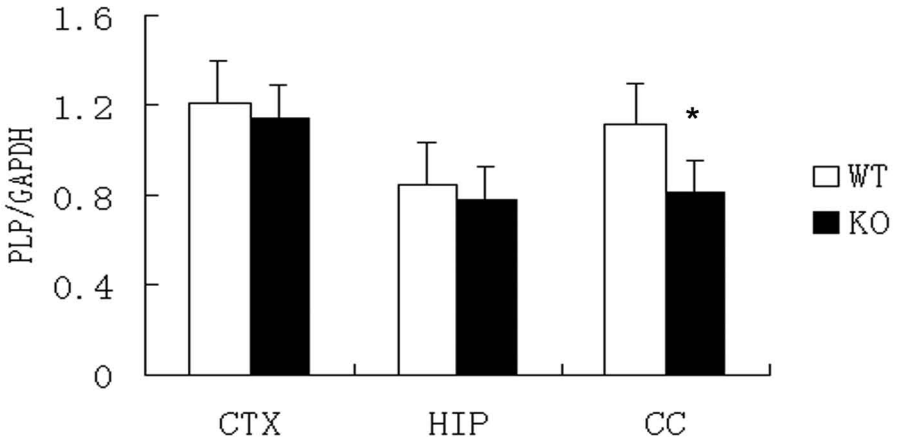
1.6
1.2
0.8
0.4
0
PLP/GAPDH
*
WT
KO
CTX
HIP
CC

was significantly ($p<0.05$) lower than that in WT mice, but there was no difference with respect to the SC-C and SC-T samples. (Figure 5.7).

5.3.4 PLP protein expression in the brains and spinal cords of 12-month-old NF-L KO and WT mice

To determine if the expression of PLP was affected by ageing in NF-L KO mice, Western blot analysis was used to investigate the protein levels of PLP in brain and spinal cord of 12-month-old WT and NF-L KO mice. The protein levels of PLP were significantly ($p<0.05$) decreased in the CC of 12-month-old NF-L KO mice, compared with age-matched WT mice (Figure 5.8). However, there was no significant change of PLP protein levels in the SC-C, SC-T and SC-L of NF-L KO mice at 12 months of age, compared to WT controls (Figure 5.9).

5.3.5 The protein expression of CNPase in the brains of 10-week-old and 12-month-old NF-L KO mice

The protein expression levels of CNPase, a structural component of myelin (Braun et al. 2004), were assessed by densitometric analysis of Western blots. The expression levels of CNPase were not significantly altered in the brain (CTX, HIP and CC) between WT and NF-L KO mice at 10 weeks (Figure 5.10) or 12 months (Figure 5.11) of age.

Figure 5.7 Western blot analysis of PLP protein expression in the SC-C, SC-T, SC-L of NF-L KO mice and WT controls at 10 weeks of age (n=3/group). Equal amounts of tissue sample were separated on a gel and labeled with PLP. Relative amounts of the protein expression of PLP were normalized against GAPDH (*$p<0.05$).

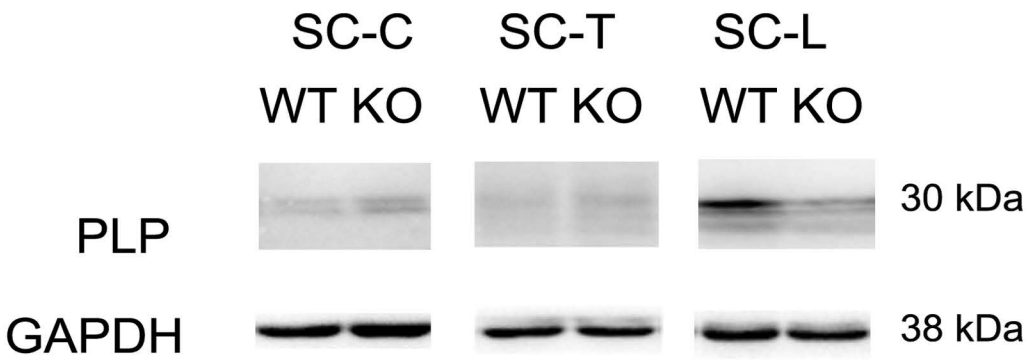
SC-C
SC-T
SC-L
WT KO
WT KO
WT KO
PLP
30 kDa
GAPDH
38 kDa

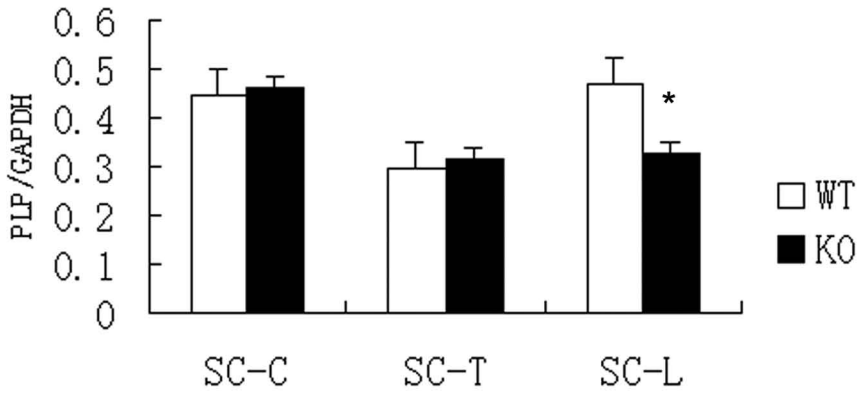
0.6
0.5
0.4
0.3
0.2
0.1
0
PLP/GAPDH
*
WT
KO
SC-C
SC-T
SC-L

Figure 5.8 Western blot analysis of PLP protein expression in the CTX, HIP and CC of NF-L KO mice and WT controls at 12 months of age (n=3/group). Equal amounts of tissue sample were separated on a gel and labeled with PLP. Relative amounts of the protein expression of PLP were normalized against GAPDH (*$p<0.05$).

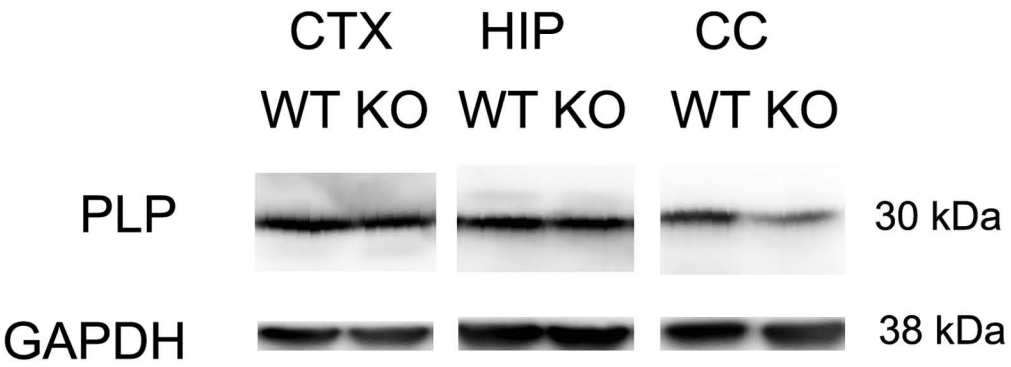
CTX
HIP
CC
WT KO
WT KO
WT KO
PLP
30 kDa
GAPDH
38 kDa

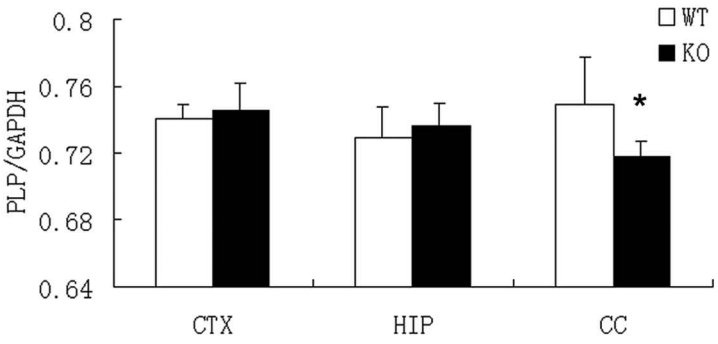
WT
KO
0.8
0.76
0.72
0.68
0.64
PLP/GAPDH
*
CTX
HIP
CC

Figure 5.9 Western blot analysis of PLP protein expression in the SC-C, SC-T, SC-L of NF-L KO mice and WT controls at 12 months of age (n=3/group). Equal amounts of tissue sample were separated on a gel and labeled with PLP. Relative amounts of the protein expression of PLP were normalized against GAPDH.

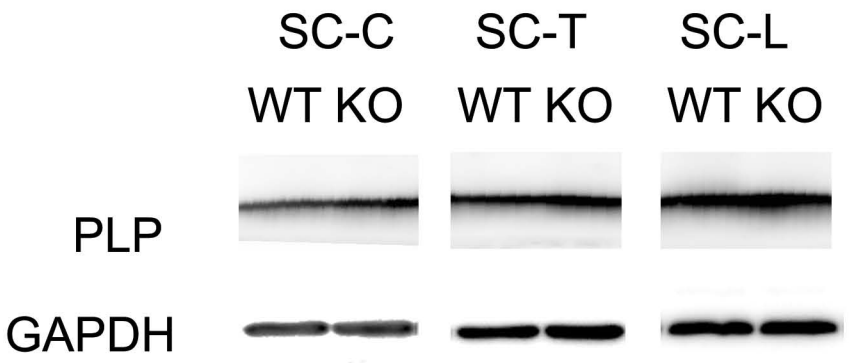
SC-C
SC-T
SC-L
WT KO
WT KO
WT KO
PLP
GAPDH

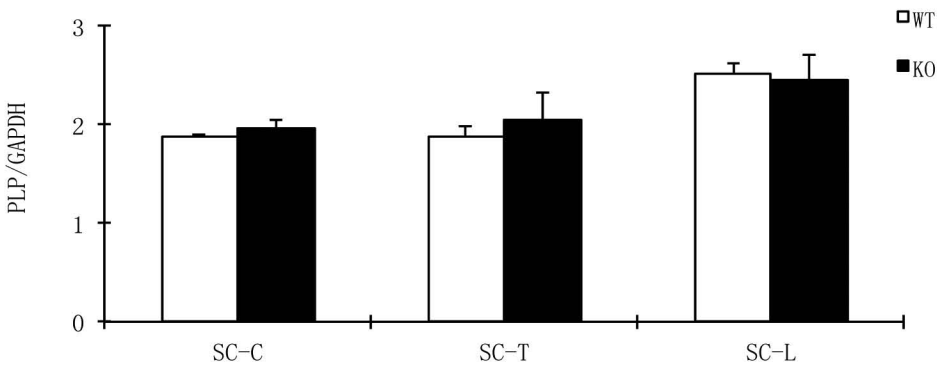
WT
KO
PLP/GAPDH
3
2
1
0
SC-C
SC-T
SC-L

Figure 5.10 Western blot analysis of CNPase protein expression in the CTX, HIP and CC of NF-L KO mice and WT controls at 10 weeks of age (n=3/group). Equal amounts of tissue sample were separated on a gel and labeled with CNPase. Relative amounts of the protein expression CNPase were normalized against GAPDH.

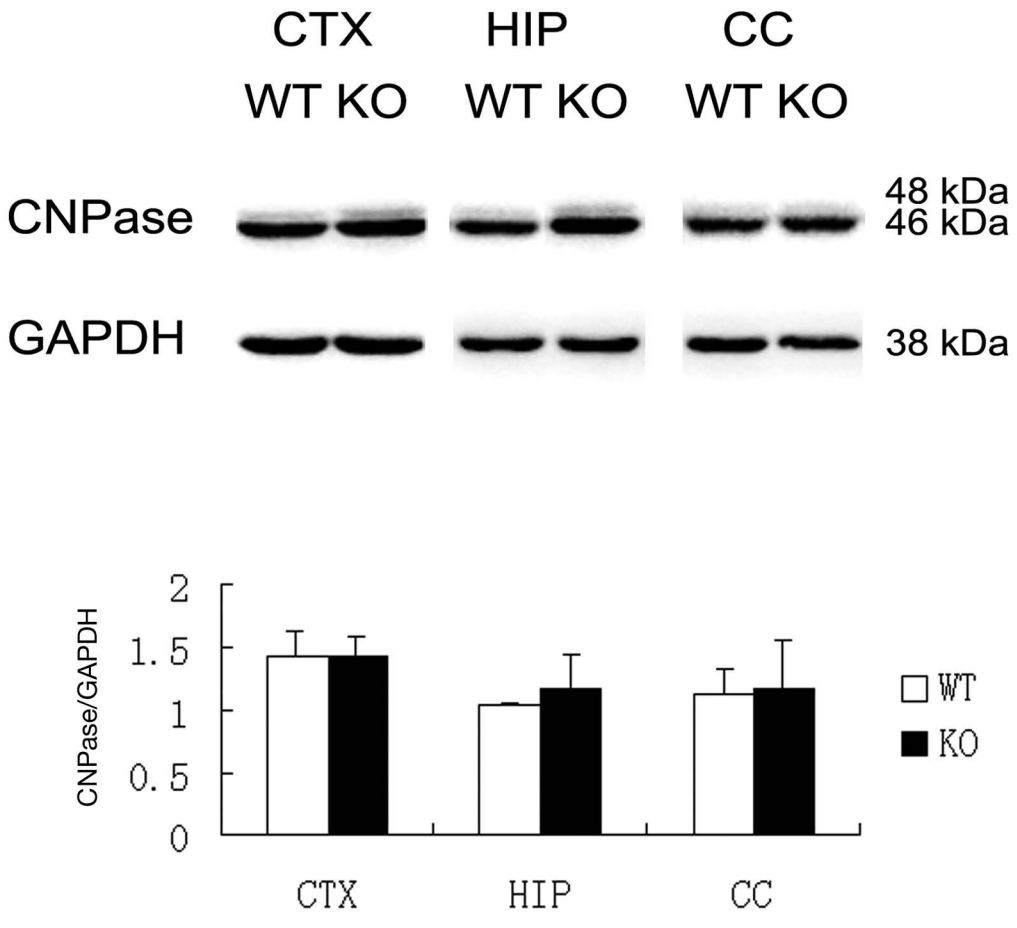
CTX
HIP
CC
WT KO
WT KO
WT KO
CNPase
GAPDH
48 kDa
46 kDa
38 kDa
CNPase/GAPDH
2
1.5
1
0.5
0
CTX
HIP
CC
WT
KO

Figure 5.11 Western blot analysis of CNPase protein expression in the CTX, HIP and CC of NF-L KO mice and WT controls at 12 months of age (n=3/group). Equal amounts of tissue sample were separated on a gel and labeled with CNPase. Relative amounts of the protein expression of CNPase were normalized against GAPDH.

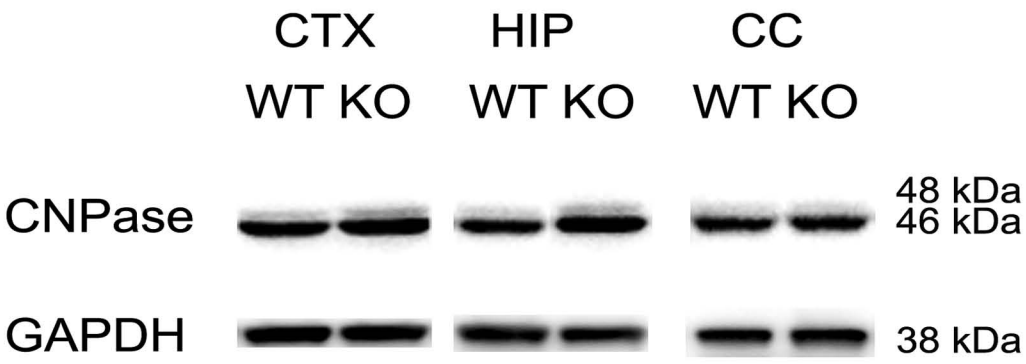
CTX
HIP
CC
WT KO
WT KO
WT KO
CNPase
GAPDH
48 kDa
46 kDa
38 kDa

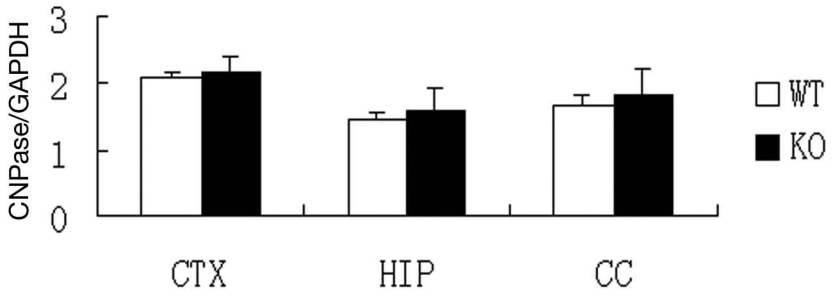
CNPase/GAPDH
3
2
1
0
CTX
HIP
CC
WT
KO

5.4 Discussion

MBP and PLP proteins are the major proteins of CNS myelin (Lazzarini, 2004). However, whether there is an interaction between NF-L and myelin in the CNS during ageing remains undefined. Based on the previous findings in Chapter 3 and 4, this chapter sought to determine the relationship between NF-L and myelin in the CNS by examing the expression of MBP, PLP and CNPase proteins in the CNS of 10-week old and 12-month old NFL-KO mice.

Previous reports have shown that the alteration in NF content in axons of NF-L KO mice results in both a decrease in axonal diameters and an increase in the thickness of myelin sheath (Zhu et al., 2007; Wu et al., 2008). These prior studies on myelin were only in the SC of NF-L KO mice up to the age of 6 months. The data presented in this chapter confirm and extend that of other studies on the myelination changes in NF-L KO mice. This chapter is the first report on the expression of MBP and PLP proteins in the CTX, HIP, CC, SC-C, SC-T, SC-L of young and aged NF-L KO mice as compared to age-matched WT controls. It was found that myelin proteins were reduced in some regions of CNS between NF-L KO and WT mice, such as MBP protein in CTX and SC-T, as well as PLP protein in CC and SC-L. However, most myelin proteins in most CNS regions investigated were not differentially expressed relative to WT samples.

The data presented in this chapter suggest that the deletion of NF-L is associated with the decrease of myelin-associated proteins in particular regions of the brain, particularly MBP proteins in the CTX and PLP protein in the CC.

In this chapter, although there were some differences in myelin protein levels in particular regions of CNS between NF-L KO and WT, most myelin proteins (such as CNPase) were not different between these groups. These results are consistent with the data reported previously that no obvious changes in expression of CNPase and MAG proteins, as OL markers, were detected in the brain and spinal cord of NF-L KO mice and WT controls at 2 and 6 months, and that the number of oligodendrocytes is maintained in young NF-L KO mice (Wu et al., 2008).

NFs are major determinants of axonal caliber in large myelinated nerve fibers and NF phosphorylation is regulated by myelination of neurons (Garcia et al., 2003; Rao et al., 2003). A previous study has shown that the absence of NF-L results in an increase in the thickness of myelin sheaths and/or decrease in the diameter of axons in the spinal cord (Wu et al., 2008). MBP, the main myelin protein in CNS, plays roles both in myelin development and homeostasis by interacting with cytoskeletal proteins, such as actin and tubulin (Harauz et al., 2004; Vassall et al., 2013). The reduced MBP protein in the SC-T and PLP protein in the SC-L of NF-L KO mice, may arise from less axons becoming myelinated in KO animals caused by NFs disruption. Alternatively, the same proportion of axons may be myelinated but the thickness may be changed. Combined with the motor dysfuntion in NF-L KO mice shown in Chapter 4, the findings in this chapter suggest that the alteration of expression of MBP and PLP proteins in some region of spinal cord may influence normal axon physiology and motor functions of NF-L KO mice.

In conclusion, the findings in this chapter suggest that the loss of NF-L can cause the reduced expression of MBP and PLP proteins in some regions of CNS in young and aged mice, potentially contributing to the motor dysfuntion, without the change of other myelin proteins (such as CNPase protein) in the CNS, under the condition of CNS compensating for the loss of NF-L described in Chapter 3 and 4.

Chapter 6: General Discussion and future studies

NF proteins play a key role in the maintenance and remodeling of the neuronal cytoskeleton, and seem to contribute to several neurodegenerative diseases. However, the detailed functions of NF proteins in the neuronal cytoskeleton, also with respect to myelination and neurodegenerative disease-related proteins, remains unknown. This thesis primarily sought to investigate the consequences of the lack of NF-L on the adaptive capacity of the neuronal cytoskeleton in adulthood and ageing, as well as the consequences related to myelination and the NF RNA-binding protein (TDP-43), in order to understand the functions of NFs in neuronal cell biology, ageing and neurodegenerative diseases.

6.1 Summary of the main findings

In summary, the data presented in this thesis suggest that the loss of NF-L causes a functional impairment, as well as interesting changes in neurodegenerative disease-related proteins such as TDP-43, but, overall, there seems to be a range of compensatory mechanisms in the CNS in response to the absence of NF-L. Additionally, the changes in cytoskeletal proteins, TDP-43 protein, myelin proteins and motor function caused by the loss of NF-L have some differences between young and aged NF-L KO mice.

6.1.1 Adaptive capacity of the cytoskeleton

It was reported in this thesis (Chapter 3) that lack of NF-L protein was associated with significantly decreased expression of dephosphorylated NFs, NF-M and INT proteins in adult (5 months) NF-L KO mice, while significantly reduced protein levels of phosphorylated NFs and increased INT protein level in aged (12 months) NF-L KO mice. For the protein levels of NF-P, there was a greater decrease in aged NF-L KO mice than in adult NF-L KO mice, compared to age-matched-WT controls. In addition, protein levels of class III neuron-specific beta-tubulin and MAP2 were significantly increased in both adult and aged NF-L KO mice. These findings from this thesis indicate that the absence of NF-L leads to disruption of other NF subunits, causing intracellular aggregation without gross structural changes in cortical neurons.

6.1.2 Reactive changes in disease-related proteins such as TDP-43 in young and aged NF-L KO mice

As described in Chapter 4, the expression of TDP-43 proteins was relatively increased in the CTX of aged (12 months) NF-L KO mice. However, there were no signifcant changes in the levels of TDP-43 protein in the CTX, HIP or CC between young (10 weeks) NF-L KO and WT mice. In addition, the changes in the spinal cord also differed from young and aged NF-L KO mice. In young mice, the expression levles of TDP-43 were significantly increased in all three regions of spinal cord, including SC-C, SC-T and SC-L; while in aged NF-L KO mice, the protein level of TDP-43 was only significantly increased in the SC-L. In both the CTX and SC-L of aged NF-L KO mice, there were no pathologic accumulations of TDP-43. For the protein levels of pTDP-43, there were no significant changes in the

CTX, HIP and CC of both young and aged NF-L KO mice relative to WT controls. Moreover, the changes in the level of pTDP-43 protein in the spinal cord differed between young and aged NF-L KO mice. The expression of pTDP43 was significantly increased in the SC-T of young NF-L KO mice and in the SC-C of aged NF-L KO mice, compared to WT controls. However, there were no significant alterations in the expression of pTDP-43 protein in the CTX, HIP and the CC of young and aged NF-L KO mice.

6.1.3 Alterations in myelin proteins

The data in Chapter 5 indicated that the deletion of NF-L resulted in the decrease of MBP proteins in the CTX, SC-T and PLP proteins in the CC in both young (10 weeks) and aged (12 months) NF-L KO mice, relative to WT mice. In addition, there was a significant decrease in the expression of PLP protien in the SC-L of young NF-L KO mice. However, there were no significant alterations of the expression of PLP proteins in the SC-C, SC-T and SC-L of ageing NF-L KO mice and no significant changes of CNPase proteins in the CTX, HIP and CC of young and aged NF-L KO mice, compared to age-matched WT controls.

6.1.4 Functional deficits

This thesis (Chapter 4) demonstrated that both young (4 months) and aged (12 months) NF-L KO mice showed motor dysfunction. Additionally, the motor dysfunction of aged NF-L mice was worse than that of young NF-L mice.

6.2 Discussion and implications of main thesis findings

The individual chapters in this thesis have discussed extensively the findings from each of the three main studies undertaken. The remainder of this discussion will therefore examine the broader findings of this thesis.

6.2.1 The cellular changes induced by loss of NF-L

The findings in this thesis illustrate that the loss of NF-L can produce cytoskeletal changes and alteration of TDP-43 and myelin proteins at the cellular level.

Cytoskeletal abnormalities have been described during neurodegenerative processes, such as in ALS (reviewed in Liu et al., 2004a). In addition, alterations in the stoichiometry of NF expression has been demonstrated in ALS (Wong et al., 2000). The data presented in this thesis suggest that the loss of NF-L affects the remainder of the cytoskeleton by causing disruption of other NF proteins as well as compensatory increase of some element proteins of MTs.

Oligodendrocytes can establish myelin and provide metabolic support to neurons (Lee et al., 2012). ALS-linked genes have been proposed to accelerate disease by directly impairing the function of oligodendrocytes (Kang et al., 2013). The data from this thesis suggest that the absence of NF-L also results in alteration of expression levels of myelin proteins in oligodendrocytes and supports the hypothesis that the loss of NF-L may cause the impaired functions of oligodendrocytes in CNS (Zhu et al., 1997; Wu et al., 2008).

6.2.2 NFs contribute to the selective vulnerability of neurons and glia to pathology

As discussed in Chapter 4, deletion of NF-L was associated with increased expression of TDP-43 proteins in the CTX and SC-L of aged animals. In addition, the data in Chapter 5 showed that the loss of NF-L resulted in the decrease in MBP protein levels in the CTX and PLP protein expression in the CC at 10 weeks and 12 months of age. It is interesting that the absence of NF-L had specific regional effects in the CNS. The data from this thesis indicated that selective vulnerability could manifest at the cellular level, with specific regions of neuronal and glial populations being differentially affected by the absence of NF-L. These findings are similar to a previous report that the accumulation of pathologic TDP-43 protein is only found in layer 5 pyramidal neurons in frontal CTX and spinal motor neurons of TDP-43 mutant transgenic mice, recapitulating the phenomenon of selective vulnerability (Wegorzewska et al., 2009). Furthermore, these findings are consistent with previous studies that NF alterations in different NF transgenic mice caused dysfunction of specific neuronal populations such as motor neurons (Cote et al., 1993; Xu et al., 1993b; Lee et al., 1994; Collard et al., 1995) and Purkinje cells of the cerebellum (Tu et al., 1997).

6.2.3 NF-L KO mice are phenotypically different from WT mice through adulthood and ageing

Although the general behavior of NF-L KO mice was indistinguishable from that of WT controls, it has been reported that, as early as 6 months, depletion of the NF-L

protein is sufficient to cause mild sensorimotor dysfunctions and spatial deficits, but without overt signs of paresis, using T-maze, stationary beam, coat hanger, rotorod and water maze tests (Dubois et al., 2005). Deficits in these tests also have been found in NF-H LacZ transgenic mice (Lalonde et al., 1999), potentially attributable to reduced motor neuron axonal caliber (Eyer and Peterson, 1994) or Purkinje cell number (Tu et al., 1997).

As discussed in Chapter 4, the data in this thesis showed that lack of NF-L resulted in motor dysfunction in both young and aged NF-L KO mice, indicating the relationship between motor function and the effects of NF-L deletion. These results suggest that the loss of NF-L is linked with gait abnormalities of animals, albeit NF-L KO mice have no overt signs of paresis (Dubois et al., 2005). The likely cause of the motor dysfunction in NF-L KO mice may be due to retarded conduction velocity of peripheral nerves, as a result of reduced axonal caliber associated with lower density of NFs in these axons (Zhu et al., 1997; Kriz et al., 2000). Moreover, the deficits may also be due to brain alterations (Dubois et al., 2005, and this thesis). It is not yet known why the NF-L KO animals show a motor deficit from early ages (4 months), and this motor deficit was amplified in the same mouse model during ageing (12 months). The most likely explanation is that the loss of NF-L causes the dysfunction of NFs and the impairment in NFs in NF-L mice increases with age.

6.2.4 The nervous system compensates for the absence of NF-L

Consistent with the previous reports (Conde et al., 1994; DeFelipe et al., 1999; Park et al., 2000; Yamashita et al., 2003), the data presented in this thesis implied that lack

of NF had no effect on overall cortical structure and there were no changes in the expression of particular myelin proteins, as well as TDP43 and pTDP43 protein in some regions of CNS, which indicated the ability of the nervous system to compensate for the loss of NF-L and reduced neurofilaments.

Increased protein expression of other cytoskeletal components (class III neuron-specific beta-tubulin and MAP2) in both adult and aged NF-L KO mice may be reflective of compensatory changes taking place in the CNS. Combined with a previous study (Zhu et al., 1997), this finding may explain why NF-L KO mice exhibit general behaviors indistinguishable from WT mice, without a major neurological/behavioural phenotype (Dubois et al., 2005). The adaptive changes in other cytoskeletal proteins underlines the inter-relationship of NFs, MTs and MFs in maintaining neuronal structure and function (reviewed in Julien et al., 2000). Associated with a recent study (Blizzard et al., 2013), the data from this thesis suggests that the loss of NF-L can partially be compensated for by increased INT expression, reflecting a partially adaptive response in which INT may act as a substitute for NF-L in the assembly of NFs, albeit the density of these structures is reduced in axons (Blizzard et al., 2011, 2013). Additionally, the small increases of TDP-43 without aggregates in some regions of the CNS in NF-L KO mice may be due to the ability of the CNS to compensate for the absence of NF-L. These findings support the hypothesis that the CNS may compensate for the lack of NFs by regulating these other elements through feedback loops which may be related to the retrograde transport of cytoskeletal proteins and resultant signalling (Zhu et al., 1997; Li et al., 2006; reviewed in Yuan et al., 2012).

6.2.5 The role of NF-L in the nervous system

Consistent with previous studies (Zhu et al., 1997; Wong et al., 2000; Li et al., 2006; Wu et al., 2008), the data presented in this thesis shows that lack of NF-L could lead to NF disruption including accumulation of other NF proteins during adulthood and ageing. This is consistent with a previous report that showed that alterations in NF-L mRNA stability were associated with intraneuronal NF aggregate formation (Ge et al., 2003). These findings indicate that, although INT may potentially compensate for the assembly of NFs, the loss of NF-L still results in NF abnormalities, supporting the previous studies on the important role that the NF-L subunit has in the assembly of NFTPs (Carter et al., 1997; Zhu et al., 1997; reviewed in Julien, 1999 and Liu et al., 2004a; reviewed in Yuan et al., 2012). These findings also support the proposal that NF-L plays an important role in the transport of NF proteins into axons by regulating the interaction between other NFs (Zhu et al.,1997; Perez-Olle et al., 2005; reviewed in Yuan et al., 2012).

Oligodendrocyte dysfunction leads to axon degeneration in several diseases (Lee et al., 2012). Increasing evidence indicates that NFs have an important role in oligodendrocyte development and myelin formation (Zhu et al.,1997; Wu et al., 2008; reviewed in Yuan et al., 2012; Blizzard et al., 2013). It has been reported that the regeneration of myelinated axons following crush injury of peripheral nerves was found to be abnormal in NF-L KO mice, which indicated that NF-L plays a critical role in the maturation of regenerating myelinated axons (Zhu et al., 1997; Blizzard et al., 2013). NF-L has been confirmed as a major determinant of axonal calibers in the ventral root of lower motorneurons of the spinal cord (Zhu et al., 1997). The

alteration in NF content in axons of NF-L KO mice resulted in both a significant decrease in axonal diameter and a significant increase in the thickness of the myelin sheath up to 6 months of age (Wu et al., 2008). The data on myelin proteins presented in this thesis confirms and extends other studies on the myelination changes in NF-L KO mice (Zhu et al., 1997; Wu et al., 2008), supporting the previous proposal that NF-L, a component of myelinated axons, and/or NF assembly, may play a direct role in maintaining the normal morphology of myelinated axons (Zhu et al., 1997; Okonkwo et al., 1998; Zhu et al., 2007; Wu et al., 2008).

6.2.6 Could loss of NF-L be a primary driver of pathology in neurodegenerative disease and/or contribute to disease pathology?

NF abnormalities related to neuronal dysfunction have been reported in many neurodegenerative disorders (Liu et al., 2004a). Additionally, TDP-43 pathology has been detected in ALS, PD, AD and FTLD (Amador-Ortiz et al., 2007a, b; Higashi et al., 2007; Bigio et al., 2008; Uryu et al., 2008). However, the relationship between TDP-43 pathology and NF abnormalities, and whether the loss of NF-L could be a primary driver of such pathology, remains unknown.

It has been reported that miRNAs could be responsible for the selective suppression of NF-L mRNA in ALS (Campos-Melo et al., 2013). Several of the proteins associated with ALS have the capacity to regulate the stability of NF-L mRNA (Volkening et al., 2009), including TDP-43 protein, which stabilizes NF-L mRNA (Strong et al., 2007). The data from this thesis indicates that the deletion of NF-L is associated with NF aggregate formation and an increase of the expression of NF

RNA-binding protein (TDP-43). These findings provide evidence of a potential link between NF-L protein loss and TDP-43 protein, suggesting that NF-L protein is potentially a negative regulator of TDP-43 in the CNS (Moisse et al., 2009) and TDP-43 may play a role in maintaining the stability of NFs (Strong et al., 2007; Volkening et al., 2009). It is not yet known how NF-L regulates TDP-43. The most likely explanation is that NF-L is involved in the regulation of TDP-43 through a cell-signaling pathway. Early loss of NFs in the pathological cascade leading to neuronal degeneration has been described in PD (Gai et al., 2004) as well as AD (Vickers et al., 1992). Combined with these previous reports, the findings in this thesis support the proposal that NF-L has a putative role in mediating the response of the neuronal cytoskeleton through the signaling pathway linked to TDP-43 and the regulation of TDP-43 (Moisse et al., 2009; Ihara al., 2013).

One of the common features of TDP-43 pathology is increased phosphorylation of this protein (Neumann et al., 2009). Several studies have shown that antibodies specific for pTDP-43 can recognize TDP-43 proteinopathies in humans (Hasegawa et al., 2008, Neumann et al., 2009) and in transgenic mice overexpressing TDP-43 (Wils et al., 2010; Igaz et al., 2011; Cannon et al., 2012). The data presented in this thesis on the band pattern of pTDP43 immunoblots are similar to previous reports on ALS/FTLD (Hasegawa et al., 2008) and FTLD-U type 3 pathology cases (Neumann et al., 2009).

As discussed in Chapter 4, although small upregulation of TDP-43 alone may not be sufficient to result in pathological accumulation of TDP-43 and extensive phosphorylation, it may be potentially linked with motor function impairments

associated with the loss of NF-L. This may be attributed to higher amounts of TDP-43 producing more neurotoxic mediators to the neurons (Swarup et al., 2011a) and the loss of NF-L in the neurons increases their vulnerability to toxic mediators.

The data presented in this thesis showed that the loss of NF-L may cause abnormally increased TDP-43, which was similar to a previous report that tau pathology generally preceded TDP-43 pathology. This indicated that TDP-43 pathology may arise as a secondary consequence of a primary proteinopathy (Clippinger et al., 2013) and/or cytoskeletal disruption. However, a previous report has shown that that NF-H protein was downregulated by 1.5-fold and NF-L protein by 2-fold in the spinal cord extracts of 10-month-old TDP-43 G348C mutant mice as compared with non-transgenic mice, because of increased expression of TDP-43 (Swarup et al., 2011a). Combined with previous studies, the findings from this thesis suggest that loss of NF-L could contribute to disease-like pathological alterations including motor dysfunction and abnormal increase of TDP-43 without aggregates, although it doesn't rule out the possibility that, in humans, the alterations of NFs are sufficient to drive TDP-43 pathology.

6.3 Future studies

In this thesis, the effects of loss of NF-L on cytoskeletal proteins, NF RNA-binding protein and myelin proteins *in vivo* have been investigated by using young and aged NF-L KO mice. These findings have provided more insight into how the absence of NF-L affects the cytoskeleton, TDP-43 and myelination. However, the cellular model of NF-L deficiency is perhaps more useful to investigate the celluar signaling linked to TDP-43. Therefore, important future work would be to study the signaling pathway *in vitro* by using cultured neurons and glia from NF-L KO mice.

In this thesis, the expression of myelin proteins including MBP, PLP and CNPase proteins in young and aged NF-L KO mice have been examined by Western blotting and immunochemistry. However, these biochemical studies are not sufficient for examining myelin structure and morphology. Therefore, studies of the thickness of myelin sheaths and diameter of myelinated axons in adult and aged NF-L KO mice are needed in future, as the information will help to more definitively delineate potential alteration of myelin sheaths in adult and aged NF-L KO mice. Thus, transmission electron microscope studies of myelin sheaths should be included in future studies.

In this thesis, the motor dysfunction associated with the loss of NF-L protein were demonstrated in 4-month-old and 12-month-old NF-L KO mice. Thus, further study may require examination of motor impairments in younger mice (eg 1, 2 or 3 months old) to confirm whether the motor dysfunction begins from earlier stages of development. In addition, future work could involve an evaluation of the progression

of the motor dysfunction of NF-L KO mice together with cognitive evaluation to investigate the effects of loss of NF-L on both spinal cord and brain functions.

6.4 Conclusions

• The absence of NF-L protein resulted in the alteration of NFs and other cytoskeletal proteins during adulthood and ageing.

• Cortical and lumbar spinal cord regions were susceptible to TDP-43 alterations in NF-L KO mice during ageing.

• NF-L protein or mRNA is potentially a negative regulator for the expression of TDP-43 in the CNS.

• The lack of NF-L protein resulted in the alteration of myelin proteins in both young and older animals.

• The deletion of NF-L protein was associated with motor dysfunction of young and aged mice.

This thesis has documented that the lack of NF-L alters the expression of cytoskeletal proteins and disrupts other NF subunits without gross structural changes in cortical neurons. In addition, the changes of NF results in the increase of TDP-43 expression level, linked with motor function impairments, without pathologic accumulation. These findings provide new insights into the roles of NF in ageing and neuro-degenerative processes.

References

Abe A, Numakura C, Saito K, Koide H, Oka N, Honma A, Kishikawa Y，Hayasaka K (2009). Neurofilament light chain polypeptide gene mutations in Charcot-Marie-Tooth disease: nonsense mutation probably causes a recessive phenotype. J Hum Genet 54:94–97.

Abhyankar MM, Urekar C, Reddi PP (2007). A novel CpG-free vertebrate insulator silences the testis-specific SP-10 gene in somatic tissues: role for TDP-43 in insulator function. J Biol Chem 282 :36143-36154.

Adalbert R, Nogradi A, Babetto E, Janeckova L, Walker SA, Kerschensteiner M, Misgeld T, Coleman MP (2009). Severely dystrophic axons at amyloid plaques remain continuous and connected to viable cell bodies. Brain 132:402-416.

Adalbert R, Coleman MP (2012). Axon pathology in age-related neurodegenerative disorders. Neuropathol Appl Neurobiol doi: 10.1111/j.1365-2990.2012.01308.x. [Epub ahead of print]

Ahlijanian MK, Barrezueta NX, Williams RD, Jakowski A, Kowsz KP, McCarthy S, Coskran T, Carlo A, Seymour PA, Burkhardt JE, Nelson RB, McNeish JD (2000). Hyperphosphorylated tau and neurofilament and cytoskeletal disruptions in mice overexpressing human p25, an activator of cdk5. Proc Natl Acad Sci USA 97: 2910-2915.

Alami NH, Jung P, Brown A (2009). Myosin Va increases the efficiency of neurofilament transport by decreasing the duration of long-term pauses. J Neurosci 29: 6625-6634.

Al-Chalabi A, Andersen PM, Nilsson P, Chioza B, Andersson JL, Russ C, Shaw CE, Powell JF, Leigh PN (1999). Deletions of the heavy neurofilament subunit tail in amyotrophic lateral sclerosis. Hum Mol Genet 8:157-164.

Al-Chalabi A, Miller CC (2003). Neurofilaments and neurological disease. Bioessays 25: 346-355.

Al-Chalabi A, Jones A, Troakes C, King A, Al-Sarraj S, van den Berg LH (2012). The genetics and neuropathology of amyotrophic lateral sclerosis. Acta Neuropathol 124:339–352.

Al-Saif A, Al-Mohanna F, Bohlega S (2011). A mutation in sigma-1 receptor causes juvenile amyotrophic lateral sclerosis. Ann Neurol:10.1002/ana.22534.

Amador-Ortiz C, Ahmed Z, Zehr C, Dickson DW (2007a). Hippocampal sclerosis dementia differs from hippocampal sclerosis in frontal lobe degeneration. Acta Neuropathol (Berl) 113:245–252.

Amador-Ortiz C, Lin WL, Ahmed Z, Personett D, Davies P, Duara R, Graff-Radford NR, Hutton ML, Dickson DW (2007b). TDP-43 immunoreactivity in hippocampal sclerosis and Alzheimer's disease. Ann Neurol 61:435–445.

Andrews H, White K, Thomson C, Edgar J, Bates D, Griffiths I, Turnbull D, Nichols P (2006). Increased axonal mitochondrial activity as an adaptation to myelin deficiency in the Shiverer mouse. J Neurosci Res 83:1533-1539.

Arai T, Mackenzie IR, Hasegawa M, Nonoka T, Niizato K, Tsuchiya K, Iritani S, Onaya M, Akiyama H (2009). Phosphorylated TDP-43 in Alzheimer's disease and dementia with Lewy bodies. Acta Neuropathol 117:125–136.

Armstrong RA, Hamilton RL, Mackenzie IR, Hedreen J, Cairns NJ (2013). Laminar distribution of the pathological changes in sporadic frontotemporal lobar degeneration with transactive response (TAR) DNA-binding protein of 43 kDa (TDP-43) proteinopathy: a quantitative study using polynomial curve fitting. Neuropathol Appl Neurobiol 39:335-347.

Arnold ES, Ling SC, Huelga SC, Lagier-Tourenne C, Polymenidou M, Ditsworth D, Kordasiewicz HB, McAlonis-Downes M, Platoshyn O, Parone PA, Da Cruz S, Clutario KM, Swing D, Tessarollo L, Marsala M, Shaw CE, Yeo GW, Cleveland DW (2013a). ALS-linked TDP-43 mutations produce aberrant RNA splicing and adult-onset motor neuron disease without aggregation or loss of nuclear TDP-43. PNAS 110:E736-745.

Arnold SJ, Dugger BN, Beach TG (2013b).TDP-43 deposition in prospectively followed, cognitively normal elderly individuals: correlation with argyrophilic grains but not other concomitant pathologies. Acta Neuropathol: [Epub ahead of print].

Arquint M, Roder J, Chia LS, Down J, Wilkinson O, Bayley H, Braun P, Dunn R (1987). Molecular cloning and primary structure of myelin-associated glycoproteins. Proc Natl Acad Sci USA 84**:**600–604.

Aruga J, Okano H, Mikoshiba K (1991). Identification of the new isoforms of mouse myelin basic protein: the existence of exon 5a. J Neurochem 56:1222–1226.

Avila J, Soares H, Fanarraga ML, Zabala JC (2008). Isolation of microtubules and

microtubule proteins. Curr Protoc Cell Biol Chapter 3:Unit 3.29

Ayala YM, Zago P, D'Ambrogio A, Xu YF, Petrucelli L, Buratti E and Baralle FE (2008). Structural determinants of the cellular localization and shuttling of TDP-43. J Cell Sci 121: 3778-3785.

Baas PW, Vidya Nadar C, Myers KA (2006). Axonal transport of microtubules: the long and short of it. Traffic 7: 490-498.

Baker M, Mackenzie IR, Pickering-Brown SM, Gass J, Rademakers R, Lindholm C, Snowden J, Adamson J, Sadovnick AD, Rollinson S, Cannon A, Dwosh E, Neary D, Melquist S, Richardson A, Dickson D, Berger Z, Eriksen J, Robinson T, Zehr C, Dickey CA, Crook R, McGowan E, Mann D, Boeve B, Feldman H, Hutton M (2006). Mutations in progranulin cause tau-negative frontotemporal dementia linked to chromosome 17. Nature 442:916–919.

Barry DM, Carpenter C, Yager C, Golik B, Barry KJ, Shen H, Mikse O, Eggert LS, Schulz DJ, Garcia ML (2010). Variation of the neurofilament medium KSP repeat sub-domain across mammalian species: implications for altering axonal structure. J Exp Biol 213:128-136.

Basso M, Giraudo S, Corpillo D, Bergamasco B, Lopiano L, Fasano M (2004). Proteome analysis of human substantia nigra in Parkinson's disease. Proteomics 4: 3943-3952.

Baumann N, Pham-Dinh D (2001). Biology of oligodendrocyte and myelin in the mammalian central nervous system. Physiol Rev 81: 871–927.

Beaulieu JM, Robertson J, Julien JP (1999a). Interactions between peripherin neurofilaments in cultured cells: disruption of peripherin assembly by the NF-M and NF-H subunits. Biochem Cell Biol 77: 41-45.

Beaulieu JM, Nguyen MD, Julien JP (1999b). Late onset death of motor neurons in mice overexpressing wildtype peripherin. J Cell Biol 147: 531–544.

Benson DL, Mandell JW, Shaw G, Banker G (1996). Compartmentation of alpha internexin and neurofilament triplet proteins in cultured hippocampal neurons. J Neurocytol 25:181–196.

Bergeron C, Beric-Maskarel K, Muntasser S, Weyer L, Somerville MJ, Percy ME (1994). Neurofilament light and polyadenylated mRNA levels are decreased in amyotrophic lateral sclerosis motor neurons. J Neuropathol Exp Neurol 53:221-230.

Berges R, Balzeau J, Takahashi M, Prevost C, Eyer J (2012). Structure-function analysis of the glioma targeting NFL-TBS.40-63 peptide corresponding to the tubulin-binding site on the light neurofilament subunit. PLoS One 7:e 49436.

Bershadsky AD,Vasiliev JM (1988). Cytoskeleton. Plenum Publishing Corporation, New York and London: 298.

Bigio EH (2008). TAR DNA-binding protein-43 in amyotrophic lateral sclerosis, frontotemporal lobar degeneration, and Alzheimer disease. Acta Neuropathol 116:135–140.

Black MM, Lasek RJ (1980). Slow components of axonal transport: two cytoskeletal networks. J Cell Biol 86 :616-623.

Blake-Hodek KA, Cassimeris L, Huffaker TC (2010). Regulation of microtubule dynamics by Bim1 and Bik1, the budding yeast members of the EB1 and CLIP-170 families of plus-end tracking proteins. Mol Biol Cell 21:2013-2023.

Blizzard CA, King AE, Haas MA, O'Toole DA, Vickers JC, Dickson TC (2009). Axonal shearing in mature cortical neurons induces attempted regeneration and the reestablishment of neurite polarity. Brain Res 1300: 24-36.

Blizzard CA, Chuckowree JA, King AE Hosie KA, McCormack GH, Chapman JA, Vickers JC, Dickson TC (2011). Focal damage to the adult rat neocortex induces wound healing accompanied by axonal sprouting and dendritic structural plasticity. Cereb Cortex 21: 281-291.

Blizzard CA, King AE, Vickers J, Dickson T (2013). Cortical murine neurons lacking the neurofilament light chain protein have an attenuated response to injury in vitro. J Neurotrauma:[Epub ahead of print].

Blokhuis AM, Groen EJ, Koppers M, van den Berg LH, Pasterkamp RJ (2013). Protein aggregation in amyotrophic lateral sclerosis. Acta Neuropathol 125:777-794.

Bouquet C, Soares S, von Boxberg Y, Ravaille-Veron M, Propst F, Nothias F (2004). Microtubule-associated protein 1B controls directionality of growth cone migration and axonal branching in regeneration of adult dorsal root ganglia neurons. J Neurosci 24: 7204-7213.

Bocquet A, Berges R, Frank R, Robert P, Peterson AC, Eyer J (2009). Neurofilaments bind tubulin and modulate its polymerization. J Neurosci 29: 11043–11054.

Boison D, Bussow H, D'Urso D, Muller HW, Stoffel W (1995). Adhesive properties of proteolipid protein are responsible for the compaction of CNS myelin sheaths. J Neurosci 15: 5502–5513.

Bradl M, Lassmann H (2010). Oligodendrocytes: biology and pathology. Acta Neuropathol 119: 37–53.

Brahic M, Roussarie JP (2009). Axon–Myelin Interactions during a Viral Infection of the Central Nervous System. PLoS Pathog 5:e1000519.

Braun PE, Lee J, Gravel M (2004). 2′,3′-cyclic nucleotide 3′-phosphodiesterase: Structure, biology and function. In Lazzarini RA (ed.), Myelin biology and disorders. San Diego, CA: Elsevier Academic Press 499–522.

Brettschneider J, Petzold A, Sussmuth SD, Ludolph AC, Tumani H (2006). Axonal damage markers in cerebrospinal fluid are increased in ALS. Neurology 66: 852-856.

Brophy PJ, Boccaccio GL, Colman DR (1993). The distribution of myelin basic protein mRNAs within myelinating oligodendrocytes. Trends Neurosci 16:515–521.

Brown A (2003). Live-cell imaging of slow axonal transport in cultured neurons. Methods Cell Biol 71:305-323.

Budini M, Buratti E, Stuani C, Guarnaccia C, Romano V, De Conti L, Baralle FE (2012). Cellular model of TAR DNA-binding protein 43 (TDP-43) aggregation based on its C-terminal Gln/Asn-rich region. J Biol Chem 287:7512-7525.

Bugiani O (2007). The many ways to frontotemporal degeneration and beyond. Neurol Sci 28:241-244.

Buki KB, Zheng JQ (2002). Growth Cone Turning Induced by Direct Local Modification of Microtubule Dynamics. J Neurosci 22: 9358-9367.

Buratti E, Baralle FE (2001). Characterization and functional implications of the RNA binding properties of nuclear factor TDP-43, a novel splicing regulator of CFTR exon 9. J Biol Chem 276:36337-36343.

Buratti E, Baralle FE (2008). Multiple roles of TDP-43 in gene expression, splicing regulation, and human disease. Front Biosci 13:867– 878.

Buratti E, De Conti L, Stuani C, Romano M, Baralle M, Baralle F (2010). Nuclear factor TDP-43 can affect selected microRNA levels. FEBS J 277: 2268–2281.

Busche MA, Eichhoff G, Adelsberger H, Abramowski D, Wiederhold KH, Haass C,

Staufenbiel M, Konnerth A, Garaschuk O (2008). Clusters of hyperactive neurons near amyloid plaques in a mouse model of Alzheimer's disease. Science 321:1686–1689.

Caccamo A, Majumder S, Deng JJ, Bai Y, Thornton FB, Oddo S (2009). Rapamycin rescues TDP-43 mislocalization and the associated low molecular mass neurofilament instability. J Biol Chem 284:27416-27424.

Camp AJ, Wijesinghe R (2009). Calretinin: Modulator of neuronal excitability. Int J Biochem Cell Biol 41:2118–2121.

Campagnoni AT, Skoff RP (2001). The pathobiology of myelin mutants reveal novel biological functions of the MBP and PLP genes. Brain Pathol 11: 74–91.

Campagnoni AT, Campagnoni CW (2004). Myelin basic protein gene. In R. A. Lazzarini (ed.), Myelin biology and disorders. San Diego, CA: Elsevier Academic Press:387–400.

Campbell GR, Mahad DJ (2011). Mitochondria as crucial players in demyelinated axons: lessons from neuropathology and experimental demyelination. Autoimmune Dis 2011:262847.

Campos-Melo D, Droppelmann CA, He Z, Volkening K, Strong MJ (2013). Altered microRNA expression profile in amyotrophic lateral sclerosis: a role in the regulation of NFL mRNA levels. Mol Brain 6:26.

Cannon A, Yang B, Knight J, Farnham IM, Zhang Y, Wuertzer CA, D'Alton S, Lin WL, Castanedes-Casey M, Rousseau L, Scott B, Jurasic M, Howard J, Yu X, Bailey R, Sarkisian MR, Dickson DW, Petrucelli L, Lewis J (2012). Neuronal sensitivity to TDP-43 overexpression is dependent on timing of induction. Acta Neuropathol 123:807-823.

Carden MJ, Trojanowski JQ, Schlaepfer WW, Lee VM (1987). Two-stage expression of neurofilament polypeptides during rat neurogenesis with early establishment of adult phosphorylation patterns. J Neurosci 7: 3489–3504.

Carpenter S (1968). Proximal axonal enlargement in motor neuron disease. Neurology 18:841–851.

Carpenter DA, Ip W (1996). Neurofilament triplet protein interactions: evidence for the preferred formation of NF-L-containing dimers and a putative function for the end domains. J Cell Sci 109:2493-2498.

Carter JE, Robertson J, Anderton BH, Gallo JM (1997). Incorporation of NF-L into

keratin filaments in transfected epithelial cells. NeuroReport 8:2225–2228.

Carter J, Gragerov A, Konvicka K, Elder G, Weinstein H, Lazzarini RA (1998). Neurofilament (NF) assembly; divergent characteristics of human and rodent NF-L subunits. J Biol Chem 273: 5101-5108.

Carter RJ, Lione LA, Humby T, Mangiarini L, Mahal A, Bates GP, Dunnett SB, Morton AJ (1999). Characterization of progressive motor deficits in mice transgenic for the human Huntington's disease mutation. J Neurosci 19:3248-3257.

Cassimeris L, Spittle C (2001). Regulation of microtubule-associated proteins. Int Rev Cytol 210:163–226.

Chernov KG, Barbet A, Hamon L, Ovchinnikov LP, Curmi PA, Pastré D (2009). Role of microtubules in stress granule assembly: microtubule dynamical instability favors the formation of micrometric stress granules in cells. J Biol Chem 284:36569-36580.

Chien CL, Liem RK (1994). Characterization of the mouse gene encoding the neuronal intermediate filament protein alpha-internexin. Gene 149:289-292.

Ching GY, Liem RK (1993). Assembly of type IV neuronal intermediate filaments in nonneuronal cells in the absence of preexisting cytoplasmic intermediate filaments. J Cell Biol 122: 1323–1335.

Ching GY, Liem RK (1998). Roles of head and tail domains in alpha-internexin's self-assembly and coassembly with the neurofilament triplet proteins. J Cell Sci 111:321-333.

Ching GY, Liem RKH (2006). Neuronal Intermediate Filaments and Neurodegenerative Diseases: Intermediate Filaments. Landes Biosciences, Austin, TX:35–51.

Chrast R, Saher G, Nave KA, Verheijen MH (2011). Lipid metabolism in myelinating glial cells: lessons from human inherited disorders and mouse models. J Lipid Res. 52:419-434.

Chuckowree JA, Vickers JC (2003). Cytoskeletal and morphological alterations underlying axonal sprouting after localized transection of cortical neuron axons in vitro. J Neurosci 23:3715-3125.

Cleveland DW, Monteiro MJ, Wong PC, Gill SR, Gearhart JD, Hoffman PN (1991). Involvement of neurofilaments in the radial growth of axons. J Cell Sci Suppl

15: 85-95.

Clippinger AK, D'Alton S, Lin WL, Gendron TF, Howard J, Borchelt DR, Cannon A, Carlomagno Y, Chakrabarty P, Cook C, Golde TE, Levites Y, Ranum L, Schultheis PJ, Xu G, Petrucelli L, Sahara N, Dickson DW, Giasson B, Lewis J (2013). Robust cytoplasmic accumulation of phosphorylated TDP-43 in transgenic models of tauopathy. Acta Neuropathol 126:39-50.

Cochard P, Paulin D (1984). Initial expression of neurofilaments and vimentin in the central and peripheral nervous system of the mouse embryo in vivo. J Neurosci 4:2080-2094.

Collard JF, Côté F, Julien JP (1995). Defective axonal transport in a transgenic mouse model of amyotrophic lateral sclerosis. Nature 375: 61-64.

Colombrita C, Zennaro E, Fallini C, Weber M, Sommacal A, Buratti E, Silani V, Ratti A (2009). TDP-43 is recruited to stress granules in conditions of oxidative insult. J Neurochem 111:1051-1061.

Conde F, Lund JS, Jacoboowitz DM, Baimbridge KG, Lewis DA (1994). Local circuit neurons immunoreactive for calretinin, calbindin D-28k or parvalbumin in monkey prefrontal cortex: distribution and morphology. J Comp Neurol 341: 95-116.

Cook C, Zhang YJ, Xu YF, Dickson DW, Petrucelli L (2008). TDP-43 in neurodegenerative disorders. Expert Opin Biol Ther 8:969-978.

Cote F, Collard JF, Julien JP (1993). Progressive neuronopathy in transgenic mice expressing the human neurofilament heavy gene: a mouse model of amyotrophic lateral sclerosis. Cell 73:35–46.

Couillard–Després S, Zhu Q, Wong PC, Price DL, Cleveland DW, Julien JP (1998). Protective effect of neurofilament heavy gene overexpression in motor neuron disease induced by mutant superoxide dismutase. Proc Natl. Acad Sci USA 95:9626–9630.

Crow JP, Ye YZ, Strong M, Kirk M, Barnes S, Beckman JS (1997). Superoxide dismutase catalyzes nitration of tyrosines by peroxynitrite in the rod and head domains of neurofilament-L. J Neurochem 69:1945-1953.

Cruts M, Gijselinck I, van der Zee J, Engelborghs S, Wils H, Pirici D, Rademakers R, Vandenberghe R, Dermaut B, Martin JJ, van Duijn C, Peeters K, Sciot R, Santens P, De Pooter T, Mattheijssens M, Van den Broeck M, Cuijt I,

Vennekens K, De Deyn PP, Kumar-Singh S, Van Broeckhoven C (2006). Null mutations in progranulin cause ubiquitin-positive frontotemporal dementia linked to chromosome 17q21. Nature 442:920–924.

Cui C, Stambrook PJ, Parysek LM (1995). Peripherin assembles into homopolymers in SW13 cells. J Cell Sci 108:3279-3284.

Cummings BJ, Head E, Ruehl W, Milgram NW, Cotman CW (1996). The canine as an animal model of human aging and dementia. Neurobiol Aging 17: 259–268.

Dashiell SM, Tanner SL, Pant HC, Quarles RH (2002). Myelin-associated glycoprotein modulates expression and phosphorylation of neuronal cytoskeletal elements and their associated kinases. J Neurochem 81:1263–1272.

De Jonghe P, Mersivanova I, Nelis E, Del Favero J, Martin JJ, Van Broeckhoven C, Evgrafov O, Timmerman V (2001). Further evidence that neurofilament light chain gene mutations can cause Charcot-Marie-Tooth disease type 2E. Ann Neurol 49:245-249.

de Waegh SM., Lee VM, Brady ST (1992). Local modulation of neurofilament phosphorylation, axonal caliber, and slow axonal transport by myelinating Schwann cells. Cell 68:451-463.

Dejesus-Hernandez M, DeJesus-Hernandez M, Mackenzie IR, Boeve BF, Boxer AL, Baker M, Rutherford NJ, Nicholson AM, Finch NA, Flynn H, Adamson J, Kouri N, Wojtas A, Sengdy P, Hsiung GY, Karydas A, Seeley WW, Josephs KA, Coppola G, Geschwind DH, Wszolek ZK, Feldman H, Knopman DS, Petersen RC, Miller BL, Dickson DW, Boylan KB, Graff-Radford NR, Rademakers R (2011). Expanded GGGGCC hexanucleotide repeat in noncoding region of C9ORF72 causes chromosome 9p-linked FTD and ALS. Neuron 72:245–256.

DeFelipe J, Gonzalez-Albo M, Del Rio M, Elston G (1999). Distribution and patterns of connectivity of interneuronscontaining calbindin, calretinin, and parvalbumin in visual areas of the occipital and temporal lobes of the macaque monkey. J Comp Neurol 412: 515−526.

Deng HX, Hentati A, Tainer JA, Iqbal Z, Cayabyab A, Hung WY, Getzoff ED, Hu P, Herzfeldt B, Roos RP, et al (1993). Amyotrophic lateral sclerosis and structural defects in Cu, Zn superoxide Dismutase. Science 261:1047–1051.

Deng Y, Li B, Liu F, Iqbal K, Grundke-Iqbal I, Brandt R, Gong CX (2008). Regulation between O-GlcNAcylation and phosphorylation of neurofilament-M and their dysregulation in Alzheimer disease. FASEB J 22: 138-145.

Deng HX, Chen W, Hong ST, Boycott KM, Gorrie GH, Siddique N, Yang Y, Fecto F, Shi Y, Zhai H, Jiang H, Hirano M, Rampersaud E, Jansen GH, Donkervoort S, Bigio EH, Brooks BR, Ajroud K, Sufit RL, Haines JL, Mugnaini E, Pericak-Vance MA, Siddique T (2011). Mutations in UBQLN2 cause dominant X-linked juvenile and adult-onset ALS and ALS/dementia. Nature 477:211–215.

Dent EW, Kalil K (2001). Axon branching requires interactions between dynamic microtubules and actin filaments. J Neurosci 21: 9757-9769.

Dent EW, Gertler FB (2003). Cytoskeletal dynamics and transport in growth cone motility and axon guidance. Neuron 40:209-227.

Dent EW, Barnes AM, Tang F, Kalil K (2004). Netrin-1 and semaphorin 3A promote or inhibit cortical axon branching, respectively, by reorganization of the cytoskeleton. J Neurosci 24: 3002-3012.

Dickson TC, Chuckowree JA, Chuah MI, West AK, Vickers JC (2005). Alpha-Internexin immunoreactivity reflects variable neuronal vulnerability in Alzheimer's disease and supports the role of the beta-amyloid plaques in inducing neuronal injury. Neurobiol Dis 18: 286-295.

Drewes G, Ebneth A, Mandelkow E (1998). MAPs, MARKs and microtubule dynamics. Trends in Biochem Sci 23:307-311.

Droppelmann CA, Keller BA, Campos-Melo D, Volkening K, Strong MJ (2013). Rho guanine nucleotide exchange factor is an NFL mRNA destabilizing factor that forms cytoplasmic inclusions in amyotrophic lateral sclerosis. Neurobiol Aging 34:248-262.

Dubois M, Strazielle C, Julien JP, Lalonde R (2005). Mice with the deleted neurofilament of low molecular weight (Nefl) gene: 2. Effects on motor functions and spatial orientation. J Neurosci Res 80:751-758.

Duyckaerts C, Potier MC, Delatour B (2008). Alzheimer disease models and human neuropathology: similarities and differences. Acta Neuropathol (Berl) 115:5–38.

Dyakin VV, Chen Y, Branch CA, Veeranna, Yuan A, Rao M, Kumar A, Peterhoff CM, Nixon RA (2010). The contributions of myelin and axonal caliber to transverse relaxation time in shiverer and neurofilament-deficient mouse

models. Neuroimage 51:1098-1105.

Edgar JM, McLaughlin M, Yool D, Zhang SC, Fowler JH, Montague P, Barrie JA, McCulloch MC, Duncan ID, Garbern J, Nave KA, Griffiths IR (2004). Oligodendroglial modulation of fast axonal transport in a mouse model of hereditary spastic paraplegia. J Cell Biol 166:121-131.

Elden AC, Kim HJ, Hart MP, Chen-Plotkin AS, Johnson BS, Fang X, Armakola M, Geser F, Greene R, Lu MM, Padmanabhan A, Clay-Falcone D, McCluskey L, Elman L, Juhr D, Gruber PJ, Rüb U, Auburger G, Trojanowski JQ, Lee VM, Van Deerlin VM, Bonini NM, Gitler AD (2010). Ataxin-2 intermediate-length polyglutamine expansions are associated with increased risk for ALS. Nature 466:1069–1075.

Elder GA, Friedrich VL Jr, Bosco P, Kang C, Gourov A, Tu PH, Lee VM, Lazzarini RA (1998a). Absence of the mid-sized neurofilament subunit decreases axonal calibers, levels of light neurofilament (NF-L), and neurofilament content. J Cell Biol. 141: 727–739.

Elder GA, Friedrich VL Jr, Kang C, Bosco P, Gourov A, Tu PH Zhang B, Lee VM, Lazzarini RA (1998b). Requirement of heavy neurofilament subunit in the development of axons with large calibers. J Cell Biol 143: 195–205.

Elder GA, Friedrich VL Jr, Margita A, Lazzarini RA (1999a). Age-related atrophy of motor axons in mice deficient in the mid-sized neurofilament subunit. J Cell Biol 146: 181–192.

Elder GA, Friedrich VL Jr, Pereira D, Tu PH, Zhang B, Lee VM, Lazzarini RA (1999b). Mice with disrupted midsized and heavy neurofilament genes lack axonal neurofilaments but have unaltered numbers of axonal microtubules. J Neurosci Res 57: 23–32.

Elvira G, Wasiak S, Blandford V, Tong XK, Serrano A, Fan X, del Rayo Sánchez-Carbente M, Servant F, Bell AW, Boismenu D, Lacaille JC, McPherson PS, DesGroseillers L, Sossin WS (2006). Characterization of an RNA granule from developing brain. Mol Cell Proteomics 5:635–651.

Encinas JM, Enikolopov G (2008). Identifying and quantitating neural stem and progenitor cells in the adult brain. Methods Cell Biol 85:243-272.

Erck C, Peris L, Andrieux A, Meissirel C, Gruber AD, Vernet M, Schweitzer A, Saoudi Y, Pointu H, Bosc C, Salin PA, Job D, Wehland J (2005). A vital role of

tubulin-tyrosine-ligase for neuronal organization. Proc Natl Acad Sci USA 102:7853-7858.

Escurat M, Djabali K, Gumpel M, Gros F, Portier MM (1990). Differential expression of two neuronal intermediate-filament proteins, peripherin and the low-molecular-mass neurofilament protein (NF-L), during the development of the rat. J Neurosci 10:764–784.

Etienne-Manneville S (2010). From signaling pathways to microtubule dynamics: the key players. Curr Opin Cell Biol 22:104-111.

Evdokimovskaya Y, Skarga Y, Vrublevskaya V, Morenkov O (2012). Release of the glucose-regulated protein 94 by baby hamster kidney cells. Cell Biochem Funct 30:558-562.

Eyer J, Peterson A (1994). Neurofilament-deficient axons and perikaryal aggregates in viable transgenic mice expressing a neurofilament-β-galactosidase fusion protein. Neuron 12:389–405.

Feiguin F, Godena VK, Romano G, D'Ambrogio A, Klima R, Baralle FE (2009). Depletion of TDP-43 affects Drosophila motoneurons terminal synapsis and locomotive behavior. FEBS Lett 583:1586–1592.

Fiesel FC, Voigt A, Weber SS, Van den Haute C, Waldenmaier A, Görner K, Walter M, Anderson ML, Kern JV, Rasse TM, Schmidt T, Springer W, Kirchner R, Bonin M, Neumann M, Baekelandt V, Alunni-Fabbroni M, Schulz JB, Kahle PJ (2010). Knockdown of transactive response DNA-binding protein (TDP-43) downregulates histone deacetylase 6. EMBO J 29:209-221.

Fletcher DA, Mullins RD (2010). Cell mechanics and the cytoskeleton. Nature 463:485-492.

Fliegner KH, Liem RK (1991). Cellular and molecular biology of neuronal intermediate filaments. Int Rev Cytol 131:109-167.

Fliegner KH, Kaplan MP, Wood TL, Pintar JE, Liem RK (1994). Expression of the gene for the neuronal intermediate filament protein alpha-internexin coincides with the onset of neuronal differentiation in the developing rat nervous system. J Comp Neurol 342: 161-173.

Friede RL, Samorajski T (1970). Axon caliber related to neurofilaments and microtubules in sciatic nerve fibers of rats and mice. Anat Rec 167: 379–387.

Fuentealba RA, Udan M, Bell S, Wegorzewska I, Shao J, Diamond MI, Weihl CC,

Baloh RH (2010). Interaction with polyglutamine aggregates reveals a Q/N-rich domain in TDP-43. J Biol Chem 285:26304-26314.

Fukushima N, Furuta D, Hidaka Y, Moriyama R, Tsujiuchi T (2009). Post-translational modifications of tubulin in the nervous system. J Neurochem 109: 683-693.

Funfschilling U, Supplie LM, Mahad D, Boretius S, Saab AS, Edgar J, Brinkmann BG, Kassmann CM, Tzvetanova ID, Möbius W, Diaz F, Meijer D, Suter U, Hamprecht B, Sereda MW, Moraes CT, Frahm J, Goebbels S, Nave KA (2012). Glycolytic oligodendrocytes maintain myelin and long-term axonal integrity. Nature 485:517–521.

Galloway PG, Mulvihill P, Perry G (1992). Filaments of Lewy bodies contain insoluble cytoskeletal elements. Am J Pathol 140: 809-822.

Garcia ML, Lobsiger CS, Shah SB, Deerinck TJ, Crum J, Young D, Ward CM, Crawford TO, Gotow T, Uchiyama Y, Ellisman MH, Calcutt NA, Cleveland DW (2003). NF-M is an essential target for the myelin-directed "outside-in" signaling cascade that mediates radial axonal growth. J Cell Biol 163:1011-1020.

Garcia ML, Rao MV, Fujimoto J, Garcia VB, Shah SB, Crum J, Gotow T, Uchiyama Y, Ellisman M, Calcutt NA, Cleveland DW (2009). Phosphorylation of highly conserved neurofilament medium KSP repeats is not required for myelin-dependent radial axonal growth. J Neurosci 29:1277-1284.

Ge WW, Leystra-Lantz C, Wen W, Strong MJ (2003). Selective loss of trans-acting instability determinants of neurofilament mRNA in amyotrophic lateral sclerosis spinal cord. J Biol Chem 6:26558–26563.

Gentil BJ, Minotti S, Beange M, Baloh RH, Julien JP, Durham HD (2012). Normal role of the low-molecular-weight neurofilament protein in mitochondrial dynamics and disruption in Charcot-Marie-Tooth disease. FASEB J 26:1194-1203.

Georgiou DM, Zidar J, Korosec M, Middleton LT, Kyriakides T, Christodoulou K (2002). A novel NF-L mutation Pro22Ser is associated with CMT2 in a large Slovenian family. Neurogenetics 4: 93-96.

Georgiou J, Tropak MP, Roder JC (2004). Myelinassociated glycoprotein gene. In R. A. Lazzarini (ed.), Myelin biology and disorders. San Diego, CA: Elsevier

Academic Press: 421–467.

Geraldo S, Gordon-Weeks PR (2009). Cytoskeletal dynamics in growth-cone steering. J Cell Sci 122: 3595-3604.

Geser F, Brandmeir NJ, Kwong LK, Martinez-Lage M, Elman L, McCluskey L, Xie SX, Lee VM, Trojanowski JQ (2008). Evidence of multisystem disorder in whole-brain map of pathological TDP-43 in amyotrophic lateral sclerosis.Arch Neurol 65:636-641.

Giordana MT, Piccinini M, Grifoni S, De Marco G, Vercellino M, Magistrello M, Pellerino A, Buccinnà B, Lupino E, Rinaudo MT (2010). TDP-43 redistribution is an early event in sporadic amyotrophic lateral sclerosis. Brain Pathol 20:351-360.

Gitcho MA, Baloh RH, Chakraverty S, Mayo K, Norton JB, Levitch D, Hatanpaa KJ, White CL 3rd, Bigio EH, Caselli R, Baker M, Al-Lozi MT, Morris JC, Pestronk A, Rademakers R, Goate AM, Cairns NJ (2008). TDP-43 A315T mutation in familial motor neuron disease. Ann Neurol 63 :535-538.

Gitcho MA, Bigio EH, Mishra M, Johnson N, Weintraub S, Mesulam M, Rademakers R, Chakraverty S, Cruchaga C, Morris JC, Goate AM, Cairns NJ (2009). TARDBP 3'-UTR variant in autopsy-confirmed frontotemporal lobar degeneration with TDP-43 proteinopathy. Acta Neuropathol 118:633-645.

Godena VK, Romano G, Romano M, Appocher C, Klima R, Buratti E, Baralle FE, Feiguin F (2011). TDP-43 regulates Drosophila neuromuscular junctions growth by modulating Futsch/MAP1B levels and synaptic microtubules organization. PLoS One 6:e17808.

Goldman RD, Grin B, Mendez MG, Kuczmarski ER (2008). Intermediate filaments: versatile building blocks of cell structure.Curr Opin Cell Biol 20: 28-34.

Gomes FC, Paulin D, Moura Neto V (1999). Glial fibrillary acidic protein (GFAP): modulation by growth factors and its implication in astrocyte differentiation. Braz J Med Biol Res 32:619-631.

Graff-Radford NR, Woodruff BK (2007). Frontotemporal dementia. Semin Neurol 27:48–57.

Guérette D, Khan PA, Savard PE, Vincent M (2007). Molecular evolution of type VI intermediate filament proteins. BMC Evol Bio l 7:164.

Haase D, Keiner S, Mawrin C, Wolf G (2009). Reduced Morg1 Expression In

Ischemic Human Brain. Neurosci Lett 455: 46-50.

Hanson KA, Kim SH, Wassarman DA, Tibbets RS (2010). Ubiquilin modifies TDP-43 toxicity in a Drosophila model of amyotrophic lateral sclerosis (ALS). J Biol Chem 285: 11068–11072.

Harauz G, Ishiyama N, Hill CMD, Bates IR, Libich DS, Farès C (2004). Myelin basic protein - diverse conformational states of an intrinsically unstructured protein and its roles in myelin assembly and multiple sclerosis. Micron 35: 503–542.

Hasegawa M, Arai T, Nonaka T, Kametani F, Yoshida M, Hashizume Y, Beach TG, Buratti E, Baralle F, Morita M, Nakano I, Oda T, Tsuchiya K, Akiyama H (2008). Phosphorylated TDP-43 in frontotemporal lobar degeneration and amyotrophic lateral sclerosis. Ann Neurol 64:60-70.

Hashimoto R, Nakamura Y, Komai S, Kashiwagi Y, Tamura K, Goto T, Aimoto S, Kaibuchi K, Shiosaka S, Takeda M (2000). Site-specificphosphorylation of neurofilament-L is mediated by calcium/calmodulin-dependent protein kinase II in the apical dendrites during long-term potentiation. J Neurochem 75: 373-382.

Hazelett DJ, Chang JC, Lakeland DL, Morton DB (2012). Comparison of parallel high-throughput RNA sequencing between knockout of TDP-43 and its overexpression reveals primarily nonreciprocal and nonoverlapping gene expression changes in the central nervous system of Drosophila. G3 (Bethesda)2 :789-802.

Herrmann H, Strelkov SV, Burkhard P, Aebi U (2009). Intermediate filaments: primary determinants of cell architecture and plasticity. J Clin Invest 119:1772-1783.

Higashi S, Iseki E, Yamamoto R, Minegishi M, Hino H, Fujisawa K, Togo T, Katsuse O, Uchikado H, Furukawa Y, Kosaka K, Arai H (2007). Concurrence of TDP-43, tau and alpha-synuclein pathology in brains of Alzheimer's disease and dementia with Lewy bodies. Brain Res 1184: 284–294.

Hill WD, Arai M, Cohen JA, Trojanowski JQ (1993). Neurofilament mRNA is reduced in Parkinson’s disease substantia nigra pars compacta neurons. J Comp Neurol 329: 328-336.

Hirano A, Nakano I, Kurland LT, Mulder DW, Holley PW, Saccomanno G (1984). Fine structural study of neurofibrillary changes in a family with amyotrophic

lateral sclerosis. J Neuropathol Exp Neurol 43:471–480.

Hirokawa N, Hisanaga S, Shiomura Y (1988). MAP2 is a component of crossbridges between microtubules and neurofilaments in the neuronal cytoskeleton: quick-freeze, deep-etch immunoelectron microscopy and reconstitution studies. J Neurosci 8: 2769–2779.

Hirokawa N (1998). Kinesin and dynein superfamily proteins and the mechanism of organelle transport. Science 279: 519-526.

Hisanaga S, Hirokawa N (1988). Structure of the peripheral domains of neurofilaments revealed by low angle rotary shadowing. J Mol Biol 202: 297-305.

Hisanaga S, Hirokawa N (1989). The effects of dephosphorylation on the structure of the projections of neurofilament. J Neurosci 9: 959-966.

Hisanaga S, Gonda Y, Inagaki M, Ikai A, Hirokawa N (1990a). Effects of phosphorylation of the neurofilament L protein on filamentous structures. Cell Regul 1:237-248.

Hisanaga S, Hirokawa N (1990b). Dephosphorylation-induced interactions of neurofilaments with microtubules. J Biol Chem 265: 21852–21858.

Hisanaga S, Kusubata M, Okumura E, Kishimoto T (1991) Phosphorylation of neurofilament H subunit at the tail domain by Cdc2 kinase dissociates the association to microtubules. J Biol Chem 266: 21798–21803.

Hitt AL, Luna EJ (1994). Membrane interactions with the actin cytoskeleton. Curr Opin Cell Biol 6: 120-130.

Hof PR, Nimchinsky EA, Morrison JH (1995). Neurochemical phenotype of corticocortical connections in the macaque monkey: quantitative analysis of a subset of neurofilament protein-immunoreactive projection neurons in frontal, parietal, temporal, and cingulate cortices. J Comp Neurol 362:109-133.

Hoffman PN, Lasek RJ (1975). The slow component of axonal transport. Identification of major structural polypeptides of the axon and their generality among mammalian neurons. J Cell Biol 66:351-366.

Hoffman PN, Cleveland DW, Griffin JW, Landes PW, Cowan N J, Price DL (1987). Neurofilament gene expression: A major determinant of axonal caliber. Proc Nat Acad Sci USA 84:3472-3476.

Hoffman PN, Griffin JW (1992). Regulation of axonal caliber. In:

Peripheralneuropathy (Dyck PJ, Thomas PK, Griffin JW, Low PA, Poduslo J, eds). New York, Raven: 389–402.

Hoogenraad CC, Bradke F (2009). Control of neuronal polarity and plasticity--a renaissance for microtubules? Trends Cell Biol 19: 669-676.

Hsieh ST, Kidd GJ, Crawford TO, Xu Z, Lin WM, Trapp BD, Cleveland DW, Griffin JW (1994). Regional modulation of neurofilament organization by myelination in normal axons. J Neurosci 14:6392–6401.

Huang C, Xia PY, Zhou H (2010). Sustained expression of TDP-43 and FUS in motor neurons in rodent's lifetime. Int J Biol Sci 6 :396-406.

Hutchins BI, Kalil K (2008). Differential outgrowth of axons and their branches is regulated by localized calcium transients. J Neurosci 28: 143-153.

Hyams JS, Lloyd CW (1994). Microtubules, Modern Cell Biology. New York: Wiley-Liss. vol. 13.

Igaz LM, Kwong LK, Lee EB, Chen-Plotkin A, Swanson E, Unger T, Malunda J, Xu Y, Winton MJ, Trojanowski JQ, Lee VM (2011). Dysregulation of the ALS-associated gene TDP-43 leads to neuronal death and degeneration in mice. J Clin Invest 121:726–738.

Ihara R, Matsukawa K, Nagata Y, Kunugi H, Tsuji S, Chihara T, Kuranaga E, Miura M, Wakabayashi T, Hashimoto T, Iwatsubo T (2013). RNA binding mediates neurotoxicity in the transgenic Drosophila model of TDP-43 proteinopathy. Hum Mol Genet :[Epub ahead of print]

Ince PG, Tomkins J, Slade JY, Thatcher NM, Shaw PJ (1998). Amyotrophic lateral sclerosis associated with genetic abnormalities in the gene encoding Cu/Zn superoxide dismutase: molecular pathology of five new cases, and comparison with previous reports and 73 sporadic cases of ALS. J Neuropathol Exp Neurol 57:895-904.

Jacomy H, Zhu Q, Couillard-Despres S, Beaulieu JM, Julien JP (1999). Disruption of type IV intermediate filament network in mice lacking the neurofilament medium and heavy subunits. J Neurochem 73: 972–984.

Johnson BS, Snead D, Lee JJ, McCaffery JM, Shorter J, Gitler AD (2009). TDP-43 is intrinsically aggregation-prone, and amyotrophic lateral sclerosis-linked mutations accelerate aggregation and increase toxicity. J Biol Chem 284: 20329–20339.

Jones JB, Safinya CR (2008). Interplay between liquid crystalline and isotropic gels in self-assembled neurofilament networks. Biophys J 95:823-835

Jordanova A, De Jonghe P, Boerkoel CF, Takashima H, De Vriendt E, Ceuterick C, Martin JJ, Butler IJ, Mancias P, Papasozomenos SCh, Terespolsky D, Potocki L, Brown CW, Shy M, Rita DA, Tournev I, Kremensky I, Lupski JR, Timmerman V (2003). Mutations in the neurofilament light chain gene (NEFL) cause early onset severe Charcot-Marie-Tooth disease. Brain 126: 590-597.

Josephs KA, Ahmed Z, Katsuse O, Parisi JF, Boeve BF, Knopman DS, Petersen RC, Davies P, Duara R, Graff-Radford NR, Uitti RJ, Rademakers R, Adamson J, Baker M, Hutton ML, Dickson DW (2007). Neuropathologic features of frontotemporal lobar degeneration with ubiquitin-positive inclusions with progranulin gene (PGRN) mutations. J Neuropathol Exp Neurol 66:142–151.

Julien JP, Mushynski WE (1981). A comparison of in vitro- and in vivo-phosphorylated neurofilament polypeptides. J Neurochem 37:1579–1585.

Julien JP, Mushynski WE (1982). Multiple phosphorylation sites in mammalian neurofilament polypeptides. J Biol Chem 257:10467–10470.

Julien JP, Mushynski WE (1983). The distribution of phosphorylation sites among identified proteolytic fragments of mammalian neurofilaments. J Biol Chem 258:4019–4025.

Julien JP, Couillard-Després S, Meier J (1998). Transgenic mice in the study of ALS: the role of neurofilaments. Brain Pathol 8:759-769.

Julien JP (1999). Neurofilament functions in health and disease. Curr Opin Neurobiol 9:554-560.

Julien JP, Beaulieu JM (2000). Cytoskeletal abnormalities in amyotrophic lateral sclerosis: beneficial or detrimental effects? J Neurol Sci 180:7-14.

Jung C, Chylinski TM, Pimenta A, Ortiz D, Shea TB (2004). Neurofilament Transport Is Dependent on Actin and Myosin. J Neurosci 24:9486–9496.

Kabashi E, Valdmanis PN, Dion P, Spiegelman D, McConkey BJ, Vande Velde C, Bouchard JP, Lacomblez L, Pochigaeva K, Salachas F, Pradat PF, Camu W, Meininger V, Dupre N, Rouleau GA (2008). TARDBP mutations in individuals with sporadic and familial amyotrophic lateral sclerosis. Nat Genet 40: 572-574.

Kabashi E, Lin L, Tradewell ML, Dion PA, Bercier V, Bourgouin P, Rochefort D,

Bel Hadj S, Durham HD, Vande Velde C, Rouleau GA, Drapeau P (2010). Gain and loss of function of ALS-related mutations of TARDBP (TDP-43) cause motor deficits in vivo. Hum Mol Genet 19: 671–683.

Kadokura A, Yamazaki T, Lemere CA, Takatama M, Okamoto K (2009). Regional distribution of TDP-43 inclusions in Alzheimer disease (ad) brains: their relation to ad common pathology. Neuropathology 29:566–573.

Kalil K, Dent EW (2005). Touch and go: guidance cues signal to the growth cone cytoskeleton. Curr Opin Neurobiol 15:521-526.

Kalwy SA, Smith R (1994). Mechanisms of myelin basic protein and proteolipid protein targeting in oligodendrocytes. Mol Membr Biol 11:67–78.

Kang SH, Li Y, Fukaya M, Lorenzini I, Cleveland DW, Ostrow LW, Rothstein JD, Bergles DE (2013). Degeneration and impaired regeneration of gray matter oligodendrocytes in amyotrophic lateral sclerosis. Nat Neurosci 16:571-579.

Kaplan MP, Chin SS, Fliegner KH, Liem RK (1990). Alpha-internexin, a novel neuronal intermediate filament protein, precedes the low molecular weight neurofilament protein (NF-L) in the developing rat brain. J Neurosci 10: 2735-2748.

Karim SA, Barrie JA, McCulloch MC, Montague P, Edgar JM, Kirkham D, Anderson TJ, Nave KA, Griffiths IR, McLaughlin M (2007). PLP overexpression perturbs myelin protein composition and myelination in a mouse model of Pelizaeus-Merzbacher disease. Glia 55:341-351.

Karp G (2005). Cell and Molecular Biology: Concepts and Experiments, Fourth. John Wiley and Sons, Hoboken, NJ:346-358.

Kasai T, Tokuda T, Ishigami N, Sasayama H, Foulds P, Mitchell DJ, Mann DM, Allsop D, Nakagawa M (2009). Increased TDP-43 protein in cerebrospinal fluid of patients with amyotrophic lateral sclerosis. Acta Neuropathol 117:55-62.

Kidd M (1964). Alzheimer's Disease--an Electron Microscopical Study. Brain 87: 307-320.

King AE, Chung JC, Vickers JC, Dickson TC (2006). Localization of glutamate receptors in developing cortical neurons in culture and relationship to susceptibility to excitotoxicity. J Comp Neurol 498: 277-294.

Kirkcaldie MTK, Dickson TC, King CE, Grasby D, Riederer BM, Vickers JC (2002). Neurofilament triplet proteins are restricted to a subset of neurons in the

rat neocortex. J Chem Neuroanat 24:163-171.

Kirkcaldie MTK (2012). Neocortex. In Watson CR, Paxinos G, Puelles L, editors. The Mouse Nervous System. 1st ed. San Diego, USA: Academic Press: 52–111.

Kirkpatrick LL, Brady ST (1999). Cytoskeleton of Neurons and Glia. In: Siegel GJ, Agranoff BW, Albers RW, et al., editors. Basic Neurochemistry: Molecular, Cellular and Medical Aspects. 6th edition. Philadelphia: Lippincott-Raven Chapter 8.

Kirkpatrick LL, Witt AS, Payne HR, Shine HD, Brady ST (2001). Changes in microtubule stability and density in myelin-deficient shiverer mouse CNS axons. J Neurosci 21: 2288-2297.

Klugmann M, Schwab MH, Pühlhofer A, Schneider A, Zimmermann F, Griffiths IR, Nave KA (1997). Assembly of CNS myelin in the absence of proteolipid protein. Neuron 18:59-70.

Koeppen AH, Robitaille Y (2002). Pelizaeus-Merzbacher disease. J Neuropathol Exp Neurol 61: 747–759.

Kong J, Tung VW, Aghajanian J, Xu Z (1998). Antagonistic roles of neurofilament subunits NF-H and NF-M against NF-L in shaping dendritic arborization in spinal motor neurons. J Cell Biol 140:1167-1176.

Kriz J, Zhu Q, Julien JP, Padjen AL (2000). Electrophysiological properties of axons in mice lacking neurofilament subunit genes: disparity between conduction velocity and axon diameter in absence of NF-H. Brain Res 885:32-44.

Kruger R, Fischer C, Schulte T, Strauss KM, Müller T, Woitalla D, Berg D, Hungs M, Gobbele R, Berger K, Epplen JT, Riess O, Schöls L (2003). Mutation analysis of the neurofilament M gene in Parkinson's disease. Neurosci Lett 351:125-129.

Ku NO, Zhou X, Toivola DM, Omary MB (1999).The cytoskeleton of digestive epithelia in health and disease. Am J Physiol 277: G1108-1137.

Kuchibhotla KV, Goldman ST, Lattarulo CR, Wu HY, Hyman BT, Bacskai BJ (2008). Abeta plaques lead to aberrant regulation of calcium homeostasis in vivo resulting in structural and functional disruption of neuronal networks. Neuron 59:214-225.

Kuczmarski ER, Rosenbaum JL (1979). Studies on the organization and localization of actin and myosin in neurons. J Cell Biol 80: 356-371.

Kuhnlein P, Sperfeld AD, Vanmassenhove B, Deerlin V, Lee VM, Trojanowski JQ, Kretzschmar HA, Ludolph AC, Neumann M (2008). Two German kindreds with familial amyotrophic lateral sclerosis due to tardbp mutations. Arch Neurol 65:1185–1189.

Kuo PH, Doudeva LG, Wang YT, Shen CK, Yuan HS (2009). Structural insights into TDP-43 in nucleic-acid binding and domain interactions. Nucleic Acids Res 37:1799–1808.

Kursula P (2008). Structural properties of proteins specific to the myelin sheath. Amino Acids 34:175-185.

Kwiatkowski TJ Jr, Bosco DA, Leclerc AL, Tamrazian E, Vanderburg CR, Russ C, Davis A, Gilchrist J, Kasarskis EJ, Munsat T, Valdmanis P, Rouleau GA, Hosler BA, Cortelli P, de Jong PJ, Yoshinaga Y, Haines JL, Pericak-Vance MA, Yan J, Ticozzi N, Siddique T, McKenna-Yasek D, Sapp PC, Horvitz HR, Landers JE, Brown RH Jr (2009). Mutations in the FUS/TLS gene on chromosome 16 cause familial amyotrophic lateral sclerosis. Science 323:1205–1208.

Lace GL, Wharton SB, Ince PG (2007). A brief history of tau: the evolving view of the microtubule-associated protein tau in neurodegenerative diseases.Clin Neuropathol 26: 43-58.

Laemmli UK (1970). Cleavage of structural proteins during the assembly of the head of bacteriophage T4. Nature 227: 680–685.

Lagier-Tourenne C, Polymenidou M, Cleveland DW (2010). TDP-43 and FUS/TLS: emerging roles in RNA processing and neurodegeneration. Hum Mol Genet 19:R46-64.

Lai C, Brow MA, Nave K-A, Noronha AB, Quarles RH, Bloom FE, Milner RJ, Sutcliffe JG (1987). Two forms of 1B236/myelin-associated glycoprotein (MAG), a cell adhesion molecule for postnatal neural development, are produced by alternative splicing. Proc Natl Acad Sci USA 84:4337–4341.

Lalonde R, Dubois M, Strazielle C, Eyer J (1999). Motor coordination and spatial orientation are affected by neurofilament maldistribution: correlations with regional brain activity of cytochrome oxidase. Exp Brain Res 126:223–234.

LaMonte BH, Wallace KE, Holloway BA, Shelly SS, Ascano J, Tokito M, Van Winkle T, Howland DS, Holzbaur EL (2002). Disruption of dynein/dynactin inhibits axonal transport in motor neurons causing late-onset progressive

degeneration. Neuron 34: 715-727.

Lariviere RC, Julien JP (2004). Functions of intermediate filaments in neuronal development and disease. J Neurobiol 58:131-148.

Lasek R J (1988). Studying the intrinsic determinants of neuronal form and function . In Intrinsic determinants of neuronal form and function. Lasek RJ, Black MM, editors. Neurology and Neurobiology. Alan R. Liss Inc., New York. 37:3-58.

Lavedan C, Buchholtz S, Nussbaum RL, Albin RL, Polymeropoulos MH (2002). A mutation in the human neurofilament M gene in Parkinson's disease that suggests a role for the cytoskeleton in neuronal degeneration. Neurosci Lett 322: 57-61.

Laule C, Vavasour IM, Kolind SH, Li DK, Traboulsee TL, Moore GR, MacKay AL (2007). Magnetic resonance imaging of myelin. Neurotherapeutics 4:460-484.

Lazzarini RA (2004). Myelin biology and disorders. Elsevier Academic Press, San Diego, CA.

Lee MK, Xu Z, Wong PC, Cleveland DW (1993). Neurofilaments are obligate heteropolymers in vivo. J Cell Biol 122: 1337–1350.

Lee MK, Cleveland DW (1996). Neuronal intermediate filaments. Annu Rev Neurosci 19: 187-217.

Lee EB, Lee VM, Trojanowski JQ (2011). Gains or losses: molecular mechanisms of TDP43-mediated neurodegeneration. Nat Rev Neurosci 13:38-50.

Lee Y, Morrison BM, Li Y, Lengacher S, Farah MH, Hoffman PN, Liu Y, Tsingalia A, Jin L, Zhang PW, Pellerin L, Magistretti PJ, Rothstein JD (2012). Oligodendroglia metabolically support axons and contribute to neurodegeneration. Nature 487: 443–448.

Leigh PN, Dodson A, Swash M, Brion JP, Anderton BH (1989). Cytoskeletal abnormalities in motor neuron disease. An immunocytochemical study. Brain 112: 521-535.

Leigh PN, Whitwell H, Garofalo O, Buller J, Swash M, Martin JE, Gallo JM, Weller RO, Anderton BH (1991). Ubiquitin immunoreactive intraneuronal inclusions in amyotrophic lateral sclerosis. Morphology, distribution, specificity. Brain 114: 775–788.

Lemmens R, Race V, Hersmus N, Matthijs G, Bosch L, Damme P, Dubois B, Boonen S, Goris A, Robberecht W (2009). TDP-43 m311v mutation in familial

amyotrophic lateral sclerosis. J Neurol Neurosurg Psychiatry 80:354–355.

Li M, Shibata A, Li C, Braun PE, McKerracher L, Roder J, Kater SB, David S (1996). Myelin-associated glycoprotein inhibits neurite/axon growth and causes growth cone collapse. J Neurosci Res 46:404–414.

Li ZH, Lu J, Tay SS, Wu YJ, Strong MJ, He BP (2006). Mice with targeted disruption of neurofilament light subunit display formation of protein aggregation in motoneurons and downregulation of complement receptor type 3 alpha subunit in microglia in the spinal cord at their earlier age: a possible feature in pre-clinical development of neurodegenerative diseases. Brain Res 1113:200-209.

Li Y, Ray P, Rao EJ, Shi C, Guo W, Chen X, Woodruff EA 3rd, Fushimi K, Wu JY (2010). A Drosophila model for TDP-43 proteinopathy. Proc Natl Acad Sci USA 107:3169–3174.

Li Y, Jung P, Browen A (2012). Axonal transport of neurofilaments: a single population of intermittently moving polymers. J Neurosci 32:746-758.

Liem RK, Messing A (2009). Dysfunctions of neuronal and glial intermediate filaments in disease. J Clin Invest 119:1814-1824.

Lin W, Szaro BG (1995). Neurofilaments help maintain normal morphologies and support elongation of neurites in Xenopus laevis cultured embryonic spinal cord neurons. J Neurosci 15:8331-8344.

Lin MJ, Cheng CW, Shen CK (2011). Neuronal function and dysfunction of Drosophila dTDP. PLoS ONE 6: e20371.

Ling SC, Albuquerque CP, Han JS, Lagier-Tourenne C, Tokunaga S, Zhou H, Cleveland DW (2010). ALS-associated mutations in TDP-43 increase its stability and promote complexes with FUS/TLS. Proc Natl Acad Sci USA 107:13318–13323.

Lippa CF, Rosso AL, Stutzbach LD, Neumann M, Lee VM, Trojanowski JQ (2009). Transactive response DNA-binding protein 43 burden in familial Alzheimer disease and Down syndrome. Arch Neurol 66:1483–1488.

Liu Q, Xie F, Siedlak SL, Nunomura A, Honda K, Moreira PI, Zhua X, Smith MA, Perry G (2004a). Neurofilament proteins in neurodegenerative diseases. Cell Mol Life Sci 61:3057-3075.

Liu Q, Xie F, Alvarado-Diaz A, Smith MA, Moreira PI, Zhu X, Perry G (2011).

Neurofilamentopathy in Neurodegenerative Diseases.Open Neurol J 5:58-62.

Liu SJ, Zhang JY, Li HL, Fang ZY, Wang Q, Deng HM, Gong CX,Grundke-Iqbel I, Iqbel K, Wang JZ (2004b). Tau becomes a more favorable substrate for GSK-3 when it is prephosphorylated by PKA in rat brain. J Biol Chem 279:50078-50088.

Liu-Yesucevitz L, Bilgutay A, Zhang YJ, Vanderweyde T, Citro A, Mehta T, Zaarur N, McKee A, Bowser R, Sherman M, Petrucelli L, Wolozin B (2010). Tar DNA binding protein-43 (TDP-43) associates with stress granules: analysis of cultured cells and pathological brain tissue. PLoS One 5:e13250.

Luduena RF (1993). Are tubulin isotypes functionally significant? Mol Biol Cell 4: 445-447.

Lupski JR (2000) Axonal Charcot-Marie-Tooth disease and the neurofilament light gene (NF-L). Am J Hum Genet 67:8-10.

Luty AA, Kwok JB, Dobson-Stone C, Loy CT, Coupland KG, Karlström H, Sobow T, Tchorzewska J, Maruszak A, Barcikowska M, Panegyres PK, Zekanowski C, Brooks WS, Williams KL, Blair IP, Mather KA, Sachdev PS, Halliday GM, Schofield PR (2010). Sigma nonopioid intracellular receptor 1 mutations cause frontotemporal lobar degeneration-motor neuron disease. Ann Neurol 68:639–649.

Maccioni RB and Cambiazo V (1995). Role of microtubule-associated proteins in the control of microtubule assembly. Physiol Rev 75(4): 835-864.

Mackenzie IR, Feldman HH (2005). Ubiquitin immunohistochemistry suggests classic motor neuron disease, motor neuron disease with dementia, and frontotemporal dementia of the motor neuron disease type represent a clinicopathologic spectrum. J Neuropathol Exp Neurol 64:730-739.

Mackenzie IR, Baborie A, Pickering-Brown S, Du Plessis D, Jaros E, Perry RH, Neary D, Snowden JS, Mann DM (2006a). Heterogeneity of ubiquitin pathology in frontotemporal lobar degeneration: classification and relation to clinical phenotype. Acta Neuropathol 112:539–549.

Mackenzie IR, Baker M, Pickering-Brown S, Hsiung GY, Lindholm C, Dwosh E, Gass J, Cannon A, Rademakers R, Hutton M, Feldman HH (2006b). The neuropathology of frontotemporal lobar degeneration caused by mutations in the progranulin gene. Brain 129:3081–3090.

Manetto V, Sternberger NH, Perry G, Sternberger LA, Gambetti P (1988). Phosphorylation of neurofilaments is altered in amyotrophic lateral sclerosis. J Neuropathol Exp Neurol 47: 642-653.

Maris C, Dominguez C, Allain FH-T (2005). The RNA recognition motif, a plastic RNA-binding platform to regulate post-transcriptional gene expression. FEBS J 272:2118–2131.

Marszalek JR, Williamson TL, Lee MK, Xu Z, Hoffman PN, Becher MW, Crawford TO, Cleveland DW(1996) Neurofilament subunit NF-H modulates axonal diameter by selectively slowing neurofilament transport. J Cell Biol 135:711-724.

Martenson RE (1992). Myelin:biology and chemistry. CRC Pres, Boca Raton, FL.

Martin LJ, Sisodia SS, Koo EH, Cork LC, Dellovade TL, Weidemann A, Beyreuther K, Masters C, Price DL (1991). Amyloid precursor protein in aged nonhuman primates. Proc Natl Acad Sci U S A 88: 1461–1465.

Martin M, Hiltner TD, Wood JC, Fraser SE, Jacobs RE, Readhead C (2006). Myelin deficiencies visualized in vivo: visually evoked potentials and T2-weighted magnetic resonance images of shiverer mutant and wild-type mice. J Neurosci Res 84:1716-1726.

Maruyama H, Morino H, Ito H, Izumi Y, Kato H, Watanabe Y, Kinoshita Y, Kamada M, Nodera H, Suzuki H, Komure O, Matsuura S, Kobatake K, Morimoto N, Abe K, Suzuki N, Aoki M, Kawata A, Hirai T, Kato T, Ogasawara K, Hirano A, Takumi T, Kusaka H, Hagiwara K, Kaji R, Kawakami H (2010). Mutations of optineurin in amyotrophic lateral sclerosis. Nature 465:223–226.

Mata M, Kupina N, Fink DJ (1992). Phosphorylation-dependent neurofilament epitopes are reduced at the node of Ranvier. J Neurocytol 21:199-210.

Matsunaga W, Miyata S, Kiyohara T (1999). Redistribution of MAP2 immunoreactivity in the neurohypophysial astrocytes of adult rats during dehydration. Brain Res 829:7-17.

Matsuyama A, Shimazu T, Sumida Y, Saito A, Yoshimatsu Y, Seigneurin-Berny D, Osada H, Komatsu Y, Nishino N, Khochbin S, Horinouchi S, Yoshida M (2002). In vivo destabilization of dynamic microtubules by HDAC6-mediated deacetylation. EMBO J 21:6820-6831.

Mattila PK, Lappalainen P (2008). Filopodia: molecular architecture and cellular functions. Nat Rev Mol Cell Biol 9: 446-454.

McGraw TS, Mickle JP, Shaw G, Streit WJ (2002). Axonally transported peripheral signals regulate alpha-internexin expression in regenerating motoneurons. J Neurosci 22: 4955-4963.

McKerracher L, David S, Jackson DL, Kottis V, Dunn RJ, Braun PE (1994). Identification of myelin-associated glycoprotein as a major myelin-derived inhibitor of neurite growth. Neuron 13: 805–811.

McLachlan DR, Lukiw WJ, Wong L, Bergeron C, Bech-Hansen NT (1988). Selective messenger RNA reduction in Alzheimer's disease. Brain Res 427: 255-261.

Mercado PA, Ayala YM , Romano M, Buratti E, Baralle FE (2005). Depletion of TDP 43 overrides the need for exonic and intronic splicing enhancers in the human apoA-II gene. Nucleic Acids Res 33:6000–6010.

Mersiyanova IV, Perepelov AV, Polyakov AV, Sitnikov VF, Dadali EL, Oparin RB, Petrin AN, Evgrafov OV (2000). A new variant of Charcot-Marie- Tooth disease type 2 is probably the result of a mutation in the neurofilament-light gene. Am J Hum Genet 67: 37-46.

Mishra M, Paunesku T, Woloschak GE, Siddique T, Zhu LJ, Lin S, Greco K, Bigio EH (2007). Gene expression analysis of frontotemporal lobar degeneration of the motor neuron disease type with ubiquitinated inclusions. Acta Neuropathol 114:81-94.

Mitew S, Kirkcaldie MTK, Halliday GM, Shepherd CE, Vickers JC and Dickson TC (2010). Focal demyelination in Alzheimer's disease and transgenic mouse models. Acta Neuropathologica 119: 567-577.

Miyasaka H, Okabe S, Ishiguro K, Uchida T, Hirokawa N (1993). Interaction of the tail domain of high-molecular-weight subunits of neurofilaments with the COOH-terminal region of tubulin and its regulation by Tau-protein kinase-II. J Biol Chem 268: 22695–22702.

Moisse K, Mepham J, Volkening K, Welch I, Hill T, Strong MJ (2009). Cytosolic TDP-43 expression following axotomy is associated with caspase 3 activation in NFL-/- mice: support for a role for TDP-43 in the physiological response to neuronal injury. Brain Res 1296:176-186.

Morell P (1984). Myelin. Plenum Press, New York.

Mosca L, Lunetta C, Tarlarini C, Avemaria F, Maestri E, Melazzini M, Corbo M, Penco S (2012). Wide phenotypic spectrum of the TARDBP gene: homozygosity of A382T mutation in a patient presenting with amyotrophic lateral sclerosis, Parkinson's disease, and frontotemporal lobar degeneration, and in neurologically healthy subject. Neurobiol Aging 33:1846.e1-4.

Mougeot JL, Li Z, Price AE, Wright FA, Brooks BR (2011). Microarray analysis of peripheral blood lymphocytes from ALS patients and the SAFE detection of the KEGG ALS pathway. BMC Med Genomics 4:74.

Mukhopadhyay G, Doherty P, Walsh FS, Crocker PR, Filbin MT (1994). A novel role for myelin-associated glycoprotein as an inhibitor of axonal regeneration. Neuron 13:757–767.

Mullins FH, Hargreaves AJ, Li JY, Dahlstrom A, McLean WG (1994). Tyrosination state of alpha-tubulin in regenerating peripheral nerve. J Neurochem 62: 227-234.

Murayama S, Bouldin TW, Suzuki K (1992). Immuno-cytochemical and ultrastructural studies of upper motor neurons in amyotrophic lateral sclerosis. Acta Neuropathol 83: 518-524.

Myers KA, He Y, Hasaka TP, Baas PW (2006). Microtubule transport in the axon: Re-thinking a potential role for the actin cytoskeleton. Neuroscientist 12:107-118.

Nardo G, Pozzi S, Pignataro M, Lauranzano E, Spano G, Garbelli S, Mantovani S, Marinou K, Papetti L, Monteforte M, Torri V, Paris L, Bazzoni G, Lunetta C, Corbo M, Mora G, Bendotti C, Bonetto V (2011). Amyotrophic lateral sclerosis multiprotein biomarkers in peripheral blood mononuclear cells. PLoS One 6:e25545.

Nave KA, Trapp BD (2008). Axon-glial signaling and the glial support of axon function. Annu Rev Neurosci 31:535-561.

Neumann M, Sampathu DM, Kwong LK, Truax AC, Micsenyi MC, Chou TT, Bruce J, Schuck T, Grossman M, Clark CM, McCluskey LF, Miller BL, Masliah E, Mackenzie IR, Feldman H, Feiden W, Kretzschmar HA, Trojanowski JQ, Lee VM (2006). Ubiquitinated TDP-43 in Frontotemporal Lobar Degeneration and Amyotrophic Lateral Sclerosis. Science 314: 130–133.

Neumann M, Kwong LK, Truax AC, Vanmassenhove B, Kretzschmar HA, Van Deerlin VM, Clark CM, Grossman M, Miller BL, Trojanowski JQ, Lee VM. (2007). TDP-43-positive white matter pathology in frontotemporal lobar degeneration with ubiquitin-positive inclusions. J Neuropathol Exp Neurol 66: 177–183.

Neumann M, Kwong LK, Lee EB, Kremmer E, Flatley A, Xu Y, Forman MS, Troost D, Kretzschmar HA, Trojanowski JQ, Lee VM. (2009). Phosphorylation of S409/410 of TDP-43 is a consistent feature in all sporadic and familial forms of TDP-43 proteinopathies. Acta Neuropathol 117:137-149.

Nguyen MD, Lariviere RC, Julien JP (2000). Reduction of axonal caliber does not alleviate motor neuron disease caused by mutant superoxide dismutase 1. Proc Natl Acad Sci USA 97:12306 –12311.

Nguyen T, Mehta NR, Conant K, Kim KJ, Jones M, Calabresi PA, Melli G, Hoke A, Schnaar RL, Ming GL, Song H, Keswani SC, Griffin JW (2009). Axonal protective effects of the myelin-associated glycoprotein.J Neurosci 29:630-637.

Nishimura AL, Zupunski V, Troakes C, Kathe C, Fratta P, Howell M, Gallo JM, Hortobágyi T, Shaw CE, Rogelj B (2010). Nuclear import impairment causes cytoplasmic trans-activation response DNA-binding protein accumulation and is associated with frontotemporal lobar degeneration. Brain 133:1763-1771.

Nixon RA, Shea TB (1992). Dynamics of neuronal intermediate filaments:a developmental perspective. Cell Motil Cytoskeleton 22:81-91.

Nixon RA (1998a). Dynamic behavior and organization of cytoskeletal proteins in neurons: reconciling old and new findings. Bioessays 20:798–807.

Nixon RA (1998b). The slow axonal transport debate. Trends Cell Biol 8:100.

Nixon RA (1998c). The slow axonal transport of cytoskeletal proteins. Curr Opin Cell Biol 10:87–92.

Noda Y, Sasaki S (2008). The role of actin remodeling in the trafficking of intracellular vesicles, transporters, and channels: focusing on aquaporin-2. Pflugers Arch 456: 737-745.

Nogales E, Wolf S G, Downing K H (1998). Structure of the αβ tubulin dimer by electron crystallography. Nature 391: 199-203.

Ohara O, Gahara Y, Miyake T, Teraoka H, Kitamura T (1993). Neurofilament deficiency in quail caused by nonsense mutation in neurofilament-L gene. J Cell

Biol 121:387–395.

Okamoto K, Hirai S, Yamazaki T, Sun XY, Nakazato Y (1991). New ubiquitin-positive intraneuronal inclusions in the extra-motor cortices in patients with amyotrophic lateral sclerosis. Neurosci Lett 129:233-236.

Okonkwo DO, Pettus EH, Moroi J, Povlishock JT (1998). Alteration of the neurofilament sidearm and its relation to neurofilament compaction occurring with traumatic axonal injury. Brain Res 784:1-6.

Omary MB, Coulombe PA, McLean WHI (2004). Mechanism of disease: Intermediate filament proteins and their associated diseases. N Engl J Med 351: 2087-2100

Ou SH, Wu F, Harrich D, García-Martínez LF, Gaynor RB (1995). Cloning and characterization of a novel cellular protein, TDP-43, that binds to human immunodeficiency virus type 1 TAR DNA sequence motifs. J Virol 69:3584 – 3596.

Pachter JS, Liem RK (1985). Alpha-Internexin, a 66-kD intermediate filament-binding protein from mammalian central nervous tissues. J Cell Biol 101:1316-22.

Palazzo A, Ackerman B, Gundersen GG (2003). Cell biology: Tubulin acetylation and cell motility. Nature 421: 230.

Pant HC (1988). Dephosphorylation of neurofilament proteins enhances their susceptibility to degradation by calpain. Biochem J 256:665-668.

Park HJ, Lee SN, Lim HR, Kong JH, Jeon CJ (2000). Calcium-binding protein calbindin D28K, calretinin,and parvalbumin immunoreactivity in the rabbit visual cortex. Mol Cells 10: 206−212.

Parry DAD, Fraser RDB (1985). Intermediate filament structure. 1. Analysis of IF protein sequence data. Int J Biol Macromol 7: 203-213.

Parysek LM, McReynolds MA, Goldman RD, Ley CA (1991). Some neural intermediate filaments contain both peripherin and the neurofilament proteins. J Neurosci Res 30:80-91.

Pasinelli P, Brown RH (2006). Molecular biology of amyotrophic lateral sclerosis: insights from genetics. Nat Rev Neurosci 7:710-723.

Patzkó A, Shy ME (2011). Update on Charcot-Marie-Tooth disease. Curr Neurol Neurosci Rep 11:78-88.

Paulussen M, Jacobs S, van der Gucht E, Hof PR, Arckens L (2011). Cytoarchitecture of the mouse neocortex revealed by the low-molecular-weight neurofilament protein subunit. Brain Struct Funct 216:183–199.

Perez-Olle R, Lopez-Toledano MA, Liem RK (2004). The G336S variant in the human neurofilament-M gene does not affect its assembly or distribution: importance of the functional analysis of neurofilament variants. J Neuropathol Exp Neurol 63: 759-774.

Perez-Olle R, Lopez-Toledano MA, Goryunov D, Cabrera-Poch N, Stefanis L, Brown K, Liem RK (2005). Mutations in the neurofilament light gene linked to Charcot-Marie-Tooth disease cause defects in transport. J Neurochem 93: 861-874.

Permana S, Hisanaga S, Nagatomo Y, Ilida J, Hotani H, Itoh TJ (2005). Truncation of the projection domain of MAP4 (microtubule-associated protein 4) leads to attenuation of microtubule dynamic instability. Cell Structure and Function 29: 147-157.

Peris L, Thery M, Fauré J, Saoudi Y, Lafanechère L, Chilton JK, Gordon-Weeks P, Galjart N, Bornens M, Wordeman L，Wehland J, Andrieux A, Job D (2006). Tubulin tyrosination is a major factor affecting the recruitment of CAP-Gly proteins at microtubule plus ends. J Cell Biol 174: 839-849.

Peris L, Wagenbach M, Lafanechère L, Brocard J, Moore AT, Kozielski F, Job D, Wordeman L, Andrieux A (2009). Motor-dependent microtubule disassembly driven by tubulin tyrosination. J Cell Biol 185:1159-1166.

Perrin FE, Boisset G, Docquier M, Schaad O, Descombes P, Kato AC (2005). No widespread induction of cell death genes occurs in pure motoneurons in an amyotrophic lateral sclerosis mouse model. Hum Mol Genet 14:3309-3320.

Perrot R, Berges R, Bocquet A, Eyer J (2008). Review of the multiple aspects of neurofilament functions, and their possible contribution to neurodegeneration. Mol Neurobiol 38: 27–65.

Perrot R, Eyer J (2009). Neuronal intermediate filaments and neurodegenerative disorders. Brain Res Bull 80:282-295.

Perry G, Rizzuto N, Autilio-Gambetti L, Gambetti P (1985). Paired helical filaments from Alzheimer disease patients contain cytoskeletal components. Proc Natl Acad Sci USA 82: 3916-3920.

Perry G, Friedman R, Shaw G, Chau V (1987). Ubiquitin is detected in neurofibrillary tangles and senile plaque neurites of Alzheimer disease brains. Proc Natl Acad Sci USA 84: 3033-3036.

Philips T, Bento-Abreu A, Nonneman A, Haeck W, Staats K, Geelen V, Hersmus N, Küsters B, Van Den Bosch L, Van Damme P, Richardson WD, Robberecht W (2013). Oligodendrocyte dysfunction in the pathogenesis of amyotrophic lateral sclerosis. Brain 136: 471-482.

Portier MM, Escurat M, Landon F, Djabali K, Bousquet O (1993). Peripherin and neurofilaments: expression and role during neural development. C R Acad Sci III 316:1124-1140.

Prahlad V, Helfand BT, Langford GM, Vale RD, Goldman RD (2000). Fast transport of neurofilament protein along microtubules in squid axoplasm. J Cell Sci 113: 3939-3946.

Price SA, Held B, Pearson HA (1998). Amyloid beta protein increases Ca^{2+} currents in rat cerebellar granule neurones. Neuroreport 9: 539-545.

Quarles RH (2002). Myelin sheaths: glycoproteins involved in their formation, maintenance and degeneration. Cell Mol Life Sci 59, 1851–1871.

Quarles RH, MacklinWB, Morell P (2006). Myelin Formation, Structure and Biochemistry. In Siegel GJ (ed.), Basic Neurochemistry: Molecular, Cellular and Medical Aspects. Philadelphia, Lippincott-Raven, Elsevier Academic Press:51–71.

Rao MV, Houseweart MK, Williamson TL, Crawford TO, Folmer J (1998) Neurofilament-dependent radial growth of motor axons and axonal organization of neurofilaments does not require the neurofilament heavy subunit (NF-H) or its phosphorylation. J Cell Biol 143:171-181.

Rao MV, Campbell J, Yuan A, Kumar A, Gotow T, Uchiyama Y, Nixon RA (2003).The neurofilament middle molecular mass subunit carboxyl-terminal tail domains is essential for the radial growth and cytoskeletal architecture of axons but not for regulating neurofilament transport rate. J Cell Biol 163:1021-1031.

Rao MV, Mohan PS, Kumar A, Yuan A, Montagna L, Campbell J, Veeranna, Espreafico EM, Julien JP, Nixon RA (2011). The myosin Va head domain binds to the neurofilament-L rod and modulates endoplasmic reticulum (ER) content and distribution within axons. PLoS One 6:e17087.

Renton AE (2011). A hexanucleotide repeat expansion in C9ORF72 is the cause of chromosome 9p21-linked ALS-FTD. Neuron.72:257–268.

Ritson GP, Custer SK, Freibaum BD, Guinto JB, Geffel D, Moore J, Tang W, Winton MJ, Neumann M, Trojanowski JQ, Lee VM, Forman MS, Taylor JP (2010). TDP-43 mediates degeneration in a novel Drosophila model of disease caused by mutations in VCP/p97. J Neurosci 30:7729–7739.

Rodriguez OC, Cheney RE (2002). Human myosin-Vc is a novel class V myosin expressed in epithelial cells. J Cell Sci 115:991–1004.

Rosenbluth J (1980). Central myelin in the mouse mutant shiverer. J Comp Neurol 194:639-648.

Roy S, Coffee P, Smith G, Liem RK, Brady ST, Black MM (2000). Neurofilaments are transported rapidly but intermittently in axons: implications for slow axonal transport. J Neurosci 20: 6849-6861.

Rudrabhatla P, Jaffe H, Pant HC (2011). Direct evidence of phosphorylated neuronal intermediate filament proteins in neurofibrillary tangles (NFTs): phosphoproteomics of Alzheimer's NFTs. FASEB J 25: 3896-3905.

Rutherford NJ, Zhang YJ, Baker M, Gass JM, Finch NA, Xu YF, Stewart H, Kelley BJ, Kuntz K, Crook RJ, Sreedharan J, Vance C, Sorenson E, Lippa C, Bigio EH, Geschwind DH, Knopman DS, Mitsumoto H, Petersen RC, Cashman NR, Hutton M, Shaw CE, Boylan KB, Boeve B, Graff-Radford NR, Wszolek ZK, Caselli RJ, Dickson DW, Mackenzie IR, Petrucelli L, Rademakers R (2008). Novel mutations in TARDBP (TDP-43) in patients with familial amyotrophic lateral sclerosis. PLoS Genet 4: e1000193.

Sakaguchi T, Okada M, Kitamura T, Kawasaki K (1993). Reduced diameter and conduction velocity of myelinated fibers in the sciatic nerve of a neurofilament-deficient mutant quail. Neurosci Lett 153:65-68.

Salzer JL, Holmes WP, Colman DR (1987). The amino acid sequences of the myelin-associated glycoproteins: homology to the immunoglobulin gene superfamily. J Cell Biol 104:957–965.

Sampson VL, Morrison JH, Vickers JC (1997). The cellular basis for the relative resistance of parvalbumin and calretinin immunoreactive neocortical neurons to the pathology of Alzheimer's disease. Exp Neurol 145:295–302.

Sánchez C, Díaz-Nido J, Avila J (2000). Phosphorylation of microtubule-associated

protein 2 (MAP2) and its relevance for the regulation of the neuronal cytoskeleton function. Prog Neurobiol 61:133-168.

Santarella RA, Skiniotis G, Goldie KN, Tittmann, P, Gross H, Mandelkow EM, Mandelkow E, Hoenger A (2004). Surface-decoration of microtubules by human tau. J Mol Biol 339: 539-553.

Sasaki T, Gotow T, Shiozaki M, Sakaue F, Saito T, Julien JP, Uchiyama Y, Hisanaga S. (2006). Aggregate formation and phosphorylation of neurofilament-L Pro22 Charcot-Marie-Tooth disease mutants. Hum Mol Genet 15: 943-952.

Schaefer AW, Kabir N, Forscher P (2002). Filopodia and actin arcs guide the assembly and transport of two populations of microtubules with unique dynamic parameters in neuronal growth cones. J Cell Biol 158: 139-152.

Schoenfeld TA, Obar RA (1994). Diverse distribution and function of fibrous microtubule-associated proteins in the nervous system. Int Rev Cytol 151: 67-137.

Schulz A, Baader SL, Niwa-Kawakita M, Jung MJ, Bauer R, Garcia C, Zoch A, Schacke S, Hagel C, Mautner VF, Hanemann CO, Dun XP, Parkinson DB, Weis J, Schröder JM, Gutmann DH, Giovannini M, Morrison H (2013). Merlin isoform 2 in neurofibromatosis type 2-associated polyneuropathy. Nat Neurosci 16: 426-433.

Schuyler SC, Pellman D (2001). Microtubule "plus-end-tracking proteins": The end is just the beginning. Cell 105:421-424.

Schwaller B, Buchwald P, Blümcke I, Celio MR, Hunziker W (1994). Characterization of a polyclonal antiserum against the purified human recombinant calcium-binding protein calretinin. Cell Calcium 14: 639-648.

Segref A, Hoppe T (2009). Think locally: control of ubiquitin-dependent protein degradation in neurons. EMBO Rep 10: 44-50.

Seiwa C, Kojima-Aikawa K, Matsumoto I, Asou H (2002). CNS myelinogenesis in vitro: myelin basic protein deficient shiverer oligodendrocytes. J Neurosci Res 69:305-317.

Shah JV, Flanagan LA, Janmey PA, Leterrier JF (2000). Bidirectional translocation of neurofilaments along microtubules mediated in part by dynein/dynactin. Mol Biol Cell 11: 3495-3508.

Shen XY, Billings-Gagliardi S, Sidman RL, Wolf MK (1985). Myelin deficient

(shimld) mutant allele: morphological comparison with shiverer (shi) allele on a B6C3 mouse stock. Brain Res 360:235-247.

Sihag RK, Jeng AY, Nixon RA (1988). Phosphorylation of neurofilament proteins by protein kinase C. FEBS Lett 233: 181-185.

Sihag RK, Nixon RA (1989). In vivo phosphorylation of distinct domains of the 70-kilodalton neurofilament subunit involves different protein kinases. J Biol Chem 264: 457-464.

Sihag RK, Nixon RA (1990). Phosphorylation of the amino-terminal head domain of the middle molecular mass 145-kDa subunit of neurofilaments. Evidence for regulation by second messenger-dependent protein kinases. J Biol Chem 265:4166-4171.

Sihag RK, Nixon, RA (1991). Identification of Ser-55 as a major protein kinase A phosphorylation site on the 70-kDa subunit of neurofilaments. Early turnover during axonal transport. J Biol Chem 266:18861-18867.

Sihag RK, JaffeH, Nixon RA, Rong X (1999). Serine-23 is a major protein kinase A phosphorylation site on the amino-terminal head domain of the middle molecular mass subunit of neurofilament proteins. J Neurochem 72:491-499.

Simons M, Lyons DA (2013). Axonal selection and myelin sheath generation in the central nervous system. Curr Opin Cell Biol pii: S0955-0674(13)00070-7.

Skibinski G, Parkinson NJ, Brown JM, Chakrabarti L, Lloyd SL, Hummerich H, Nielsen JE, Hodges JR, Spillantini MG, Thusgaard T, Brandner S, Brun A, Rossor MN, Gade A, Johannsen P, Sørensen SA, Gydesen S, Fisher EM, Collinge J (2005). Mutations in the endosomal ESCRTIII- complex subunit CHMP2B in frontotemporal dementia. Nat Genet 37:806–808.

Skre H (1974).Genetic and clinical aspects of Charcot-Marie-Tooth's disease.Clin Genet 6:98-118.

Sosa-Ortiz AL, Acosta-Castillo I, Prince MJ (2012). Epidemiology of Dementias and Alzheimer's Disease. Archives of Medical Research 43:600-608.

Sreedharan J, Blair IP, Tripathi VB, Hu X, Vance C, Rogelj B, Ackerley S, Durnall JC, Williams KL, Buratti E, Baralle F, de Belleroche J, Mitchell JD, Leigh PN, Al-Chalabi A, Miller CC, Nicholson G, Shaw CE (2008). TDP-43 Mutations in Familial and Sporadic Amyotrophic Lateral Sclerosis. Science 319:1668–1672.

Staal JA, Alexander SR, Liu Y, Dickson TD, Vickers JC (2011). Characterization of

Cortical Neuronal and Glial Alterations during Culture of Organotypic Whole Brain Slices from Neonatal and Mature Mice. PLoS ONE 6: e22040.

Stallings NR, Puttaparthi K, Luther CM, Burns DK, Elliott JL (2010). Progressive motor weakness in transgenic mice expressing human TDP-43. Neurobiol Dis 40:404-414.

Starr R**,** Attema B, DeVries GH, Monteiro MJ (1996)**.** Neurofilament phosphorylation is modulated by myelination. J Neurosci Res 44:328-337.

Steinert PM, Roop DR (1988).The molecular and cellular biology of intermediate filaments. Annu Rev Biochem 57: 593-625.

Sternberger LA, Sternberger NH (1983). Monoclonal antibodies distinguish phosphorylated and nonphosphorylated forms of neurofilaments in situ. Proc Natl Acad Sci U S A 80:6126–6130.

Strong MJ, Sopper MM, Crow JP, Strong WL, Beckman JS (1998). Nitration of the low molecular weight neurofilament is equivalent in Biophys Res Commun 248:157-164.

Strong MJ, Volkening K, Hammond R, Yang W, Strong W, Leystra-Lantz C, Shoesmith C (2007). TDP43 is a human low molecular weight neurofilament (hNFL) mRNA-binding protein. Mol Cell Neurosci 35: 320-327.

Strong MJ (2010). The evidence for altered RNA metabolism in amyotrophic lateral sclerosis (ALS). J Neurol Sci 288:1-12.

Sunil N, Lee S, Shea TB (2012). Interference with kinesin-based anterograde neurofilament axonal transport increases neurofilament-neurofilament bundling. Cytoskeleton 69:371-379.

Swarup V, Phaneuf D, Bareil C, Robertson J, Rouleau GA, Kriz J, Julien JP (2011a). Pathological hallmarks of amyotrophic lateral sclerosis/frontotemporal lobar degeneration in transgenic mice produced with TDP-43 genomic fragments. Brain 134:2610-2626.

Swarup V, Phaneuf D, Dupré N, Petri S, Strong M, Kriz J, Julien JP (2011b). Deregulation of TDP-43 in amyotrophic lateral sclerosis triggers nuclear factor κB-mediated pathogenic pathways. J Exp Med 208:2429-2447.

Szaro BG, Strong MJ (2010). Post-transcriptional control of neurofilaments: New roles in development, regeneration and neurodegenerative disease. Trends Neurosci 33:27–37.

Terry RD (1963). The Fine Structure of Neurofibrillary Tangles in Alzheimer's Disease. J Neuropathol Exp Neurol 22: 629-642.

Terry RD, Gonatas NK, Weiss M (1964). Ultrastructural Studies in Alzheimer's Presenile Dementia. Am J Pathol 44: 269-297.

Theriot JA (1994). Regulation of the actin cytoskeleton in living cells. Semin. Cell Biol 5: 193-199.

Tomkins J, Usher P, Slade JY, Ince PG, Curtis A, Bushby K, Shaw PJ (1998). Novel insertion in the KSP region of the neurofilament heavy gene in amyotrophic lateral sclerosis (ALS). Neuroreport 9:3967-3970.

Toyoshima I, Kato K, Sugawara M, Wada C, Okawa S, Kobayashi M, Masamune O,Watanabe S (2000). Massive accumulation of M and H subunits of neurofilament proteins in spinal motor neurons of neurofilament deficient Japanese quail, Quv. Neurosci Lett 287: 175–178.

Trapp BD (1990). Myelin-associated glycoprotein. Location and potential functions. Ann N Y Acad Sci 605:29-43.

Trimmer PA, Borland MK, Keeney PM, Bennett JP Jr, Parker WD Jr (2004). Parkinson's disease transgenic mitochondrial cybrids generate Lewy inclusion bodies. J Neurochem 88: 800-812.

Tu PH, Robinson KA, de Snoo F, Eyer J, Peterson A, Lee VM, Trojanowski QJ (1997). Selective degeneration of Purkinje cells with Lewy body-like inclusions in aged NFHLACZ transgenic mice. J Neurosci 17:1064–1074.

Uchida A, Alami NH, Brown A (2009). Tight functional coupling of kinesin-1A and dynein motors in the bidirectional transport of neurofilaments. Mol Biol Cell 20: 4997-5006.

Uchida A, Sasaguri H, Kimura N, Tajiri M, Ohkubo T, Ono F, Sakaue F, Kanai K, Hirai T, Sano T, Shibuya K, Kobayashi M, Yamamoto M, Yokota S, Kubodera T, Tomori M, Sakaki K, Enomoto M, Hirai Y, Kumagai J, Yasutomi Y, Mochizuki H, Kuwabara S, Uchihara T, Mizusawa H, Yokota T (2012). Non-human primate model of amyotrophic lateral sclerosis with cytoplasmic mislocalization of TDP-43. Brain 135:833-846.

Uryu K, Nakashima-Yasuda H, Forman MS, Kwong LK, Clark CM, Grossman M, Miller BL, Kretzschmar HA, Lee VM, Trojanowski JQ, Neumann M (2008). Concomitant TAR-DNA-binding protein 43 pathology is present in Alzheimer

disease and corticobasal degeneration but not in other tauopathies. J Neuropathol Exp Neurol 67:555–564.

Utreras E, Jiménez-Mateos EM, Contreras-Vallejos E, Tortosa E, Pérez M, Rojas S, Saragoni L, Maccioni RB, Avila J, González-Billault C (2008). Microtubule-associated protein 1B interaction with tubulin tyrosine ligase contributes to the control of microtubule tyrosination. Dev Neurosci 30: 200-210.

Van Deerlin VM, Leverenz JB, Bekris LM, Bird TD, Yuan W, Elman LB, Clay D, Wood EM, Chen-Plotkin AS, Martinez-Lage M, Steinbart E, McCluskey L, Grossman M, Neumann M, Wu IL, Yang WS, Kalb R, Galasko DR, Montine TJ, Trojanowski JQ, Lee VM, Schellenberg GD, Yu CE (2008). TARDBP mutations in amyotrophic lateral sclerosis with TDP-43 neuropathology: A genetic and histopathological analysis. Lancet Neurol 7:409–416.

Van der Gucht E, Hof PR, Van Brussel L, Burnat K, Arckens L (2007). Neurofilament protein and neuronal activity markers define regional architectonic parcellation in the mouse visual cortex. Cerebral Cortex 17:2805-2819.

Van der Vaart B, Akhmanova A, Straube A (2009). Regulation of microtubule dynamic instability. Biochem Soc Trans 37 (5): 1007-1013.

Van der Zee J, Gijselinck I, Pirici D, Kumar-Singh S, Cruts M, Van Broeckhoven C (2007). Frontotemporal lobar degeneration with ubiquitin-positive inclusions: a molecular genetic update. Neurodegener Dis 4:227-235.

Vance C, Rogelj B, Hortobagyi T, De Vos KJ, Nishimura AL, Sreedharan J, Hu X, Smith B, Ruddy DM, Wright P, Ganesalingam J, Williams KL, Tripathi V, Al-Saraj S, Al-Chalabi A, Leigh PN, Blair IP, Nicholson G, de Belleroche J, Gallo JM, Miller CC, Shaw CE (2009). Mutations in FUS, an RNA processing protein, cause familial amyotrophic lateral sclerosis type 6. Science 323:1208-1211.

Vanden Broeck L, Naval-Sánchez M, Adachi Y, Diaper D, Dourlen P, Chapuis J, Kleinberger G, Gistelinck M, Van Broeckhoven C, Lambert JC, Hirth F, Aerts S, Callaerts P, Dermaut B (2013). TDP-43 loss-of-function causes neuronal loss due to defective steroid receptor-mediated gene program switching in Drosophila. Cell Rep 3:160-172.

Vassall KA, Bessonov K, De Avila M, Polverini E, Harauz G (2013).The Effects of

Threonine Phosphorylation on the Stability and Dynamics of the Central Molecular Switch Region of 18.5-kDa Myelin Basic Protein. PLoS One 8:e68175.

Verhey KJ, Hammond JW (2009). Traffic control: regulation of kinesin motors. Nat Rev Mol Cell Biol 10: 765-777.

Verma A (2011). Altered RNA metabolism and amyotrophic lateral sclerosis.Ann Indian Acad Neurol 14:239-244.

Vickers JC, Costa M (1992). The neurofilament triplet is present in distinct subpopulations of neurons in the central nervous system of the guinea-pig. Neuroscience 49:73-100.

Vickers JC, Morrison JH, Friedrich VL, Elder G.A, Perl DP, Katz RN, Lazzarini RA (1994). Age-associated and cell-type-specific neurofibrillary pathology in transgenic mice expressing the human midsized neurofilament subunit. The Journal of neuroscience: the official journal of the Society for Neuroscience 14:5603-5612.

Vickers JC, Chin D, Edwards AM, Sampson V, Harper C, Morrison J (1996). Dystrophic neurite formation associated with age-related beta amyloid deposition in the neocortex: clues to the genesis of neurofibrillary pathology. Experimental Neurology 141:1-11.

Volkening K, Leystra-Lantz C, Yang W, Jaffee H, Strong MJ (2009). Tar DNA binding protein of 43 kDa (TDP-43), 14-3-3 proteins and copper/zinc superoxide dismutase (SOD1) interact to modulate NFL mRNA stability. Implications for altered RNA processing in amyotrophic lateral sclerosis (ALS). Brain Res 6:168–182.

Wagner OI, Ascaño J, Tokito M, Leterrier JF, Janmey PA, Holzbaur EL (2004). The interaction of neurofilaments with the microtubule motor cytoplasmic dynein. Mol Biol Cell 15:5092-5100.

Walker KL, Yoo HK, Undamatla J, Szaro BG (2001). Loss of neurofilaments alters axonal growth dynamics. J Neurosci 21:9655–9666.

Wang L, Ho CL, Sun D, Liem RK, Brown A (2000). Rapid movement of axonal neurofilaments interrupted by prolonged pauses. Nat Cell Biol 2:137-141.

Wang L, Brown A (2002). Rapid movement of microtubules in axons. Curr Biol 12: 1496-1501.

Wang HY, Wang IF, Bose J and Shen CK (2004). Structural diversity and functional implications of the eukaryotic TDP gene family. Genomics 83: 130-139.

Wang IF, Wu LS, Chang HY, Shen CK (2008). TDP-43, the signature protein of FTLD-U, is a neuronal activity-responsive factor. J Neurochem.105:797–806.

Wang JW, Brent JR, Tomlinson A, Shneider NA, McCabe BD (2011). The ALS-associated proteins FUS and TDP-43 function together to affect Drosophila locomotion and life span. J Clin Invest 121: 4118–4126.

Watts GD, Wymer J, Kovach MJ, Mehta SG, Mumm S, Darvish D, Pestronk A, Whyte MP, Kimonis VE (2004). Inclusion body myopathy associated with Paget disease of bone and frontotemporal dementia is caused by mutant valosin-containing protein. Nat Genet 36:377–381.

Waxman SG, Bangalore L (2004). Electrophysiological consequences of myelination. In R. A. Lazzarini (ed.), Myelin biology and disorders. San Diego, CA: Elsevier Academic Press:117–141.

Webster DR, Wehland J, Weber K, Borisy GG (1990). Detyrosination of alpha tubulin does not stabilize microtubules in vivo. J Cell Biol 111:113-122.

Wegorzewska I, Bell S, Cairns NJ, Miller TM, Baloh RH (2009). TDP-43 mutant transgenic mice develop features of ALS and frontotemporal lobar degeneration. Proc Natl Acad Sci. USA 106: 18809–18814.

Westermann S, Weber K (2003). Post-translational modifications regulate microtubule function. Nat Rev Mol Cell Biol 4: 938-947.

Whitehouse PJ, Price DL, Struble RG, Clark AW, Coyle JT, Delon M (1982). Alzheimer's disease and senile dementia: loss of neurons in the basal forebrain. Science 215: 1237-1239.

Wightman G, Anderson VE, Martin J, Swash M, Anderton BH, Neary D, Mann D, Luthert P, Leigh PN (1992). Hippocampal and neocortical ubiquitin-immunoreactive inclusions in amyotrophic lateral sclerosis with dementia. Neurosci Lett 139:269-274.

Willard M, Simon C (1983). Modulations of neurofilament axonal transport during the development of rabbit retinal ganglion cells.Cell 35:551-559.

Williamson TL, Bruijn LI, Zhu Q, Anderson KL, Anderson SD, Julien JP, Cleveland DW (1998). Absence of neurofilaments reduces the selective vulnerability of motor neurons and slows disease caused by a familial

amyotrophic lateral sclerosis-linked superoxide dismutase 1 mutant. Proc Natl Acad Sci USA 95:9631–9636.

Wils H, Kleinberger G, Janssens J, Pereson S, Joris G, Cuijt I, Smits V, Ceuterick-de Groote C, Van Broeckhoven C, Kumar-Singh S (2010). TDP-43 transgenic mice develop spastic paralysis and neuronal inclusions characteristic of ALS and frontotemporal lobar degeneration. Proc Natl Acad Sci U S A 107:3858-3863.

Wilson AC, Dugger BN, Dickson DW, Wang DS (2011). TDP-43 in aging and Alzheimer's disease - a review. Int J Clin Exp Pathol 4:147-155.

Windebank AJ, Word P, Bunge RP, Dyck PJ (1985). Myelination determines the caliber of dorsal root ganglion neurons in culture. J Neurosci 5:1563–1567.

Winton MJ, Igaz LM, Wong MM, Kwong LK, Trojanowski JQ, Lee VM (2008). Disturbance of nuclear and cytoplasmic TAR DNA-binding protein (TDP-43) induces disease-like redistribution, sequestration, and aggregate formation. J Biol Chem 283:13302–13309.

Wong NK, He BP, Strong MJ (2000). Characterization of neuronal intermediate filament protein expression in cervical spinal motor neurons in sporadic amyotrophic lateral sclerosis (ALS). J Neuropathol Exp Neurol 59: 972-982.

Woodhouse A, Shepherd CE, Sokolova A, Carroll VL, King AE, Halliday GM, Dickson TC, Vickers JC (2009). Cytoskeletal alterations differentiate presenilin-1 and sporadic Alzheimer's disease. Acta Neuropathol 117:19-29.

Wu YJ, Tang YF, Xiao ZC, Bao ZM, He BP (2008). NG2 cells response to axonal alteration in the spinal cord white matter in mice with genetic disruption of neurofilament light subunit expression. Mol Neurodegener 3:18.

Wu LS, Cheng WC, Hou SC, Yan YT, Jiang ST, Shen CK (2010). TDP-43, a neuro-pathosignature factor, is essential for early mouse embryogenesis. Genesis 48:56–62.

Wu W, Gu W, Xu X, Shang S, Zhao Z (2012). Downregulation of CNPase in a MeCP2 deficient mouse model of Rett syndrome. Neurol Res 34:107-113.

Xia CH, Roberts EA, Her LS, Liu X, Williams DS, Cleveland DW, Goldstein LS (2003). Abnormal neurofilament transport caused by targeted disruption of neuronal kinesin heavy chain KIF5A. J Cell Biol 161:55-66.

Xu Z, Cork LC, Griffin JW, Cleveland DW (1993). Increased expression of neurofilament subunit NF-L produces morphological alterations that resemble

the pathology of human motor neuron disease. Cell 73:23–33.

Xu YF, Gendron TF, Zhang YJ, Lin WL, D'Alton S, Sheng H, Casey MC, Tong J, Knight J, Yu X, Rademakers R, Boylan K, Hutton M, McGowan E, Dickson DW, Lewis J, Petrucelli L (2000a). Wild-type human TDP-43 expression causes TDP-43 phosphorylation, mitochondrial aggregation, motor deficits, and early mortality in transgenic mice. J Neurosci 30:10851-10859.

Xu Z (2000b). Mechanism and treatment of motoneuron degeneration in ALS: what have SOD1 mutants told us? Amyotroph Lateral Scler Other Motor Neuron Disord 1:225-234.

Xu YF, Gendron TF, Zhang YJ, Lin WL, D'Alton S, Sheng H, Casey MC, Tong J, Knight J, Yu X, Rademakers R, Boylan K, Hutton M, McGowan E, Dickson DW, Lewis J, Petrucelli L (2010). Wild-type human TDP-43 expression causes TDP-43 phosphorylation, mitochondrial aggregation, motor deficits, and early mortality in transgenic mice. J Neurosci 30:10851-10859.

Yabe JT, Pimenta A, Shea TB(1999). Kinesin-mediated transport of neurofilament protein oligomers in growing axons. J Cell Sci 112: 3799-3814.

Yamashita A, Valkova K, Gonchar Y, Burkhalter A (2003). Rearrangement of synaptic connections with inhibitory neurons in developing mouse visual cortex. J Comp Neurol 464:426-437.

Yang X, Yang Y, Lou Y, Li G, Wang J, Yang ES (2009). Hyperphosphorylation and accumulation of neurofilament proteins in transgenic mice with Alzheimer presenilin 1 mutation. Cell Mol Neurobiol 29: 497-501.

Yates DM, Manser C, De Vos KJ, Shaw CE, McLoughlin DM, Miller CC (2009). Neurofilament subunit (NFL) head domain phosphorylation regulates axonal transport of neurofilaments. Eur J Cell Biol. 88:193-202.

Yokoseki A, Shiga A, Tan CF, Tagawa A, Kaneko H, Koyama A, Eguchi H, Tsujino A, Ikeuchi T, Kakita A, Okamoto K, Nishizawa M, Takahashi H, Onodera O (2008). TDP-43 mutation in familial amyotrophic lateral sclerosis. Ann Neurol 63:538-542.

Yuan A, Rao MV, Kumar A, Julien JP, Nixon RA (2003). Neurofilament transport in vivo minimally requires hetero-oligomer formation. J Neurosci 23: 9452-9458.

Yuan A, Nixon RA, Rao MV (2006a). Deleting the phosphorylated tail domain of the neurofilament heavy subunit does not alter neurofilament transport rate in

vivo. Neurosci Lett 393: 264-268.

Yuan A, Rao MV, Sasaki T, Chen Y, Kumar A, Veeranna, Liem RK, Eyer J, Peterson AC, Julien JP, Nixon RA (2006b). Alpha-Internexin is structurally and functionally associated with the neurofilament triplet proteins in the mature CNS. J Neurosci 26:10006–10019.

Yuan A, Rao MV, Veeranna, Nixon RA (2012). Neurofilaments at a glance. J Cell Science 125: 3257-3263.

Yum SW, Zhang J, Mo K, Li J, Scherer SS (2009). A novel recessive Nefl mutation causes a severe, early-onset axonal neuropathy. Ann Neurol 66: 759-770.

Yin X, Crawford TO, Griffin JW, Tu Ph, Lee VM, Li C, Roder J, Trapp BD (1998). Myelin-associated glycoprotein is a myelin signal that modulates the caliber of myelinated axons. J Neurosci 18:1953-1962.

Zhang Z, Casey DM, Julien JP, Xu Z (2002). Normal dendritic arborization in spinal motoneurons requires neurofilament subunit L. J Comp Neurol 450:144-152.

Zhang YJ, Xu YF, Dickey CA, Buratti E, Baralle F, Bailey R, Pickering-Brown S, Dickson D, Petrucelli L (2007). Progranulin mediates caspase-dependent cleavage of TAR DNA binding protein-43. J Neurosci 27:10530–10534.

Zhang YJ, Gendron TF, Xu YF, Ko LW, Yen SH, Petrucelli L (2010). Phosphorylation regulates proteasomal-mediated degradation and solubility of TAR DNA binding protein-43 C-terminal fragments. Mol Neurodegener 5:33.

Zhang YJ, Caulfield T, Xu YF, Gendron TF, Hubbard J, Stetler C, Sasaguri H, Whitelaw EC, Cai S, Lee WC, Petrucelli L (2013). The dual functions of the extreme N-terminus of TDP-43 in regulating its biological activity and inclusion formation. Hum Mol Genet:[Epub ahead of print].

Zheng YL, Li BS, Veeranna, Pant HC (2003). Phosphorylation of the head domain of neurofilament protein (NF-M): a factor regulating topographic phosphorylation of NF-M tail domain KSP sites in neurons. J Biol Chem 278:24026-24032.

Zhu Q, Couillard-Després S, Julien JP (1997). Delayed maturation of regenerating myelinated axons in mice lacking neurofilaments. Exp Neurol 148:299-316.

Zhu Q, Lindenbaum M, Levavasseur F, Jacomy H, Julien JP (1998). Disruption of the NF-H gene increases axonal microtubule content and velocity of neurofilament transport: relief of axonopathy resulting from the toxin beta,

beta'-iminodipropionitrile. J Cell Biol 143:183-193.

Appendix

1. General Solutions

0.01M phosphate buffered saline (PBS, pH 7.4), 1000ml

100ml NaCl (Sigma)- 90g/L stock solution
40ml $Na_2HPO_412H_2O$ (Sigma) - 28.4g/L stock solution
10ml $NaH_2PO_4.H_2O$ (Sigma)- 31.2g/L stock solution
850ml Milli-Q water
pH 7.4

2. Immunohistochemistry solutions

4% paraformaldehyde (PFA), 100ml

4g PFA (Sigma)
4g sucrose (Sigma)
10ml $NaH_2PO_4.H_2O$ (Sigma)- 31.2g/L stock solution
40ml NaH_2PO_4 (Sigma)- 28.4g/L stock solution
50ml Milli-Q water
dissolved by heating (~80°C) on stirrer hotplate in fume hood

Diluent solution (0.3% Triton X-100 in 0.01M PBS)

600μL Triton X-100 (Sigma)
200mL 0.01M PBS

18% / 30% Sucrose, 1000ml

180/300g sucrose (Sigma)
1000 ml 0.01M PBS

Tissue Storage Solution, 1000ml

1g azide (Sigma)
1000ml PBS

0.01M Citrate buffer, 1000ml

2.94g Trisodium citrate in 800ml Milli-Q water
Dessolve and adjust to pH 6 with 0.1M citic acid, then Add Milli-Q water to reach the final volume 1000ml

3. Western blot solutions

10 x transfer buffer, 1000ml

144g Glycine (Sigma)
30.3g Tris base (Sigma)
Add Milli-Q water to reach the final volume 1000ml

10 x TBS, 1000ml

87.66 g NaCl (Sigma)
12.11g Tris base (Sigma)
Add Milli-Q water to reach the final volume 1000ml

10 x running buffer, 1000ml

144g Glycine (Sigma)
30.3g Tris base (Sigma)
10g SDS (Sigma)
Add MilliQ water to reach the final volume 1000ml

1 x running buffer, 1000ml

100 ml 10 x running buffer
900 ml MilliQ water

1 x transfer buffer, 1000ml

100 ml 10x transfer buffer
100 ml Methanol
800 ml MilliQ water

1 x TBST buffer, 1000ml

100 ml 10 x TBS
900 ml MilliQ water
1 ml Tween 20 (Bio-Rad Laboratories)

Blocking buffer, 50ml

2.5g Skim dry milk (Coles)
50 mL 1x TBST